Inflatable Glazing

Prototyping of a dynamic thin glass unit
with a switchable thermal insulation

Patrick Ullmer

Inflatable Glazing

Prototyping of a dynamic thin glass unit
with a switchable thermal insulation

Building Technology Graduation Project

[Author]

Patrick Ullmer

5604966

June 20, 2023

[1st Mentor]

Prof. James O'Callaghan

Architectural Glass

TU Delft / EOC Engineers

[2nd Mentor]

Dr. Marcel Bilow

Building Product Innovation

TU Delft

TU Delft

Acknowledgements

Working on this thesis over the past few months has been the most challenging and exciting experience of my studies. My time at TU Delft, following the Building Technology track, provided me with a valuable skillset in building envelope design that I was able to apply extensively. I am grateful for the connections I made with inspiring and knowledgeable people who helped me accomplish a project I am truly proud of.

Firstly, a sincere thank you to my mentors, James and Marcel. Your guidance and support were invaluable in every aspect of this journey.

Alongside being a remarkable mentor, James has influenced me to grow my passion for façade engineering. He connected me with leading companies in the glass industry, and made this thesis feel like genuine product development. He provided assistance as we detailed prototypes and encouraged me to explore the vast field of glass design.

Marcel has not only been a great mentor but also an inspirational figure. Since the start of my studies at TU Delft, he made me understand the challenge of bringing an idea from sketch paper to real life. He helped me develop a fully functional prototype and taught me the importance of neat and accurate working. I am grateful for the patience and fun times at his workshop.

To my thesis committee member Christian van Ees, I really appreciate your time and interest in this project.

I also want to express my gratitude to Christian Scherer from Kömmerling | H.B. Fuller and Marco Zaccaria from AGC. Both have been closely involved in significant parts of this thesis and have generously devoted their time to assisting in the design and supply of key materials to manufacture the prototypes.

A special thanks goes to my co-workers, Joep Hövels and Leonie van Ginkel from Frontwise Facades. They not only supported me throughout my entire studies but also took the time to provide valuable input for my thesis.

This journey would not have been half as fun without my friends from Delft, Eindhoven and back in Germany. I thank every one of them for being there for me and for the moments we spent together.

This thesis is dedicated to my family, whose unconditional love and support always kept me positive and motivated. I am thankful for the great moments I could spend with my parents, brother, and grandparents during the course of this thesis.

Thank you all,

Patrick

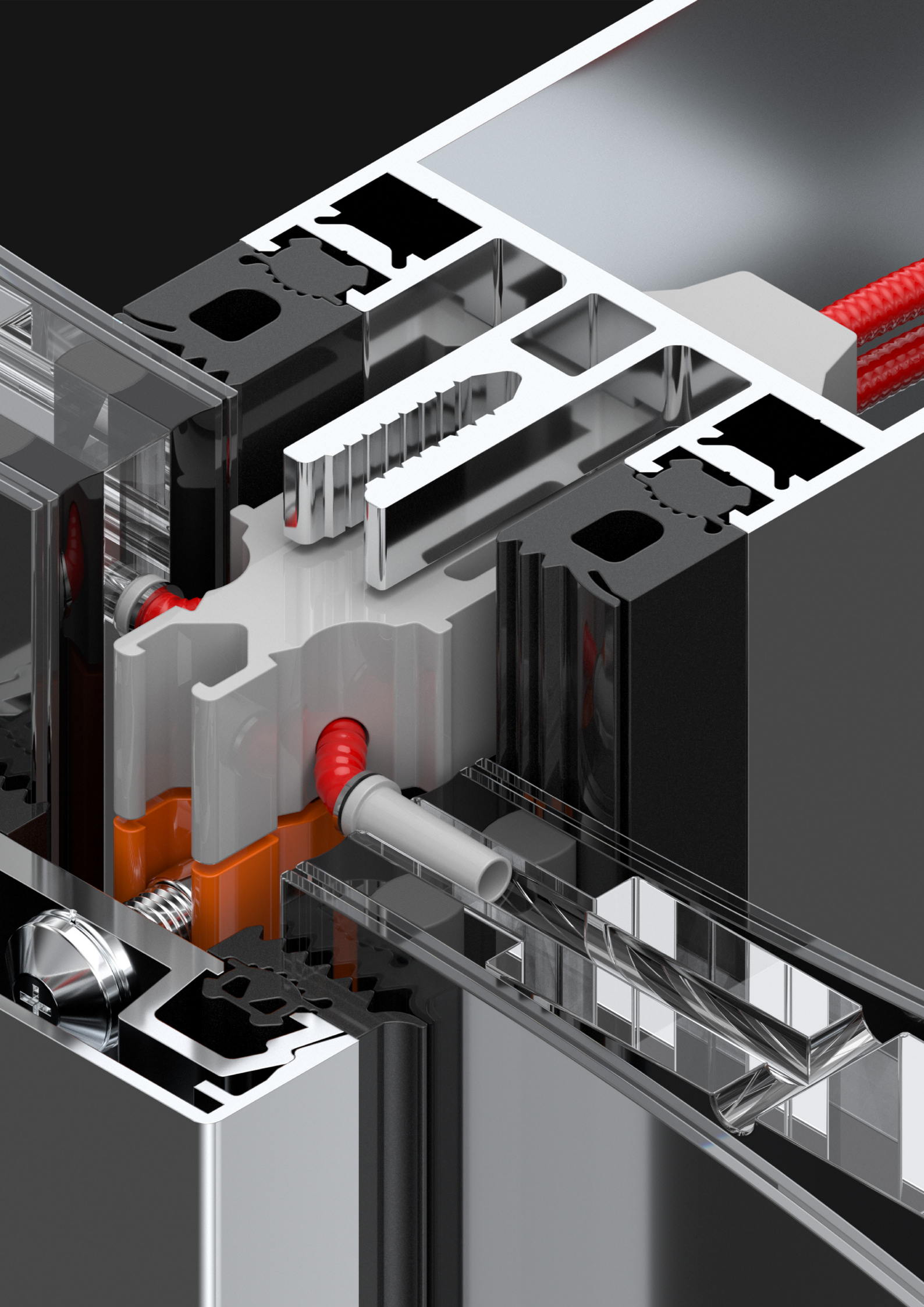

Abstract

Building energy regulations worldwide are increasingly advocating for better-insulated facades since improved insulation in facades can significantly reduce a building's heating energy demand. However, research indicates that super-insulated buildings are already at risk of overheating due to high internal heat storage and low heat loss. In addition, over the past decades, the climatic trend demonstrated a significant rise in surface temperatures. As a result, well-insulated commercial buildings have become increasingly dependent on cooling.

On the other hand, approximately 85% of Europe's glazing comprises single glazing and uncoated double glazing. This prevalence leads to high demand for heating and cooling energy. Therefore, there is an urgent need to enhance the insulation of these buildings' glazing while maintaining the existing window frames.

A glass unit prototype with switchable insulation has been developed and assessed to address these issues. The findings of this thesis demonstrate that in mixed climate zones, the utilization of switchable insulation can lead to a reduction in total energy demand by as much as 33% compared to the use of present high-performance glazing technologies.

When advantageous, Inflatable Glazing can be activated on-demand or controlled by internal and external sensors. The heat transfer coefficient of the facade, known as the U-value, can be switched from a low insulating value to a high conducting value. During the cooling period, this technology can be employed to increase the heat flux of the glass unit, thereby enhancing heat dissipation. Conversely, Inflatable Glazing can provide excellent insulation and highly effective solar gain during the heating period.

This thesis investigates the potential of a switchable insulating glass unit for buildings in mixed and mild climate zones, where selecting the appropriate U-value can be complex. The focus is set on building and testing a fully transparent glass unit with a switchable U-value. The innovative material, thin glass, serves as the primary dynamic component due to its advantageous bending properties and strength.

Keywords:

Thin glass, thermal performance, switchable insulation

Table of Contents

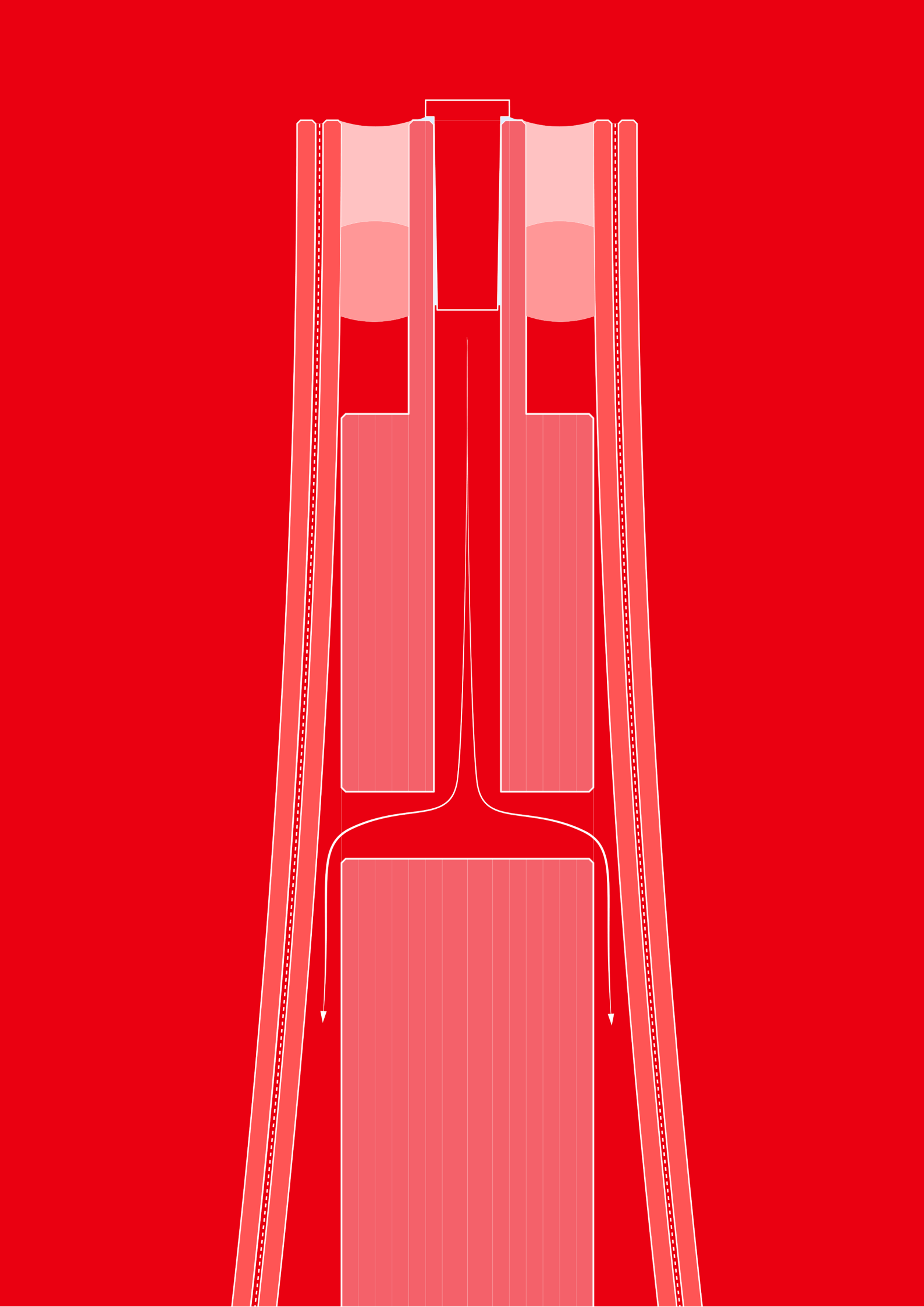

1. Introduction

The master's thesis explores the production design of a thin glass unit with switchable insulation. To fully comprehend the different fields of research, some background is provided. This background discusses topics such as thermal insulation, the composition of Insulated Glass Units (IGUs), the current smart-glazing market, and the innovative material of thin glass. These topics will establish the basis for subsequent simulations and experiments.

In the chapters, 4 and 5, the conceptual design and development of the glass unit are explored. The technology's working principle is outlined, and the design criteria are specified. Additionally, the design process is documented, highlighting its evolution over the course of the thesis. Furthermore, a plausible manufacturing process is proposed.

Following that, chapters 6, 7, and 8 assess the thermal, energy, and structural performance of Inflatable Glazing. These topics are vital for determining the feasibility and efficacy of the unit. The computational workflow is disclosed in each of these chapters, and the simulations are documented. Finally, the results are discussed on a per-topic basis.

Chapter 9 addresses the manufacturing and functionality tests of various prototypes, with the unit constructed as closely as possible to the actual product. A 3D scan is then performed to measure and evaluate the surface of the prototype, providing the necessary input data for both thermal and energy simulations.

Chapter 10 will present visuals of the product and its application in architecture, along with close-up renders to better understand the product's installation and assembly. Furthermore, the aesthetic quality of the unit is discussed.

The thesis closes with a conclusion where the research questions are answered, and recommendations for further research are provided.

2. Research Framework

2.1 Problem statement

A high level of insulation in buildings can lead to increased cooling load and overheating risks. Studies, such as those by Berger et al. (2016) and McLeod et al. (2013), have shown that with additional insulation in place, the cooling demand in summer increases as it tends to slow down (nocturnal) cooling processes. Buildings with high amounts of insulation are particularly vulnerable to overheating, with occupants often reporting better thermal comfort in winter than in summer. The risk of overheating in these buildings is highly dependent on factors such as solar transmission, internal heat gains, the presence of shading devices, the glazing-to-wall ratio, the orientation of the glazed areas, and thermal mass (Pflug, 2016)

The thesis emphasizes two climate scenarios in which selecting the appropriate level of insulation poses difficulties.

1. Choosing an appropriate U-value for glazing in mixed climate zones, where regions experience cold winters and hot summers, is complex due to the contrasting requirements for thermal insulation throughout the year. In cold winters, glazing with a low U-value are desirable as they provide better insulation, reducing heat loss and lowering heating energy demand.
Conversely, during hot summers, a higher U-value might be beneficial for allowing heat transfer and promoting natural cooling. Selecting a single U-value for windows in mixed climate zones requires balancing these competing needs to optimize energy efficiency and maintain comfortable indoor temperatures all year round.

2. In warm or temperate climate zones, single glazing is commonly used due to its lower cost and adequate performance under milder weather conditions. These regions typically experience less extreme temperature fluctuations, and the primary concern is often to allow natural light and ventilation while providing a basic level of insulation. However, single glazing is disadvantageous in winter because it offers poor thermal insulation. The single layer of glass has a high U-value, which means it allows more heat to escape from the building, leading to increased energy consumption for heating and reduced indoor comfort.

On the other hand, a higher U-value can be advantageous in warm or temperate climates, as it allows for easier heat ejection due to a higher thermal flux. This can be beneficial in situations where there are significant internal heat loads that need to be expelled from the building, such as when appliances or occupants generate excess heat. The higher U-value of single glazing promotes more effective heat

transfer, helping to maintain comfortable indoor temperatures and reduce the reliance on mechanical cooling systems.

The problem statement is formulated as follows:

Selecting an appropriate U-value for windows in mixed and mild climate zones poses a challenge due to the need to balance conflicting thermal insulation requirements for both hot summers and cold winters while optimizing energy efficiency and indoor comfort.

2.2 Studio choice

The Transparent Structures and Glass Design Studio focuses on developing innovative solutions for more sustainable buildings using glass. The primary concept for achieving switchable insulation in windows involves opening and closing a cavity. In conventional insulated glass units (IGUs), glass panes are separated by spacers, creating a cavity that lowers conductance and provides an insulation layer. If the cavities in an IGU were eliminated, the glass panes would make direct contact and become fully conductive, resulting in properties similar to single glazing.

Thin glass, an innovative material, was chosen for this application due to its desirable bending properties and high design strength. The goal of this thesis is to enable the opening and closing of one or more cavities within a glass unit merely using gas pressure.

2.3 Research Question

Based on the problem statement, certain climate zones could benefit from switchable insulating glazing to improve a building's energy efficiency. The use of thin glass and the concept of a collapsible cavity leads to the following research question:

How can thin glass be utilized as a dynamic component to enable a switchable U-value in an insulated glass unit?

The research and design assignment will also answer the following sub-questions:

1. What are the resulting U-values when the unit's cavity is either open or collapsed?

2. What is the effect on energy efficiency of a building with Inflatable Glazing equipped and where is it the most effective?

3. What are the main challenges in manufacturing a dynamic thin glass unit and how could the process be improved?

4. What are the desired cavity widths to achieve the best thermal results and which pressures and stresses can be expected?

5. What is the resulting inflation geometry and curvature of the inflated thin glass unit?

2.4 Objective

The problem statement highlights that the insulation value of static insulated glazing is not beneficial in the desribed climatic zones over the whole year. A glass unit with an adjustable insulation value would enable the building to collect, store, and release heat as needed. The insulation value could be controlled by means of interior and exterior sensors, as well as weather predictions.

General objective

This study aims to build a functional prototype of an inflatable glass unit capable of significantly changing its insulation. The hard criteria for the prototype include variable cavity widths ranging from 0.0 to 16.0 mm and a resulting U-value close to single- (5.6 W/m^2K) and triple-glazing properties (0.7 W/m^2K). The soft criteria involve delivering a structurally sound panel, preferably with modern facade panel dimensions. The actual prototype should demonstrate a stable and consistent double curvature, which can be measured and fed into the thermal simulation. Additionally, the thickness of the resulting insulated glass unit should be compatible with standard facade profile openings.

The prototype will undergo laboratory testing to evaluate its inflated geometry. The prototype will be 3D modelled and simulated for various thermal calucaltions to determine achievable U-values. Finite Element Analysis will be used to calculate the necessary material thicknesess, predicting the principal stresses and the maximum deformations. Ultimately, an estimate of the annual energy demand will be calculated to verify its performance compared to different static glazing

options. Furthermore, this study aims to provide a deeper understanding of thin glass bending through air pressure and pave the way for future research in this field.

Final products

1. Technical drawings of the glass edge for the theoretical production design and prototypes.

2. Custom U-value Python plug-in for Grasshopper according to EN673:2011 to determine the the average, maximum and minimum U-value on an irregularily curved surface. The plug-in will be able to always find the best glass build-up using a machine learning algorithm.

3. Finite Element Analysis to determine the thicknesses, stresses and w-deformations of the theoretical units and actual prototypes.

4. Energy model simulations in Honeybee to determine the products performance and find the ideal location.

5. Prototypes to demonstrate the functionality of inflation as well as a protoype which will undergo 3D scanning. Thus, the exact shape can be determined and fed back into the U-value script.

6. Product visuals - 3D renderings of an architectural case study and product renders of the glass edge in a custom mullion.

7. Report and presentation with literature research to build the fundamental base of the project.

Boundary conditions

This thesis focuses on innovative glass solutions and, in particular, the use of thin glass. Therefore, the starting point is to use thin glass as the primary deformable material. The dimensions of the prototype will depend on the material dimension that the author receives from suppliers and the dimensions of the testing equipment available at the TU Delft. The main objective of this study is the proof of concept on both a theoretical and a practical basis.

2.5 Methodology

The thesis has been planned as follows:

Phase 1: Literature research and preliminary design
Phase 2: Thermal simulations and Finite Element Analysis
Phase 3: Functionality tests, material procurement and Energy simulation
Phase 4: Final manufacturing, 3D scanning and reporting

Phase 1 deals with fundamental research to comprehend the principles of the building envelope design. A preliminary draft design of the glass edge has been developed to initiate discussions with industry professionals. A functional prototype using PETG has been produced to prove the concept of the inflation principle.

Phase 2 focuses on verifying the thermal performance of the glass unit through computational simulations. Finite Element Analyses play a crucial role in demonstrating the theoretical structural capabilities, as well as obtaining results for required thicknesses, permissible stresses, and expected deformations in the actual prototype.

In Phase 3, the first thin glass prototype has been tested to validate the functionality. The double curvature and inflation was consitent, so the glass edge design has been considered as ready for final production. In this phase, the procurement of materials and tools took place, and alongside that, an energy simulation was conducted to demonstrate the product's performance.

Phase 4 involves producing the final glass unit after receiving all materials. In the glass lab, three versions of the final prototype are built for: functionality tests, 3D scanning, and exhibition purposes. The results have been assessed and documented in a presentation and report.

2.6 Relevance

Societal relevance:

Inflatable glazing tackles societal issues by reducing a building's energy demand and enhancing the thermal comfort of its occupants. Unlike other smart glazing products, the technology allows occupants to maintain an unobstructed view. Furthermore, there is a high potential of reducing material usage and thus lowering the CO2 footprint of the facade. The product offers renovation possibilities due to its thickness, and with reduced weight, it also lowers labor intensity.

Scientific relevance:

The thermal performance of dynamic IGUs with uneven surfaces has been simulated, paving the way for further research. Additionally, the energy efficiency of switchable insulation technology has been modeled, leading to conclusions about its optimal use and locations. The structural performance of thin glass panes under gas pressure has also been theoretically assessed using Finite Element Analysis and compared with simple laboratory tests. To understand the extent of double curvature, the inflation geometry of thin glass panes has been evaluated using 3D scanners. Finally, the project has investigated the flexibility and durability of innovative edge seals to ensure the product's airtightness and adhesion.

(streetcommunication, 2021)

3. Background

The background serves to comprehend the four research areas for the project of inflatable glazing. The key takeaways for each field are:

1. Solar control and thermal insulation: The building physical parameters of static glazing that affect an indoor temperature depends on solar control and thermal insulation. These factors are crucial to control thermal comfort depending on the climate zone and building type.

2. Insulated glass unit build-up: The edge seal of an IGU is the most important in terms of durability. The latest spacer innovations offer higher flexibility to counter movements caused by pressure. In addition, flexible edge seals and spacers offer opportunities for dynamic products.

3. Smart glazing market: This section looks at innovative, dynamic products that change their properties to control solar heat gain. The main takeaway is that the market is still quite small due to the complexity and costs of the products. However, this market is evolving and offers promising technologies. The market of switchable thermal insulation products is not yet established. However, it shows feasible concepts and approaches to change the U-value significantly.

4. Thin glass: The bending properties and the resulting stiffness when thin glass is flexed offer a range of opportunities. The chapter examines the evolution, production, tempering and physical properties of the material.

5. Opportunity: An IGU that is able to adjust the cavity width would have a variable U-value and could be an opportunity to enter the smart glazing market with reduced complexity. A variable insulation value of a facade would allow to better control thermal insulation and be less reliant on HVAC systems.

3.1 Solar Control and Thermal Insulation

Facades have a dual role in the design and functionality of a building. Their primary function is to serve as a physical barrier that separates the building's internal environment and occupants from the external weather and climatic conditions. The second function of facades is to contribute to the aesthetic and visual appearance of the building. The facade is often the most visible element of a building, and it plays a significant role in creating a structure's overall image.

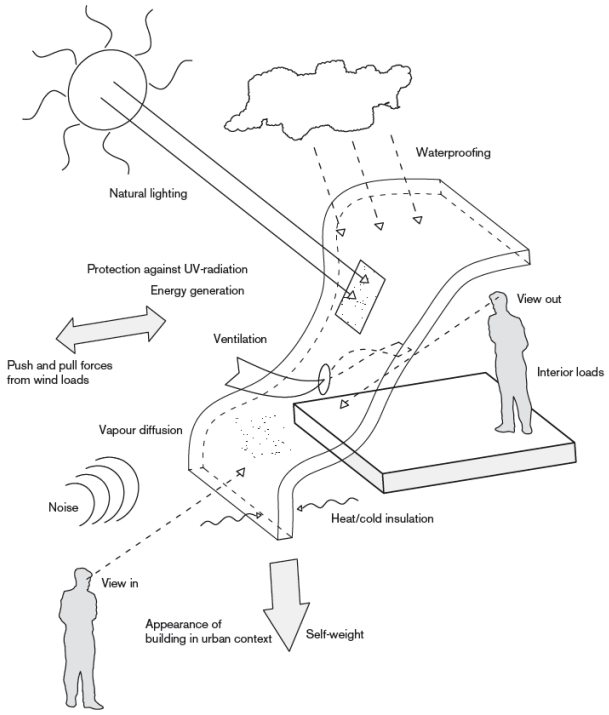

Figure 3.0 | Facade functions according to Knaack et al. (2014)

The following paragraph focuses on the primary function of the facade. Ultimately, the fundamental physics of solar radiation and the principles of thermal insulation.

Solar radiation

The intensity of solar radiation [*q*] hitting the building skin can reach up to 900 [W/m^2], depending on the season and the direction of the building's faces (van der Linden, 2018). The amount of radiation entering a building also significantly influences the interior temperature. Although the provision of natural light, exterior views, and ventilation necessitate the inclusion of windows in specific locations, they also contribute significantly to thermal discomfort or overheating.

Solar radiation occurs as direct solar radiation, diffuse solar radiation (scattered sunlight by the atmosphere), and radiation reflected off the ground. The latter two contribute less significantly than direct solar radiation but are still crucial for accurate calculations.

Greenhouse effect

As described by van der Linden (2018), glass is a material that does not allow longwave infrared radiation to pass through it, but it is permeable to sunlight. This means that when sunlight enters a room through glass windows, it heats up the surfaces and objects inside the room passively. The wavelength of the radiation from the sunlight is around 10 micrometers, which is too big to pass through glass. As a result, the heat energy from the sunlight gets trapped inside the room, creating a warming effect, commonly known as the greenhouse effect.

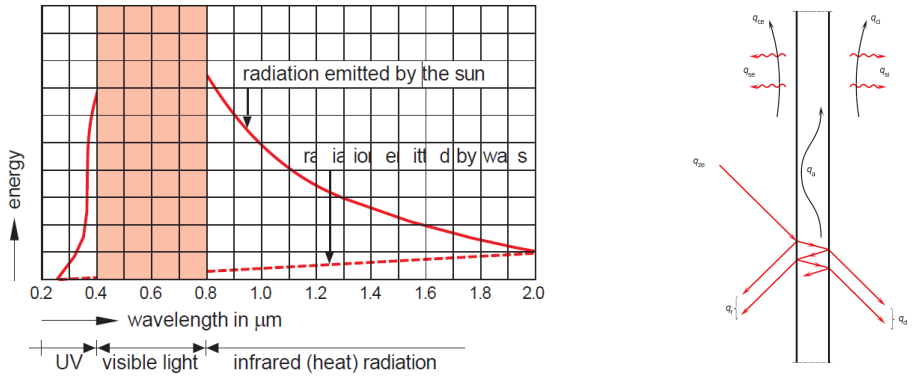

Figure 3.1 | Solar energy wavelength distribution (left) and all solar energy flows on a glas pane (right) (van der Linden, 2018)

Solar & thermal effects on glass

Figure 3.1 (right) illustrates all energy flows resulting from solar radiation on a glass pane in a schematic section according to van der Linden (2018). The energy flows are defined as follows:

q_{ze} the totality of solar energy directed at the building
q_r radiation that is reflected
q_d radiation that is admitted
q_a radiation that is absorbed
q_{ce} heat that is given off outside through convection
q_{se} heat radiation that is given off outside
q_{ci} heat that is given off inside through convection
q_{si} heat radiation that is given off inside

Thermal insulation

Temperature differences within a material cause heat to flow from warmer to cooler areas through conduction, convection, and radiation.

Conduction occurs within the material itself as heat moves from one molecule to another, while convection involves molecular movement in liquids and gases due to density variations caused by temperature fluctuations. Radiation involves the emission of electromagnetic energy from heated objects.

Insulating glazing minimizes heat transfer by limiting conduction and convection using a cavity filled with a thermally insulating gas and a low-emissivity coating between glass layers. This design effectively reduces heat flux, improving energy efficiency in buildings (AGC, 2010).

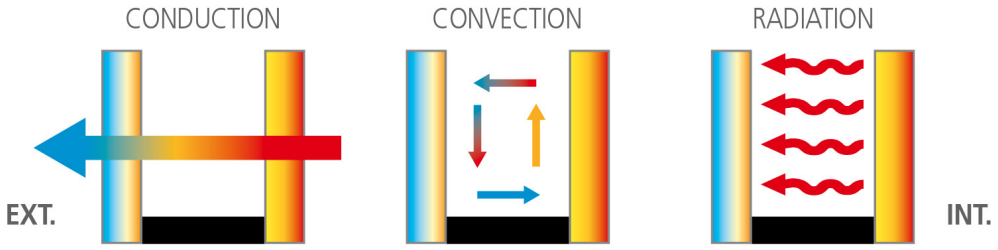

Figure 3.2 | Fundamental mechanisms of heat transmission through a glazing (AGC, 2010)

Insulated glass units (IGUs) consist of two or more glass panes that are separated by a spacer and sealed around the edges to create an airtight space called a cavity. This cavity is essential in keeping the conduction of an IGU as low as possible, thus reducing the amount of heat flux transferred through the glass. The type of glass, cavity width, material thickness, and inert gas are the main drivers to determine the insulation value of an IGU.

The heat conduction coefficient lambda [λ], measured in [W/(m·K)], indicates the heat transfer rate through a material with a thickness of 1 [m], a surface area of 1 [m2], and a temperature difference of 1 [K]. The U-value is the inverse of the absolute thermal resistance, also called the R_T-value. For calculating the R-value, one must know the heat conduction coefficient [λ], the thickness of a material [d] in [m], and the outside- R_{so} and inside air film R_{si}. The following formulae give a basic idea on how the U-value is determined in building construction components:

$$R_m = \frac{d}{\lambda} \qquad R_T = R_{si} + R_c + R_{se}$$

EN-673 is a European standard that outlines a method for calculating the thermal transmittance of glazing including uncoated glass, coated glass, and multiple glazing. The calculation determines the U-value (thermal transmittance) in the any point of the glazing, but does not include edge effects due to thermal bridges or energy transfer from solar radiation. The standard is used for product comparison and for predicting heat loss, conduction heat gains, condensation, and the solar factor. This calculation is more complex and will be further disucussed in chapter 6 (Thermal Performance).

Solar control

The solar transmission properties of a building are represented by the solar transmission factor (g) and the convection factor (CF). The g factor represents the amount of solar energy that enters a room, while the CF represents the amount of energy that enters as convective heat and directly affects the air temperature. Both factors are important in determining the solar transmission quality of a construction. They can be calculated as such:

$$g = \frac{q_d + q_{ci} + q_{si}}{q_{ze}}$$

$$CF = \frac{q_{ci}}{q_d + q_{ci} + q_{si}}$$

So to speak, the g factor of a glass unit indicates the percentage of incoming solar energy transmitted through the glass unit, while the convection factor represents the percentage of the convective part of that energy. The g factor is particularly important in situations where solar energy is desired, such as in heating-dominated climates. In warmer regions, the g factor is typically kept low to prevent excessive solar energy from entering the building and to maintain a cooler interior.

The most efficient way to control solar heat gain is through external sun shading, which blocks the sun's rays before they reach the glass unit, thus reducing the amount of heat entering the building. External sun shading solutions like vertical blinds, roll-up screens, and canopy blinds are commonly used, but they have several downsides. These include partial opacity that obstructs views, instability in strong winds, high maintenance requirements, and aesthetic limitations. Interior sun shading and between-pane shading are less effective in controlling solar heat gain, but they are commonly used due to their aesthetic appeal and cost-effectiveness.

Secondary shading methods are an additional layer of protection against solar heat gain, and they include coatings, films, tints or frit patterns. These methods are applied to the glass surface of windows and are designed to reduce the amount of solar radiation that enters the building. Currently, the use of coatings and films is a prevalent practice as they provide high transparency while effectively controlling solar heat gain.

Spectrally selective coatings and films can be applied to the glass to reflect or absorb certain wavelengths of light. This allows natural light to enter the building while reducing heat gain. They work by reflecting or absorbing the sun's infrared (IR) and ultraviolet (UV) radiation, which are the main sources of heat gain. Generally, they can provide the same effectiveness of solar control, however, coatings are much more durable than window films (Aguilar-Santana, 2019).

3.2 Insulated Glass Unit Build-Up

Early IGUs were developed in the 1930s, but it wasn't until the 1970s that they became widely used in commercial and residential construction. Today, IGUs are standard in most new construction and retrofit projects and continue to improve in their energy efficiency, sound insulation, and overall performance.

Despite advances in technology, windows are still a significant contributor to energy loss in buildings, accounting for 30-50% of energy lost through building envelopes (Van Den Bergh, 2013). This has led to a high demand for more energy efficient windows. As a result, research has been focused on improving the insulation and durability of window panes and their components. The upcoming sections will discuss the general composition of an IGU and its individual parts.

Components of an IGU

IGUs are made up of multiple glass panes sealed together along their edges, held structurally in place by various types of edge seal systems. The primary function of these edge seals is to maintain an equal distance between the panes and to act as a barrier against water vapor or prevent exfiltration of the gas infill. As shown in Figure 3.3, the edge seal system is composed of components like a spacer bar with desiccant, and sealant, which are often combined to serve multiple purposes (Van Den Bergh, 2013).

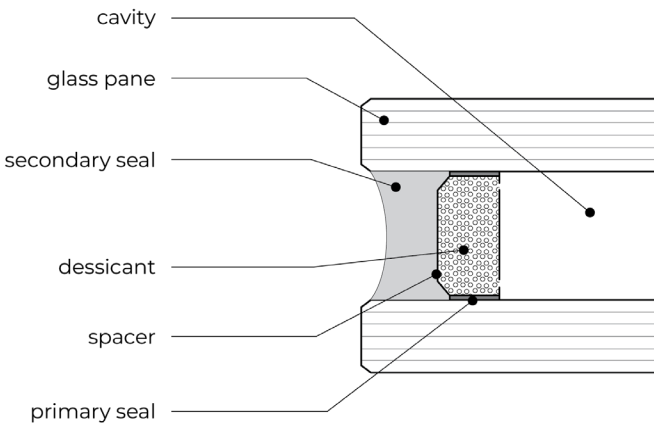

Figure 3.3 | Typical edge section of an IGU (Author)

Spacer

The spacer bar is used to hold the glass panes at a fixed distance from each other and determine the size of the interpane space. The typical profile width varies between 4-8 mm and common spacer thicknesses are 12 and 16 mm. Both hollow and solid spacer bars are available on the market (AGC, 2010).

Desiccant

Desiccants are used in IGUs to prevent the inside glass surfaces from fogging due to condensation of moisture vapor or organic vapors that may be present in the interpane space. These vapors can be trapped during manufacturing or permeate through the edge seal during use. Desiccants prolong the windows' service life by adsorbing moisture and organic vapor until they are saturated. Commonly used desiccants in the IG industry are molecular sieves or a blend of silica gel with molecular sieves.

Edge seals

The system of spacer bar and secondary sealant provides the strength to hold two panes of glass at a fixed distance apart. The primary seal does not contribute to the structural integrity of the IG unit. It is responsible for keeping the inert gas, such as argon or krypton, that is filled between the panes inside the IGU, and preventing it from leaking out. It also helps to prevent moisture and other external elements from entering the interpane space.
It is essential that the secondary sealant adheres over the long term to the glass, glass coatings, and spacer bar materials. To ensure a long service life for the IG unit, the secondary seal must also be flexible to accommodate glass movement under a variety of continuous mechanical stresses. These include pressure differences between the interpane space and the outside atmosphere that are introduced during

manufacturing, transportation, and installation of the glazing unit. Other factors are stresses during the service life of the IG unit from environmental conditions such as solar radiation, temperature differences, wind loads, and barometric pressure (Van Den Bergh, 2013).

The primary sealant, typically made of polyisobutylene. The secondary sealant, is typically made of polyurethane, silicone, or polysulfide. It functions as an adhesive that unites the glass panes and spacer bar and prevents excessive movement under different environmental stresses. The thickness of the primary sealant is typically 0.2-0.6mm and the secondary seal width is about 4mm. The minimum width of secondary sealant is 3mm to cover the primary sealant and protect it from contact with moisture (Van Den Bergh, 2013).

Edge spacer categories

The main categories of spacers are metal and non-metal spacers (see Figure 3.4). Metal spacers are further divided into aluminum, galvanized steel, stainless steel and thermally improved metal spacers. Non-metal spacers are divided into composite, structural foam and thermoplastic spacers. Hybrid spacers and thermally broken aluminum spacers are special types of metal spacers that have improved thermal performance.

Non-metal spacers are considered to be a promising future direction for improving thermal performance of edge seals as they greatly reduce heat loss through the edge-of-glass region. They often incorporate a metalized foil to ensure low water vapor and gas permeability. Thermoplastic spacers are made from PIB with integrated desiccant, and are extruded directly between the glass panes, creating a homogeneous and continuous edge seal (Van Den Bergh, 2013).

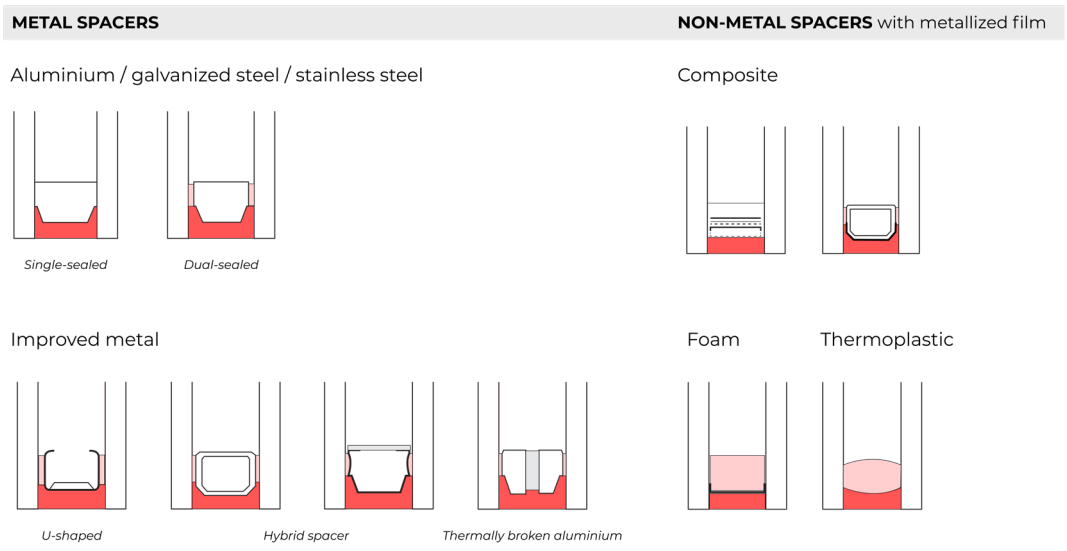

Figure 3.4 | Spacer categories (Author)

Conclusion

Facades belong to the shearing layer of “skin” and have an expected lifespan of about 25+ years (Overbey, 2022). The durability of an IGU edge detail is the most crucial since it affects the lifespan of a facade the most. To address this, many companies provide different edge sealants, spacers, and desiccants solutions. IGUs need to be more flexible to accommodate movements, decrease vapor transport, reduce thermal conduction and have better adhesion to the glass and the adhesive itself. New edge seal components also offer better manufacturability by reducing and simplifying steps in the process. The thermoplastic spacers seem to be a good choice in designs where high flexibility and durability is needed.

3.3 Smart Glazing Market

Smart glazing or dynamic glazing is the umbrella term for glazing which is able to change it’s properties with an external stimulus such as an electrical current, heat, mechanics or light. By changing its properties, these types of glazing have an effect on thermal comfort and the reduction of a buildings energy demand. They can be categorized in active and passive smart glazing. The following section will discuss the main innovations in smart glazing and identify their functioning according to Rezaei, 2017.

Passive systems

Thermochromic glazing

Thermochromic glazing is a type of window coating that changes color and optical properties when the temperature changes. This can help to increase the energy efficiency of buildings by controlling the amount of light and solar radiation that enters the building. The most common material used for this type of coating is vanadium oxide (VO2). The performance of these coatings is measured by their ability to control the amount of solar energy that passes through the window. Despite research, there is still no commercial window that meets the demands of this type of coating.

Phase changing materials (PCMs) based windows

Phase changing materials can be used in windows to decrease energy load during peak hours and prevent temperature fluctuations by absorbing and releasing heat. PCMs can be placed between window glass panes and absorb infrared radiation, but have poor visual transmittance. The use of PCMs in windows can decrease temperature fluctuations and reduce energy demand. While translucent PCM

windows are commercially available, their light quality transmittance needs to be improved.

Active systems

Electrochromic glazing (EC)

Electrochromic glazing changes color and optical properties when a small DC voltage is applied. Both inorganic and organic materials are used, and multiple layers are required. The process involves inserting or extracting ions through an electrolyte layer under an external electric field. High modulation of visible light transmittance and fast switching time are achievable. Research is currently focused on developing EC layers that can alter near-infrared transmittance without changing the visible light transmittance.

Gasochromic glazing (GC)

Gasochromic windows change color and transparency based on the exposure to hydrogen gas. The transparency level can be adjusted by varying the amount of hydrogen and can be restored by exposing the window to oxygen. GC windows are simpler in structure compared to electrochromic windows but require additional equipment for control. Studies have shown that GC windows can achieve a transparency range from 0.77 to 0.06 and have the potential for energy efficiency by reducing HVAC loads in buildings.

Suspended particle (SP) and Liquid crystal (LC) glazing

Suspended particle and Liquid crystal windows are electroactive devices which change transparency when an AC voltage is applied. SP windows generally have 3-5 layers and become transparent when the randomly scattered and oriented particles align. LC windows appear white and translucent when the voltage is off and scatter light. The transparency of SP windows can be adjusted and the response time is faster than EC windows but energy consumption is higher. LC windows are used for privacy purposes. Research is being conducted to improve the energy efficiency of these windows.

Conclusion

In conclusion, smart glazing technologies primarily block solar radiation by adjusting their opacity. This can also eliminate the need for traditional shading elements, thus, enhancing the design freedom and aesthetic appeal of a building. Additionally, these technologies can greatly reduce the workload on HVAC systems. However, it should also be noted that smart glazing systems are complex, with

many components that may wear down over time. They also tend to have limited control options and can consume high amounts of energy. Furthermore, research on smart glazing has primarily been focused on controlling solar radiation, with less emphasis on variable thermal insulation. In regions where solar heat gain is already effectively managed through other means, such as large canopies, variable thermal insulation becomes a more crucial aspect to consider. Following section will explore concepts for building products with a switchable U-value.

Switchable U-value building products

According to research from Pflug et al. (2018b) several concepts with a switchable U-value have been explored in the past. Examples include physically removing insulation (Sodha et al., 1982), filling or emptying cavities with insulating foam (Olbrich, 1989), rear-ventilation of insulation systems (Stazi et al., 2012), collapsing (Kimber et al., 2014b) or removing (Pflug et al., 2017) air cavities. Following section depicts three concepts of building products with a switchable insulation.

According to the reviewed papers, there is not yet a product with a switchable insulation value on the market. The following example is a patented invention of (Kvasnin, 2014), and features a series of air-filled cavities separated by opaque films, that can be rolled up or down. The U-value varies from 0.35 W/m2K in the insulating state to 2.7 W/m2K. Building simulations for an office space in a continental European climate were conducted, and results showed that the new concept could reduce the sum of heating and cooling demands by 29-31%.

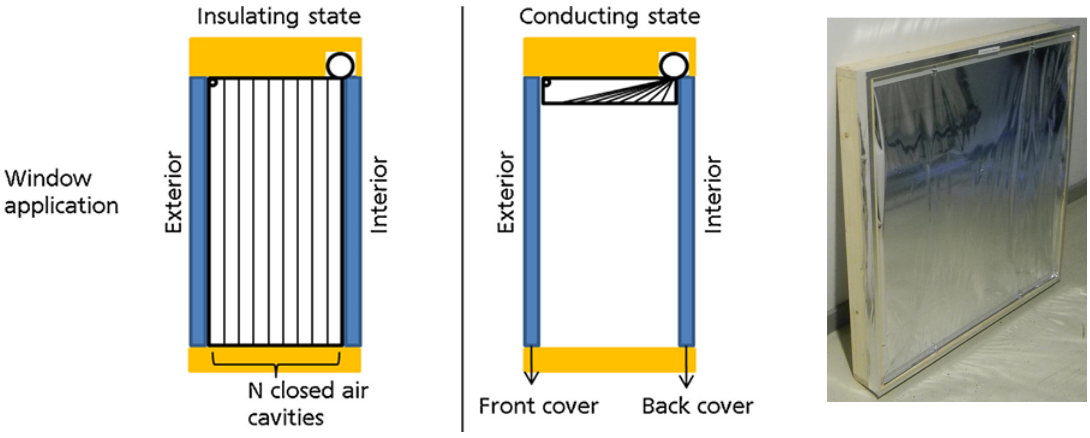

Figure 3.5 | Left: Schemaic section of the removable switchable insulation, Right: prototype with insulation rolled down (Pflug et al., 2017)

The article by Kimber et al. (2014) discusses a theoretical approach to a switchable insulation concept. The concept involves dividing a large air cavity into smaller ones separated by thin polymer membranes to achieve insulation. The conductive state is achieved by collapsing the wall, removing the air, and compressing the membranes into a single layer. The main challenge in creating this concept is switching between

the insulated and conductive states. Kimber et al. suggest using the building's HVAC system to inflate the wall for insulation and deflate it for conduction (Kimber, 2014). However, it should be noted that this concept has not yet been successfully implemented. A low U-value of 0.26 W/m2K and a high conducting value of 3.47 W/m2K could be achieved.

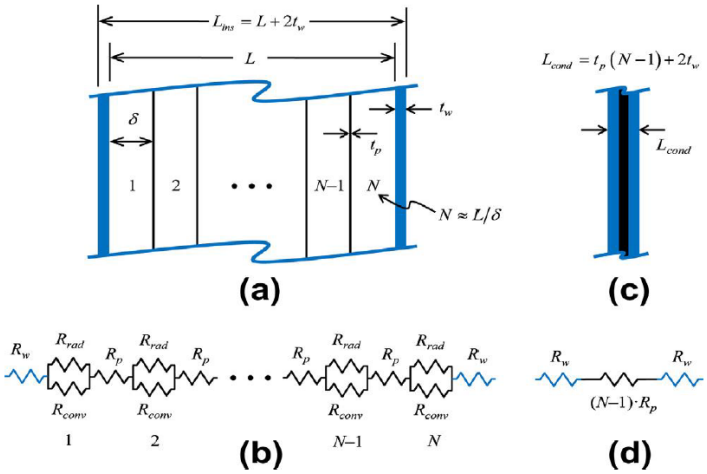

Figure 3.6 | Schematic sketch of the switchable insulation with N internal air layers: {a) extended wall (insulated) and (c) collapsed wall (conductive) configurations. The related resistance networks used by Kimber et al. for the heat flux analysis are shown in {b) and {d) for, respectively, the insulated and conductive configurations (Kimber, 2014).

A closed translucent element with switchable insulation has been developed by Pflug (2016). It is based on controlled convection inside a closed module containing one or several insulating panes. The element can be in two states: in the insulating state, the insulation panel is at the top, and in the conducting state, the insulation panel is moved to a vertical middle position. The U-value of a prototype with 30mm thick vertical air gaps and a 30mm thick insulation panel has been tested and could be switched from about 0.9 W/m2K in the insulating state to 1.7 W/m2K in the conducting state.

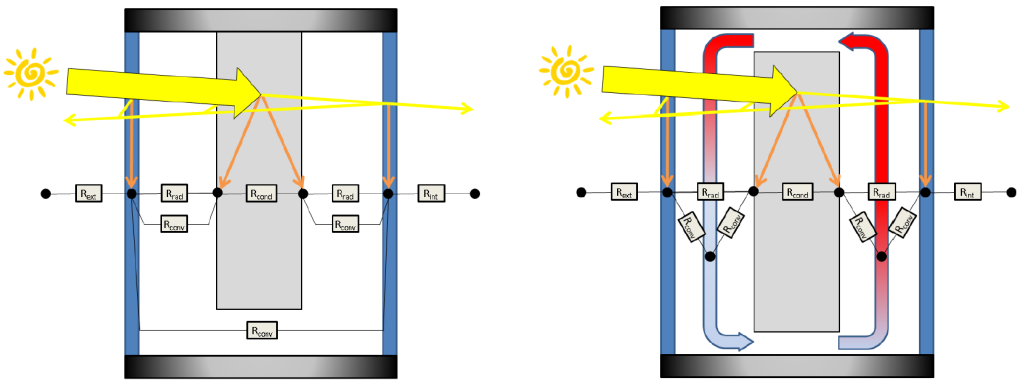

Figure 3.7 | Left: The switchable insulating panel in the insulating state and (right) in the conductive state

A switchable insulation technology by Dabbagh and Krarti (2021) evaluates the energy savings potential of optimal controls of switchable transparent insulation systems (STIS) applied to smart windows for US residential buildings. The technology works by synchronously rotating insulation baffles to any desired rotation angle, allowing for independent adjustment of the overall thermal resistance of the shade-window system. The results demonstrate that optimized controls of STISs can save up to 81.8% in daily thermal loads and reduce electrical peak demand by up to 49.8% compared to a simplified rule set. A range of U-values has not been stated in the article.

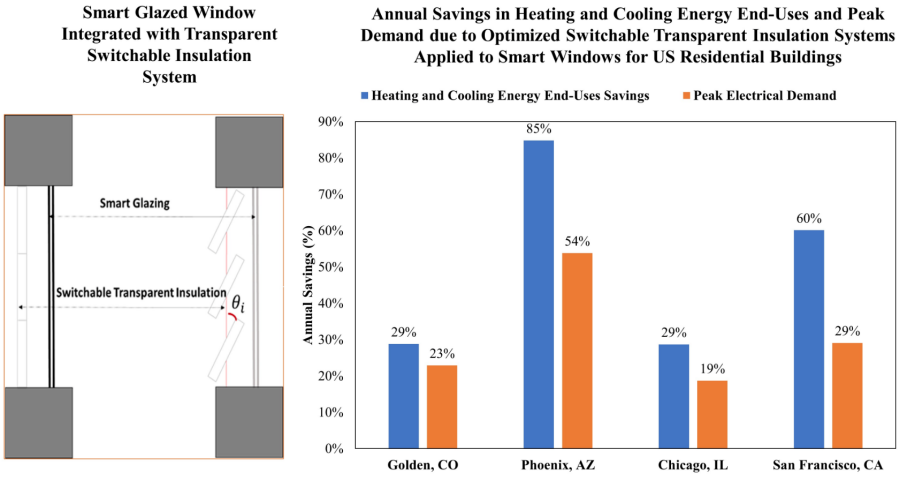

Figure 3.8 | Left: The conceptual build-up of the technology, Right: annual savings on peak demand with the switchable thermal insulation

Conclusion

Research shows that there are various approaches on switchable insulation systems. High savings in heating/cooling demand could be achieved, however, most of these concepts were merely tested as prototypes and further analyzed in energy simulation software. Also, most of the mentioned innovations are not permanently transparent, meaning their optical appearance can be similar to the ones of smart glazing. The STIS technology presented by Dabbagh and Krarti (2021) is the most similar to this thesis since it can be fully transparent, however, lots of high tech solutions are integrated. The following chapter focuses on thin glass as an innovative bendable material which could potentially be used in achieving a fully transparent glass unit with a switchable U-value.

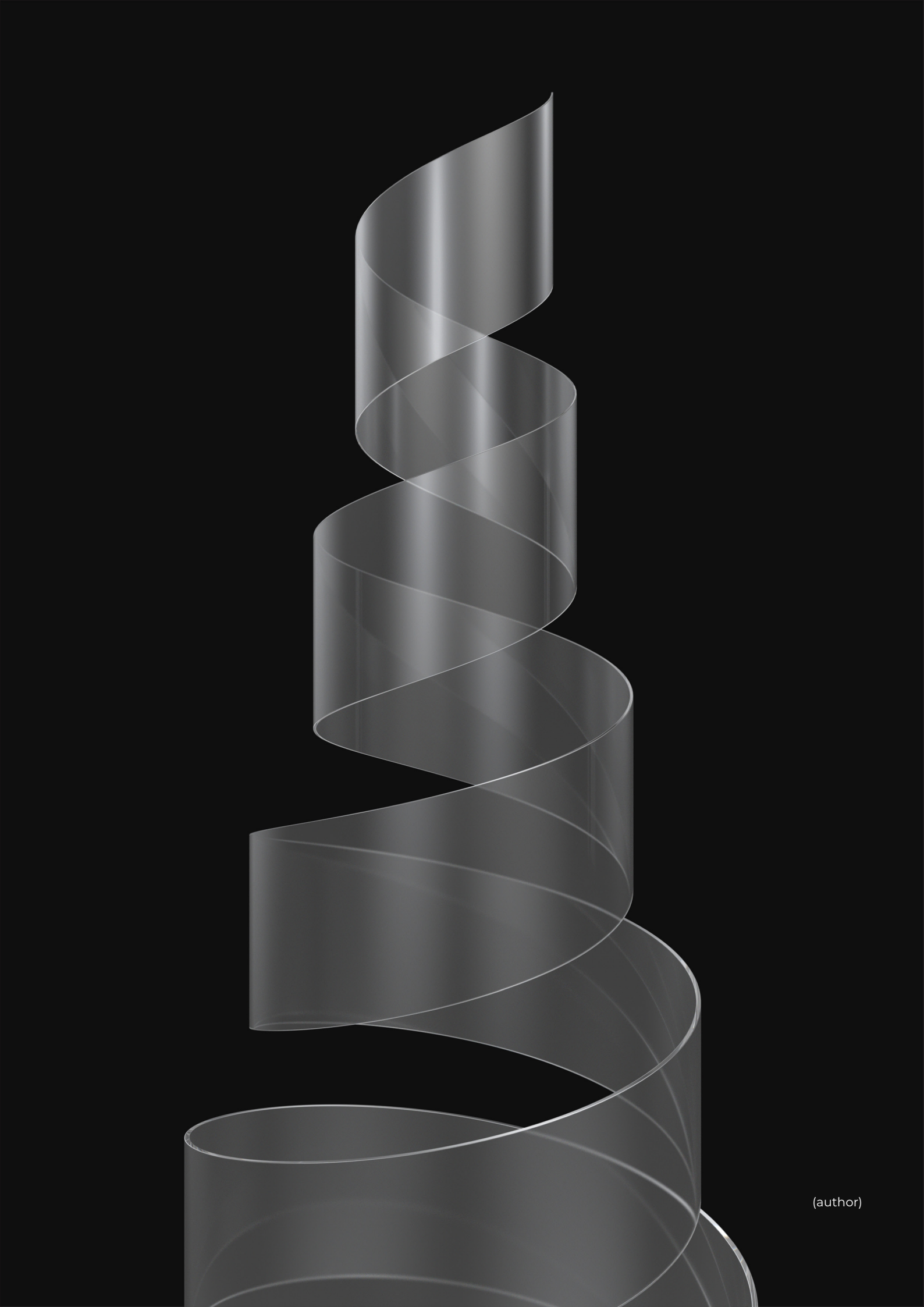

(author)

3.4 Thin Glass

The evloution of thin glass

Corning created the ultrathin and strong glass material known as Gorilla Glass through a process of experimentation and innovation. The process began in 1952 when Corning Glass Works chemist Don Stookey accidentally overheated a sample of photosensitive glass, causing it to transform into a milky white plate that was much stronger than regular glass. This material, known as Pyroceram, was the first synthetic glass-ceramic and was used in a variety of applications.

In the 1960s, Corning scientists developed a method of reinforcing glass by dousing it in a bath of hot potassium salt. They discovered that adding aluminum oxide to the glass composition before the dip would result in remarkable strength and durability. This glass, known as Chemcor, was incredibly strong but did not find widespread commercial success.

Figure 3.9 | Apple's innovation and investment with Corning fueled the creation of Ceramic Shield for the iPhone 12 (Apple, 2021)

In 2007, Apple approached Corning with a request for millions of square feet of ultrathin, ultrastrong glass for their new iPhone. Corning revisited their Chemcor technology and reformulated it to create a glass that was 1.3 mm thick and had better visual characteristics. They used a fusion draw process to manufacture the glass on a large scale. The result was Gorilla Glass, an ultrathin and ultrastrong material that has become widely used in smartphones and other devices (Corning, n.d.).

The material: glass

Glass is a rigid, amorphous material made from inorganic silicate, characterized by its isotropic properties. Its characteristics remain the same in every direction.

Glass mainly consists of natural raw materials such as silica sand, lime, and soda.

Although glass can be made from various materials as long as the melt cools quickly enough to maintain an amorphous structure without crystallizing, silica sand is most commonly used as the base material (Rammig, 2022).

Borosilicate glass is challenging to temper, both thermally and chemically, due to its lower thermal expansion and limited alkali ions. Consequently, an aluminosilicate glass mixture is used to produce thin glass. This blend comprises silica sand (SiO2), soda (Na2O), lime (CaO), magnesia (MgO), alumina (Al2O3), and boron-oxide (B2O3). The focus is specifically on alkali aluminosilicate glasses, as their high alkali content makes them better suited for ion exchange, significantly enhancing surface compressive strength. In addition, chemically tempered alkali aluminosilicate glass offers high transformation temperatures and exceptional mechanical properties such as hardness and scratch resistance (Schlösser, 2018).

Composition		
Silica sand	SiO2	62%
Soda	Na2O	1%
Lime	CaO	8%
Magnesia	MgO	7%
Alumina	Al2O3	17%
Boron-oxide	B2O3	5%

Figure 3.10 | Composition of aluminiosilicate glass (Schlösser, 2018)

Thin glass production

Thin glass production involves two main fabrication methods that result in the lightweight, strong, and scratch-resistant glass. One method for making thin glass is the down-draw or up-draw process, which involves pulling molten glass vertically through a series of rollers and dies to achieve a consistent thickness (Schott, 2023). As the glass is drawn downward or upward, it cools and solidifies, leading to a thin sheet of glass with a uniform thickness and high surface quality.

The second method for producing thin glass is the overflow-fusion process. In this process, molten glass overflows from a V-shaped container and fuses over a series of rollers, creating a continuous sheet of glass. This method allows for precise control of the glass thickness and results in an exceptionally smooth surface, reducing the need for additional polishing. The down-drawn and overflow-fusion processes have been crucial in developing thin glass technology (Corning, n.d.).

These methods enable the production of high-quality, durable glass sheets that are excellent for various applications, such as screens for electronic devices or solar panels. Furthermore, as the demand for thin glass continues to grow, more advancements in manufacturing processes are expected, leading to even thinner and stronger glass materials in the future.

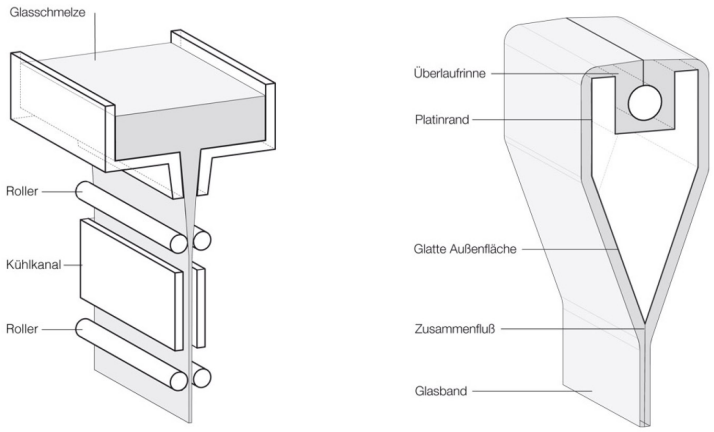

Figure 3.11 | Left: Down-draw process, Right: Overflow fusion process (Albus & Robanus, 2014)

Glass tempering

According to Schlösser (2018) glass strengthening involves various methods to increase its resistance to breakage. The four primary categories of strengthened glass, in increasing order of strength, are annealed glass (also known as float glass), heat-strengthened glass (semi-tempered or partly toughened), fully tempered glass, and chemically tempered glass. Each method leads to pre-stressing the glass.

Annealed glass behaves uniformly and flexibly until it suddenly breaks. Breakage depends on the existence of flaws, stress levels, and the duration of the applied load. Since glass doesn't plastically deform, it experiences brittle failure.

Thermal tempering involves heating annealed glass to about 620-675°C, rendering the glass pliable. Afterward, the glass is quickly cooled using cold air jets, producing compressive residual stresses on the surface and tension inside. Both heat-strengthened and fully tempered glass undergo this process, with the only difference being the slower cooling rate for heat-strengthened glass.

Chemical tempering submerges annealed glass in a molten alkali salt bath at approximately 500°C. During this process, alkali ions near the glass surface are replaced with ions from the molten salt, leading to compressive stresses on the surface. Chemical tempering results in higher surface compression and increased strengthening compared to thermal tempering. Benefits of this method include

negligible optical distortion, the capability to reinforce ultra-thin and irregularly-shaped plates, and the option to cut, grind, or drill the glass after the process. However, drawbacks consist of vulnerability to flaws, high expenses, size limitations due to prolonged bath immersion, and restrictions for alkali-containing glass (Schlösser, 2018).

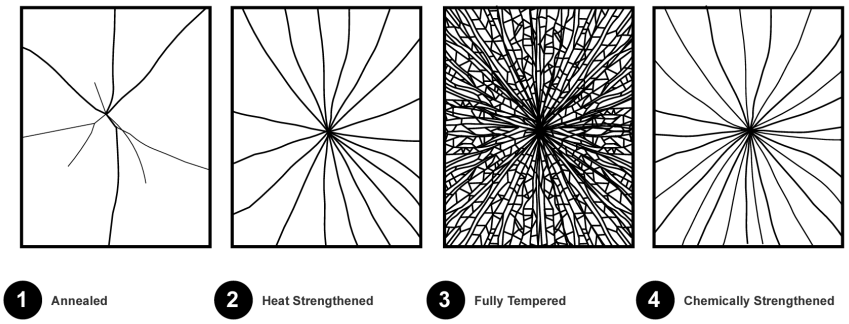

Figure 3.12 | Glass breakage patterns with different degrees of strengthening (Rammig, 2022)

The tensile strength of tempered glass varies significantly depending on the method employed, allowing it to serve specific requirements in a multitude of applications according to Rammig (2022). These individual values and benefits are the following:

Annealed glass, with a tensile strength of 45 MPa, is the least robust but provides a cost-effective solution for less demanding uses.

Heat-strengthened glass, exhibiting tensile strength between 50 and 80 MPa, offers enhanced durability and resilience over annealed glass, making it suitable for instances where additional support is necessary.

Fully tempered glass boasts a tensile strength of 150 MPa, providing substantial structural integrity and impact resistance, making it ideal for high-stress environments such as doors and building facades.

Chemically tempered glass surpasses all other types with an impressive tensile strength of 700 MPa or more, offering unparalleled durability and protection.

There are also several benefits of thermal tempering compared to chemical tempering. Thermally tempered glass usually possesses a stronger tension layer, causing the broken glass to disintegrate into tiny pieces. Although these fragments may cause injury, they pose a significantly lower risk than the larger shards resulting from fractured chemically tempered glass (Brandon, 2020).

Polyvinyl butyral (PVB) interlayers have become a crucial component in enhancing the safety and performance of architectural glass applications. By laminating PVB between two or more glass panels, it creates a strong bond that significantly

improves the structural integrity of the glass. In the event of impact or breakage, PVB prevents the glass from shattering into dangerous fragments, instead retaining the broken pieces within the laminate structure. This greatly reduces the risk of injury and property damage. Furthermore, PVB interlayers offer additional benefits, such as noise reduction and enhanced UV protection, making them an invaluable asset in modern architectural glass design (Saflex, 2023).

Edge treatment

The failure strength of glass is largely influenced by the imperfections in its surface, making edge quality crucial (Feldmann et al, 2014). Figure 3.13 demonstrates common glass edge treatment steps (cut edge not inlcuded):

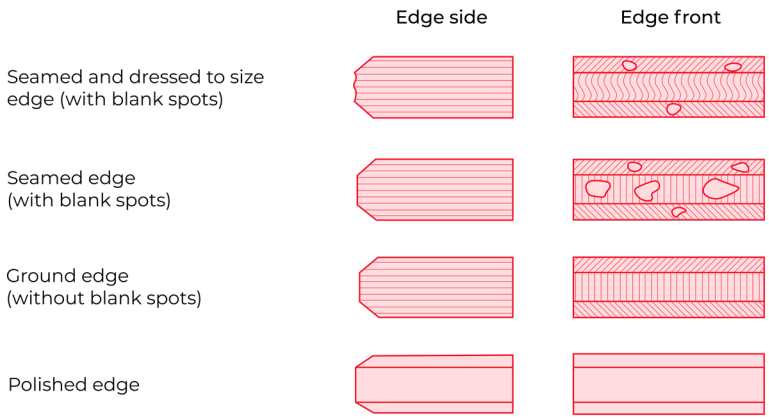

Figure 3.13 | Glass edge treatment according to Feldmann et al, 2014, changed by author

Next to the cut edge which is a rough edge from the factory cut there are four main processes of treating a glass edge (Rammig, 2022):

1. Seamed edge: The top and bottom edges are ground in this treatment to minimize injury risk, but the face retains the broken edge.

2. Ground edge: Often specified for curtain wall applications with four-side support, this edge is arrised and ground smooth, eliminating any visible blank spots.

3. Polished edge: Structural glass applications typically require polished edges, where both the arris and the edge are polished for full transparency.

4. Adequate edge treatment not only enhances edge strength but also reduces the likelihood of thermal shock fractures during the tempering process .

Conclusion

Thin glass, an innovative material, has yet to achieve widespread use in architectural applications. However, valuable research is currently being conducted in the facade segment, exploring concepts for integrating the bending and lightweight properties of thin glass into building envelopes. This material has not yet been explored for use in switchable insulation systems.

As the concept of switchable insulation technology relies on opening and closing a cavity, thin glass may be the ideal material due to its bendability. The tensile strength and edge treatment are likely to play critical roles in this project, as high stresses are anticipated. It is essential to use high-quality glass without imperfections when inflating it, as microcracks are the primary cause of larger cracks or shattering.

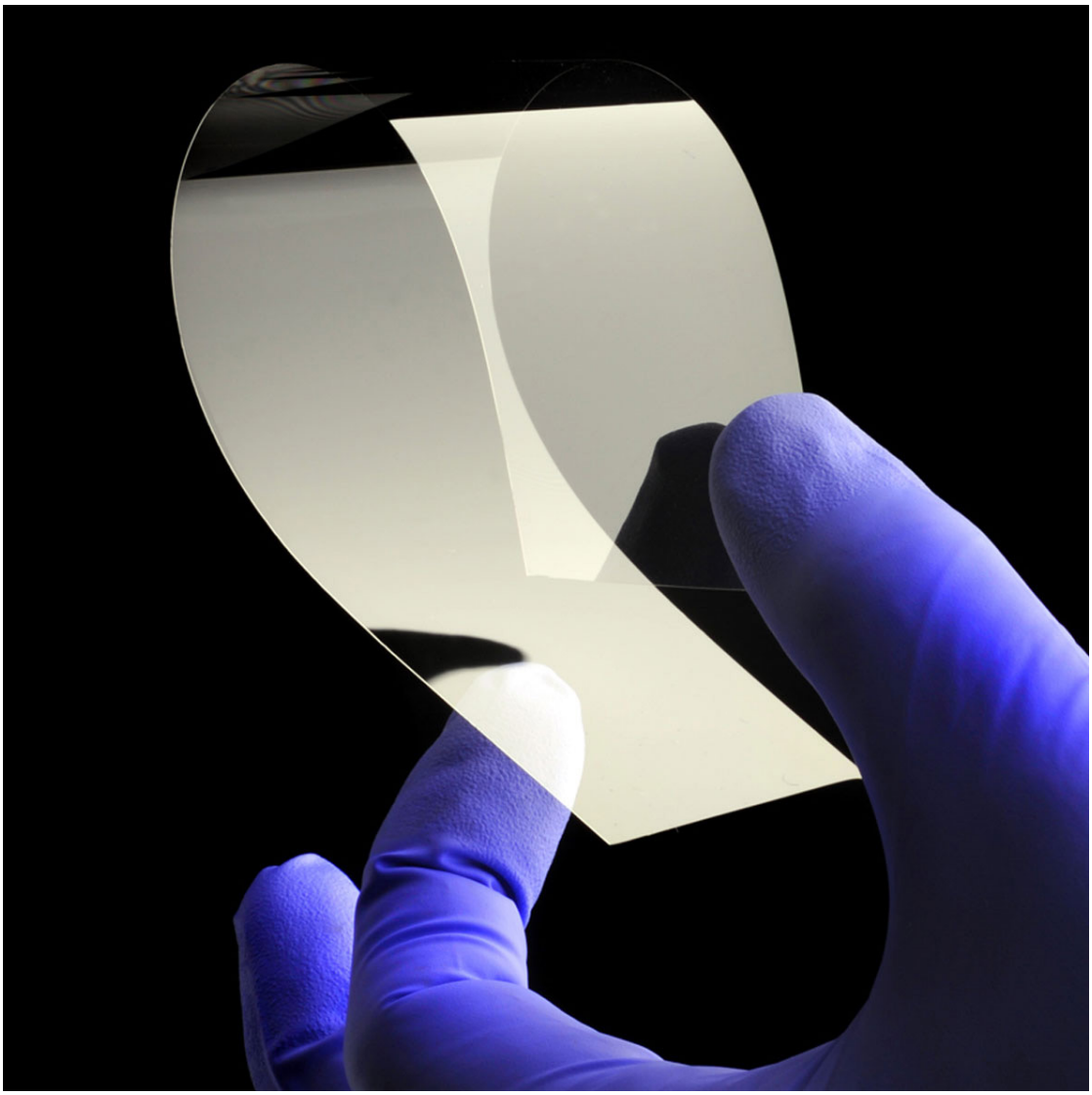

Figure 3.14 | Ultra-thin willow glass developed by Corning (Corning, 2016)

(arquitecturaviva, 2021)

4. Conceptual design

4.1 Overheating Issues of Buildings

Buildings are increasingly experiencing overheating due to a combination of factors, including climate change, urban heat island effect, and inadequate design choices. According to the Intergovernmental Panel on Climate Change, global temperatures have risen by approximately 1.2°C since the preindustrial era, resulting in more frequent and intense heatwaves (IPCC, 2021). This exacerbates the urban heat island effect, a phenomenon where cities experience higher temperatures than their surrounding rural areas due to the concentration of buildings and infrastructure and the reduction of vegetation (US EPA, 2023).

Moreover, poor design choices, such as the amount of insulation, the use of heat-absorbing materials, and a lack of natural ventilation, contribute to the overheating issue. Research by Mavrogianni et al. (2012) shows that many modern buildings, particularly those with extensive glass facades, trap heat inside and struggle to dissipate it effectively.

The study also highlighted the role of energy-efficient measures, such as improved insulation and airtightness, which results in trapping heat within buildings (Mavrogianni et al., 2012). To mitigate this issue, architects and urban planners must prioritize sustainable design practices that consider rising global temperatures and the need for buildings to remain thermally comfortable for their occupants.

A paper by Dodoo et al. (2014) studied the impact of future climate change scenarios on residential buildings in Växjö, Sweden, on both conventional and passive houses. The study found that the risk of overheating increases under climate change scenarios, with passive buildings more vulnerable. The analysis showed a reduction in space heating demand and an increase in cooling demand. The results underscore the need to consider potential overheating risks and implement measures to prevent them.

Evidence suggests that Passivhaus and super-insulated dwellings in the UK, Ireland, and Northern Europe are at risk of overheating due to the rapid transition to zero-carbon buildings (R. R. McLeod et al., 2013). By 2050, average internal temperatures in such dwellings in London could exceed 25°C for 5-10% of the year. Overheating risks can be reduced by optimizing whole-life design, but active cooling systems may become necessary within 30-40 years (R. R. McLeod et al., 2013).

4.2 Factors Contributing to Overheating of Buildings

External factors

- Climate change: Increasing global temperatures, hotter summers, and frequent heatwaves
- Urban heat island effect: Heat-absorbing materials in densely populated areas increase local temperatures.
- Poor building design:
- Inadequate insulation
- Improper orientation
- Lack of shading elements
- Building materials and construction methods that do not match the thermal requirements

Internal factors

- Inefficient cooling systems:
- Insufficient cooling capacity during heat waves
- Poor maintenance and improper sizing
- Inadequate ventilation:
- Poor heat dissipation within buildings
- Importance of proper ventilation in energy-efficient buildings with high airtightness.
- High internal heat gains from:
- IT equipment, lighting, occupants and appliances
- Occupant behavior: excessive use of appliances or high occupancy levels

4.3 Working principle of Inflatable Glazing

As previously highlighted, the issue of overheating is generally connected to variable factors such as construction type, shading, ventilation, and occupancy. The building skin of well-insulated buildings can be considered quite impermeable. Due to high insulation, heat transfer through the construction, whether it is an exterior wall or high-performance glazing, is notably slow.

Conversely, buildings in warmer climates are designed differently. Single glazing is common since insulation is not needed for most of the year. Internal gains are a concern, and heat ejection is vital to maintain a comfortable internal environment. However, even in warm climate zones, winter can be cold enough to require heating. This heating demand is significant for fully glazed buildings, mainly as heating costs are much higher than cooling costs. The primary objective of Inflatable Glazing is to change its insulation properties. If the system could alter its insulation value from that of high-performance triple glazing to the properties of single glazing, one could make the building envelope more or less permeable for heat transfer. This way, the heat flux could be sped up or slowed down to maintain a comfortable internal temperature.

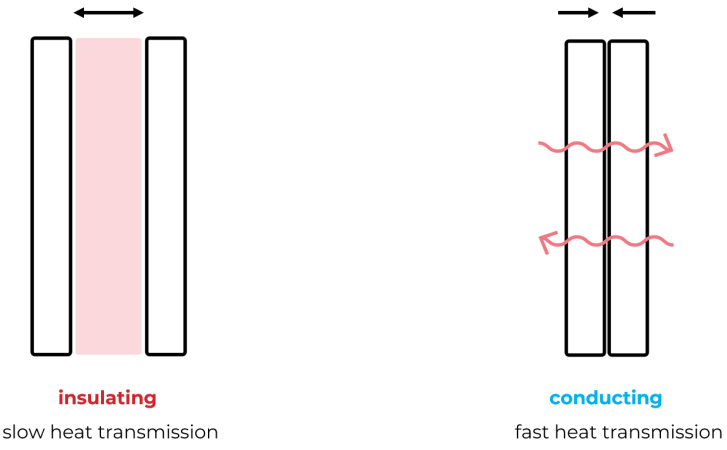

Figure 4.0 | The concept of dynamic insulation - opening an closing a cavity (Author).

Penguins possess an excellent dynamic insulation system that illustrates nature's remarkable adaptation strategies. Penguins fluff up their feathers in freezing temperatures, which traps pockets of air within their plumage. This process creates an insulating air cavity that effectively conserves their body heat, shielding them against the harsh cold. The trapped air layer acts as a thermal buffer, minimizing heat loss and keeping the penguins warm during the frigid periods. However, when temperatures rise, they need to prevent overheating. Penguins adjust their feather layer to regulate their internal temperature, effectively opening it. This action

exposes their skin to the external environment, enabling the dissipation of excess body heat into the cooler outside air. Furthermore, the fluffing up of the feathers happens in the blink of an eye, making it highly adjustable to quickly changing conditions.

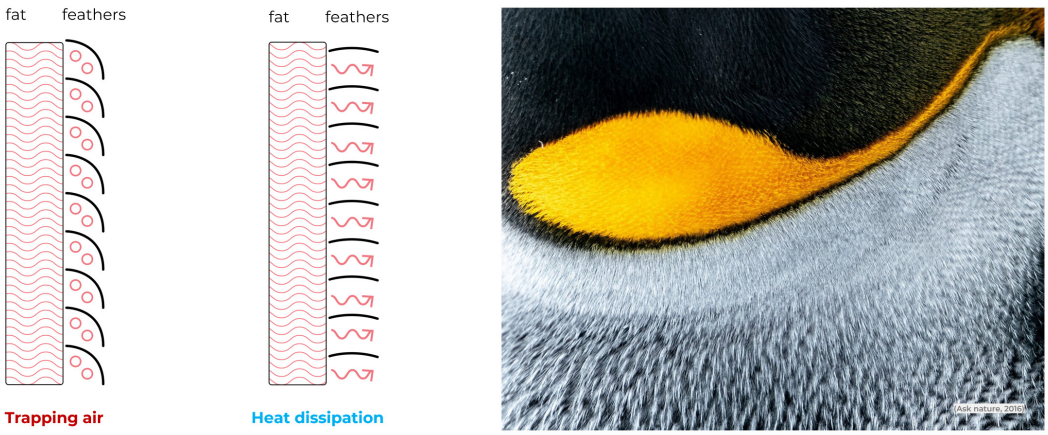

Figure 4.1 | Warm blooded penguin skin thermal insulation principle (Author), (Ask Nature, 2016).

The concept of Inflatable Glazing aims to achieve the same rapid response time as birds' feathers by using an air pressure system that can inflate or deflate the glass unit within a fraction of a second. This allows for quick adaptation to changing external conditions anticipated by sensors or meteorological data. By stabilizing the internal temperature with Inflatable Glazing, the demand on the HVAC system is reduced, resulting in lower energy consumption. The primary goal is to improve thermal comfort and decrease energy demand in buildings. Inflatable Glazing can perform well in several scenarios, although it is not limited to these. Overall, it should be able to collect, store, and eject heat on demand:

1. Nocturnal cooling/heating:
During the night, insulation can be reduced to dissipate heat from the building, taking advantage of cooler outdoor temperatures. Alternatively, heat can be stored by increasing insulation.

2. Rapid temperature changes:
Inflatable Glazing can adapt to rapid and unexpected temperature or weather changes depending on the climate zone, season, or day. For instance, it can accommodate temperature fluctuations on partly cloudy days or during cold spells.

3. Seasonal changes:
Seasonal adjustments are crucial, as the technology alters insulation values based on colder or warmer seasons. For example, insulation may be mostly high during winter months.

4. Internal loads:

Internal loads are becoming increasingly critical due to technological advancements. Smarter buildings generate more heat due to the amount of equipment they contain. Additionally, peak loads from occupants can be problematic. By lowering insulation, these heat loads can be more easily expelled, consequently reducing the energy demand on the HVAC system.

Figure 4.2 | Useful scenarios of Inflatable Glazing (Author).

5. Design Development

5.1 Design criteria

Design criteria are the fundamental requirements, objectives, and considerations that guide the development of a product. The following criteria were developed according to industry standards and state-of-the-art manufacturing processes to achieve a successful and functional design. They help streamline the design process, ensuring the end result meets the desired expectations and performance levels. By outlining key aspects such as functionality, durability, or aesthetics, design criteria serve as a blueprint for designers and engineers to follow throughout the project, reducing the likelihood of overlooking critical elements and ultimately leading to a more efficient and effective design outcome.

The design criteria are the following:

- Achieve full transparency for unobstructed views in all insulation states. Although reflections might occur, maintaining full transparency would enhance the aesthetic quality and visual comfort, setting the product apart from other smart glazing technologies.

- Adjust the U-value from single glazing properties to triple glazing properties to cover the full range of typical U-values. This way, all climatic scenarios could be addressed, and there would be no advantage to using a static system. These values generally range from around 0.7 W/m^2K to 5.6 W/m^2K.

- Ensure compatibility with current manufacturing processes, allowing for the production on a typical IGU production line with minimal alterations to the machines. Spacers and sealants currently available in the market should be used for manufacturing the unit.

- Maintain uniform curvature of the inflated glass to enable a consistent and controlled U-value change. This uniformity is also important for enhancing visual quality and having control over the unit's behavior.

- Prioritize safety to protect both occupants and individuals surrounding buildings with Inflatable Glazing installed.

- Ensure compatibility with standard facade frame profiles so that the glass unit can be used in both new and renovated buildings. Additionally, the ease of glass replacement should be considered.

5.2 Design evolution

The base design began with a 2D sketch seen in figure 5.1 that explored the potential functionality of the product. The sketch included ideas that remain applicable in the final design. The primary question was whether thin glass could be double-curved with a typical IGU seal around the pane's perimeter. In addition, there was speculation about the most suitable shape, whether rectangular, square, or round. Another question was about the number of achievable cavities and the integration of spacers. The initial design featured an inflation and deflation system that maintained a curvature in both the insulating and non-insulating state with a convex or concave shape, respectively. However, the initial drawing also suggested a fully relaxed (deflated) option, where the materials are flat and in direct contact. Since thin glass is not inherently stiff, incorporating a structural core pane in the middle appeared to be a good starting point.

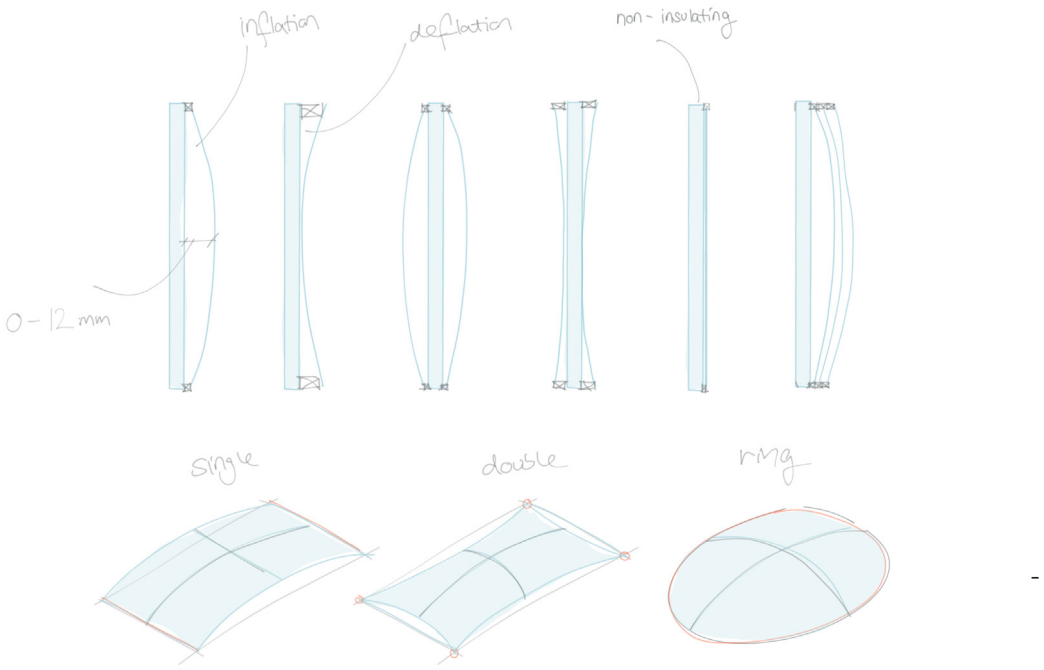

Figure 5.1 | Initial design exploration of possible configurations (author)

It was quickly determined that using triple glazing, with thin glass on both sides of the core pane, would maximize the product's potential. The core pane serves as both a structural component and a separating layer to create two cavities. Since the core pane is protected by the durable and scratch-resistant thin glass panes, there was an opportunity to use PMMA as the core material. In contrast to glass, PMMA has higher transparency and is much lighter. As it is protected from both sides, there are also no concerns about scratches. The choice of PMMA opened up even

more possibilities, leading to the next design phase.
The inflation and deflation process involving convex and concave shapes seemed overly complex (Figure 5.2) and would not provide any advantages over having a relaxed state (with flat material in direct contact) and an inflated state. Consequently, an edge design needed to be developed that would allow the thin glass pane to lie flat on the PMMA pane while still maintaining an airtight seal (Figure 5.3).

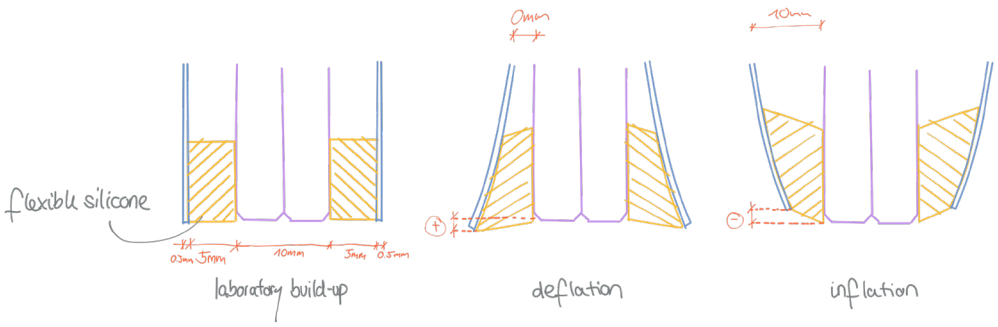

Figure 5.2 | Early sketch - inflation and deflation with deformation of sealants - Glass core pane (author)

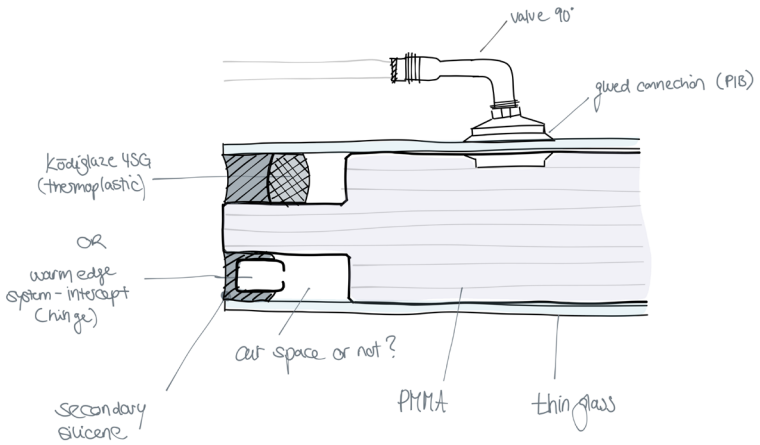

Figure 5.3 | Early sketch - updated edge design with groove in the PMMA pane & spacers - PMMA core pane (author)

The updated edge design features a groove around the perimeter of the PMMA pane, which can be sawn or milled. Implementing this groove in a glass pane would be challenging, as it would necessitate stacking multiple glass panes or using a custom mold. Figure 5.3 also illustrates two distinct spacer systems. The bottom “warm edge system intercept,” has a C-shape and was initially considered due to its resemblance to a hinge. It was thought that the pane could lift the spacer, making this a feasible option. The second option involved using a thermoplastic spacer, known for its excellent flexibility and adhesion to glass. However, the inflation system had not been fully considered, given that the valve connection would need to pass through the glass, which would be less than ideal.

The base design with milled edges appeared promising, and an initial construction drawing was developed (Figure 5.4), which did not include the inflation system. This construction drawing was used to establish contact with the chemical company Kömmerling/HB Fuller to seek their expertise in warm edge spacer design.

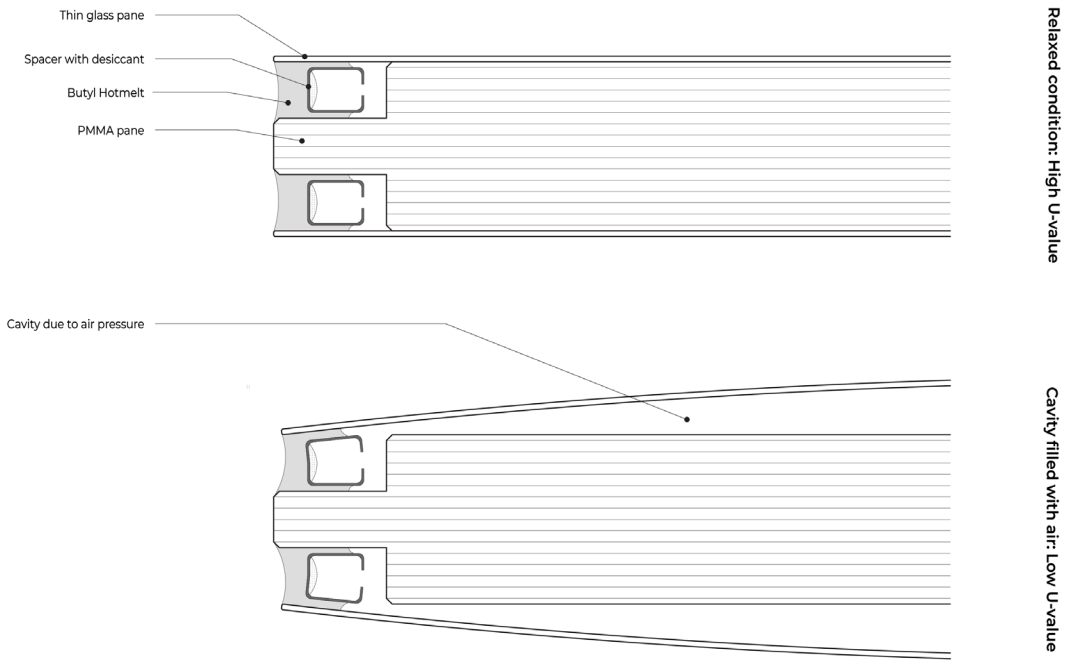

Figure 5.4 | First construction drawing - featuring the milled PMMA edge with a warm edge system intercept (author)

The selection of the right spacer system was crucial, as it would determine the durability and flexibility of the unit's edge bond. Kömmerling recommended using a thermoplastic spacer, as they provide the best bonding to glass and offer the highest flexibility. They also expressed concerns about the permeability of gas through the PMMA. This was not a significant concern during the prototyping phase since the gas content could be adjusted through the gas supply. However, the PMMA has a higher coefficient of thermal expansion than glass. This could certainly cause problems in real-world applications with significant temperature fluctuations.

Another suggestion was to use a full glass design, as the thermoplastic spacer would form a chemical bond with the glass, offering the best durability. Kömmerling's product, Ködispace 4SG, is therefore an optimal choice for glazing that needs to accommodate high movements. This is typically a phenomenon experienced by IGUs with high expansions due to pressure differences caused by thermal fluctuations.

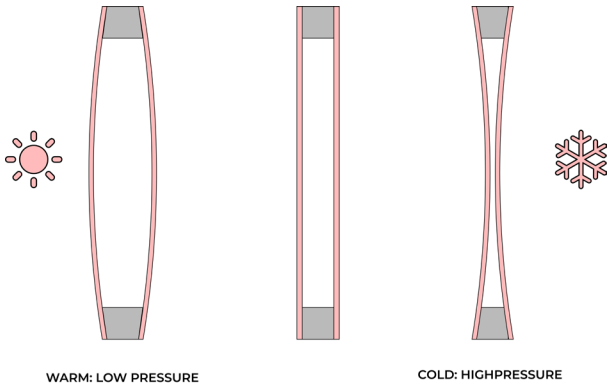

Figure 5.5 | Expansion and contraction of an IGU due to thermal fluctuations (author)

From Kömmerling's comments, it became clear that a full glass design would be more beneficial than incorporating a PMMA core. However, for ease of assembly, lightweight construction, and proof of concept, the PMMA core still seemed like the right choice for a prototype. Later in the thermal calculations, we will also learn that a glass core performs better than the PMMA core. Ultimately, the decision was made, and the primary spacer for Inflatable Glazing was designed using the 4SG spacer from Kömmerling. As a secondary sealant, Ködiglaze S, a 2-component silicone was proposed due to its high durability and excellent adhesion.

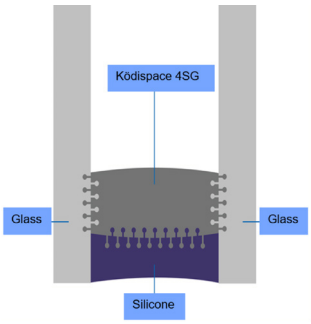

Figure 5.6 | Ködispace 4SG Insulating Glass Warm Edge Spacer (Kömmerling, n.d.)

The next question concerned how gas could be supplied to the cavities. Three main ideas were discussed:

1. The infill would pass through the thin glass and be directly injected into the cavity. This had the advantage of achieving a relatively thin unit since the core pane could be merely structural, and the edge seals of the pane could be as small as possible. The connection would be glued, similar to how bicycle valves are "welded" on the rubber tube of a bicycle tire. However, this option seemed ambitious and would also require a laser-cut hole before the tempering of the glass. Additionally, the aesthetic quality would decrease with this option. Therefore, it was not considered viable.

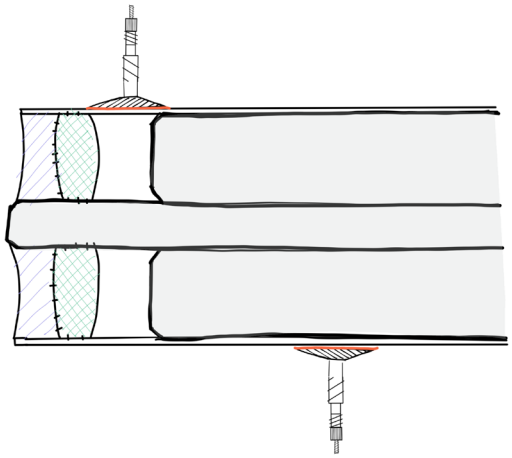

Figure 5.7 | Option 1 - Gas infill through the glass (author)

2. The second option involved having one valve penetrating through each edge bond of the glass unit (see Figure 5.8). This would provide high control over the unit, as each cavity could be inflated individually and valves could be protected inside the frame. Here, the core pane could be as thin as structurally possible. The concept of drilling through a spacer is done, for example, when performing manual gas infills or using valves for pressure equalization when shipping at higher altitudes. However, it had a flaw that would require two very small valves in diameter to keep the edge bond as small as possible. It was determined that prototyping only allows for generic bicycle or car valves ranging from 6-8mm in diameter. This would mean that the unit's thickness would be significantly higher than anticipated. Therefore, this option was not considered for the prototype.

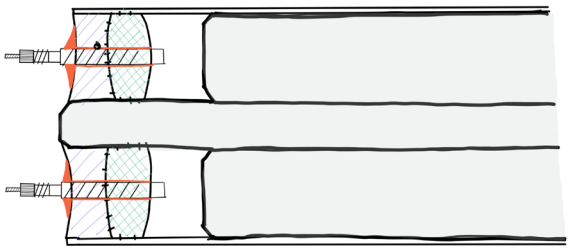

Figure 5.8 | Option 2 - Gas infill through the edge seal (author)

3. The final and most suitable option was found to be a locally drilled air channel through the edge of the PMMA pane. With this approach, the gas supply could be reduced to having only one valve controlling the inflation of both cavities simultaneously. The T-channel could be easily drilled with a common electric drill and would reduce the overall thickness of the unit. Moreover, with this design, it was still possible to use two valves at different locations if the gas supply were to work in

both directions, namely supply and suction. Finally, the appropriate valve had to be selected to complete the unit's edge design.

Figure 5.9 | Comparison of different valve types. From left to right: Sclaverand, Dunlop and Schrader valve (Luplow, 2021)

There are generally three types of common valves for tires on the market. The Schrader valve, also known as the car valve, is optimal for compressor filling but has a large diameter of 7.5mm. The Dunlop valve is prevalent in the Netherlands; however, it offers the same diameter as the Schrader valve and a lower pressure capacity. Lastly, the Sclaverand valve provides a small diameter of 6mm, a high pressure capacity, slow exfiltration, and compressor compatibility.

The Sclaverand valve was consequently added to the final prototype design and integrated with a silicone seal around it to prevent gas leakage and ensure a tight bond. The final edge design can be seen in Figure 5.10.

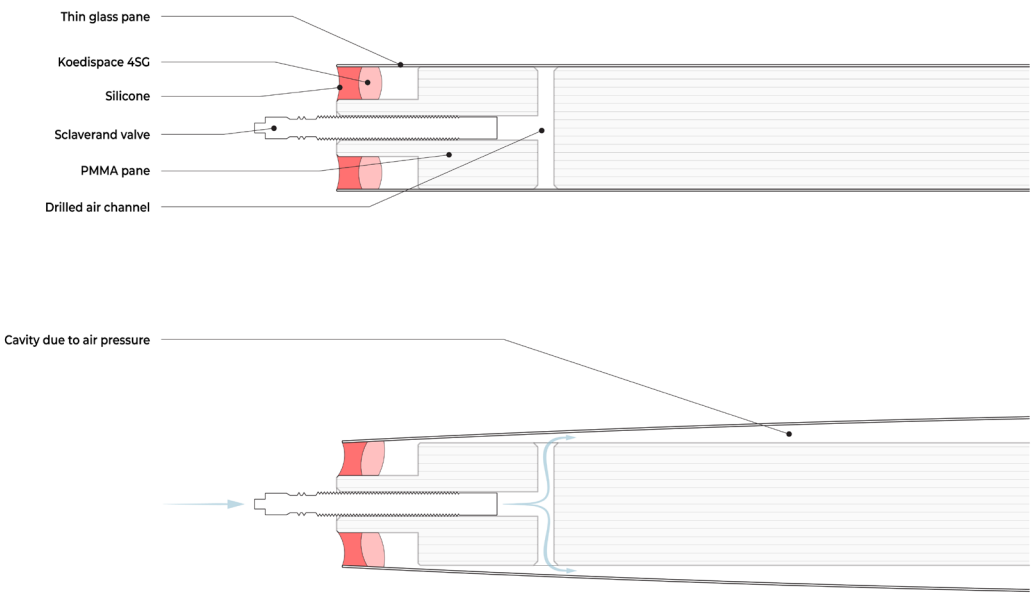

Figure 5.10 | Option 3 - final option with gas infill through PMMA edge (author)

5.3 Manufacturing

The manufacturing of the unit should ideally be carried out in an automated glass assembly facility to reduce labor, enhance quality, and ensure a long service life. The 4SG Ködispace spacer can be applied using a CNC automated dispenser, which presses the thermoplastic material uniformly onto the glass with high precision. The reactive spacer then chemically bonds with the glass, ensuring excellent durability. This spacer type also ensures lower psi-values, which are associated with reduced thermal transmission. Moreover, this spacer offers an attractive visual quality due to its completely black appearance, unlike conventional aluminum spacer systems.

The following step-by-step list outlines the ideal production process for Inflatable Glazing. The glass assembly is ideally done on a automated high tech line as similar to figure 5.11. Due to a limited timeframe, this process could not be precisely achieved; however, Chapter 9 will discuss the actual assembly of the prototype in greater detail.

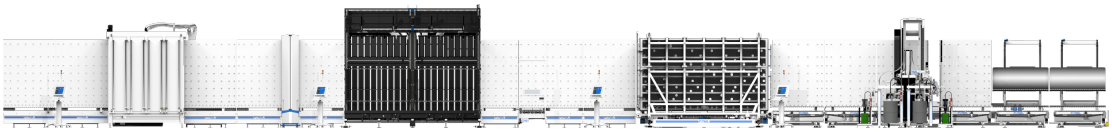

Figure 5.11 | High Tech Line for Insulated Glass assembly (Forel, 2023)

Step 1: Mill the PMMA pane around the perimeter with a CNC machine from both sides and drill the T-channel. The CNC bevels the upper and lower corners of the PMMA pane to avoid contact with the later-applied thermoplastic spacer. Afterward, all holes, sharp edges, and corners of the PMMA pane should be chamfered.

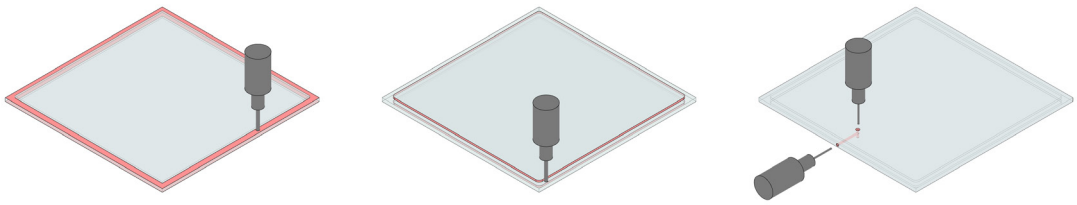

Figure 5.12 | CNC milling of the PMMA pane - 1. Milling the groove, 2. Filleting the corners, 3. Drilling the T-channel (author)

Step 2: Place the factory-laminated thin glass pane on the automated IGU assembly machine. Enter the measurements into the control system. Once the pane reaches the CNC applicator, the thermoplastic spacer will be applied in one round. The spacer bead does not have sharp corners after the application, which is why it is necessary to bevel the corners in step 1.

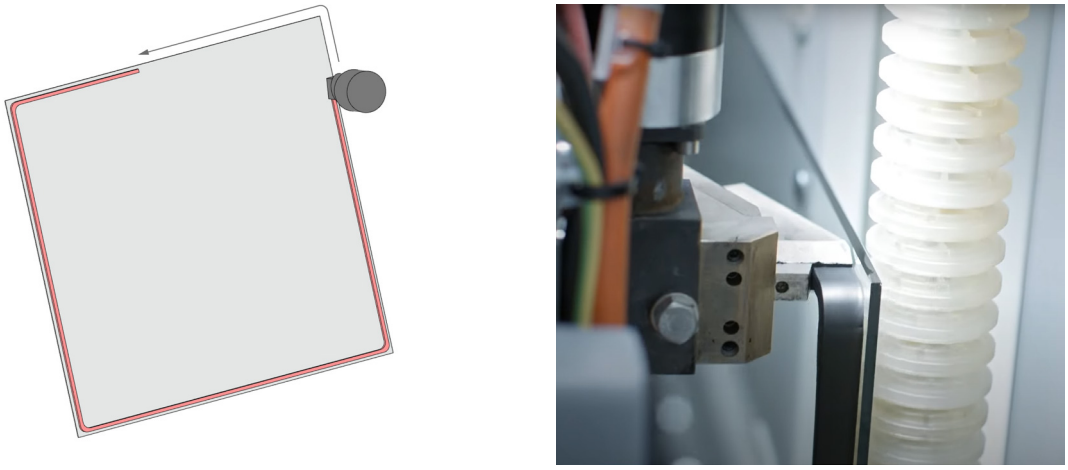

Figure 5.13 | Left: CNC applicator of 4SG spacer (author) - Right: snapshot of production video from Forel (2023)

Step 3: In the flat coupling press, which can also be used for gas filling, the machine presses the PMMA pane onto the thin glass pane. Rear panel suction cups will ensure a straight and accurate placement of the thin glass pane. This is essential since the thin glass is likely to bend without additional support.

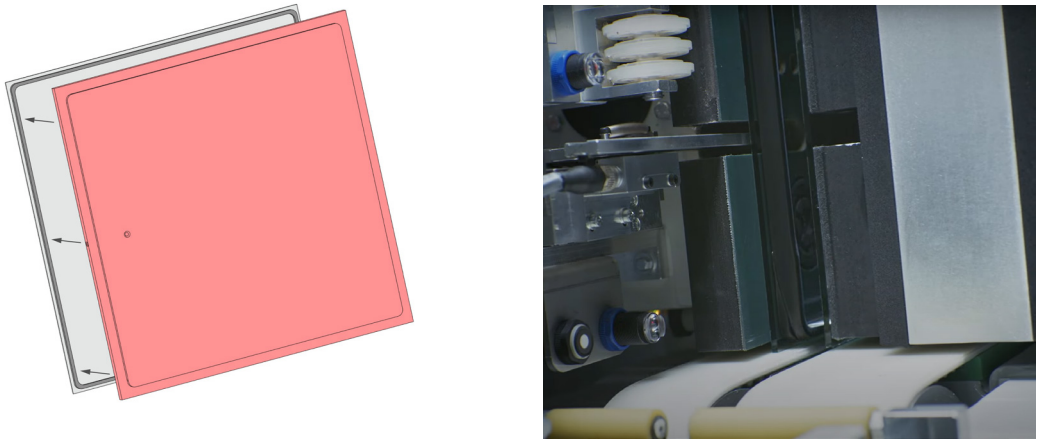

Figure 5.14 | Left: Coupling of PMMA pane and thin glass (author) - Right: snapshot of production video from Forel (2023)

Step 4: The prototype is being removed from the production line with a glass unloader and placed at the start again, where it will move directly into the coupling press again, now turned by 180 degrees. The second thin glass pane also enters the production line, and the 4SG spacer will be applied identically to step 2. In the coupling press, the half-finished and reversed unit will now be pressed onto the second thin glass pane.

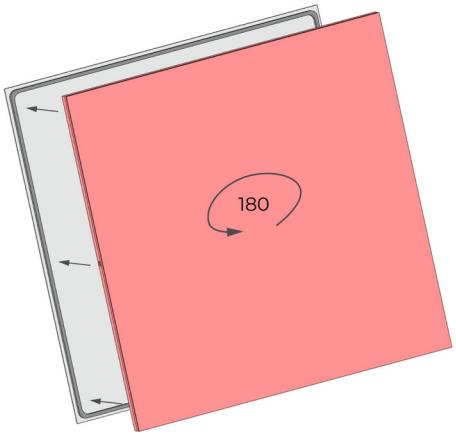

Figure 5.15 | Left: Coupling of bonded panes with second thin glass pane (author)

Step 5: The unit is now fully connected and only missing the structural bond. A sealing robot will automatically apply the secondary sealant around the unit with a seamless finish. The sealant is a 2-component silicone that will cure quickly and provide almost immediate adhesion.

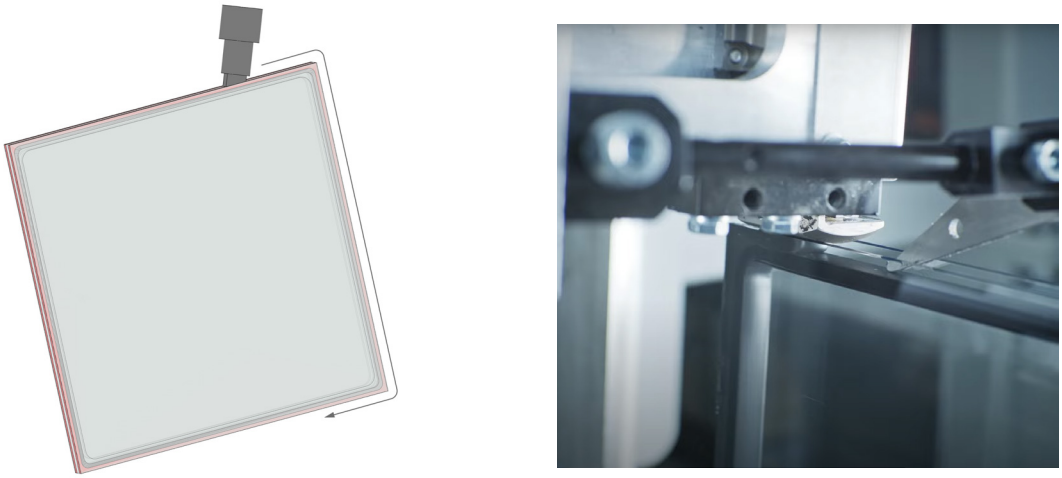

Figure 5.16 | Left: Secondary sealant application (author) - Right: snapshot of production video from Forel (2023)

Step 6: The unit is being removed from the production line again with the glass unloader. The suction cups will securely handle the unit and place it on adaptive supports on the glass unit rack. Consequently, the production of the unit is complete.

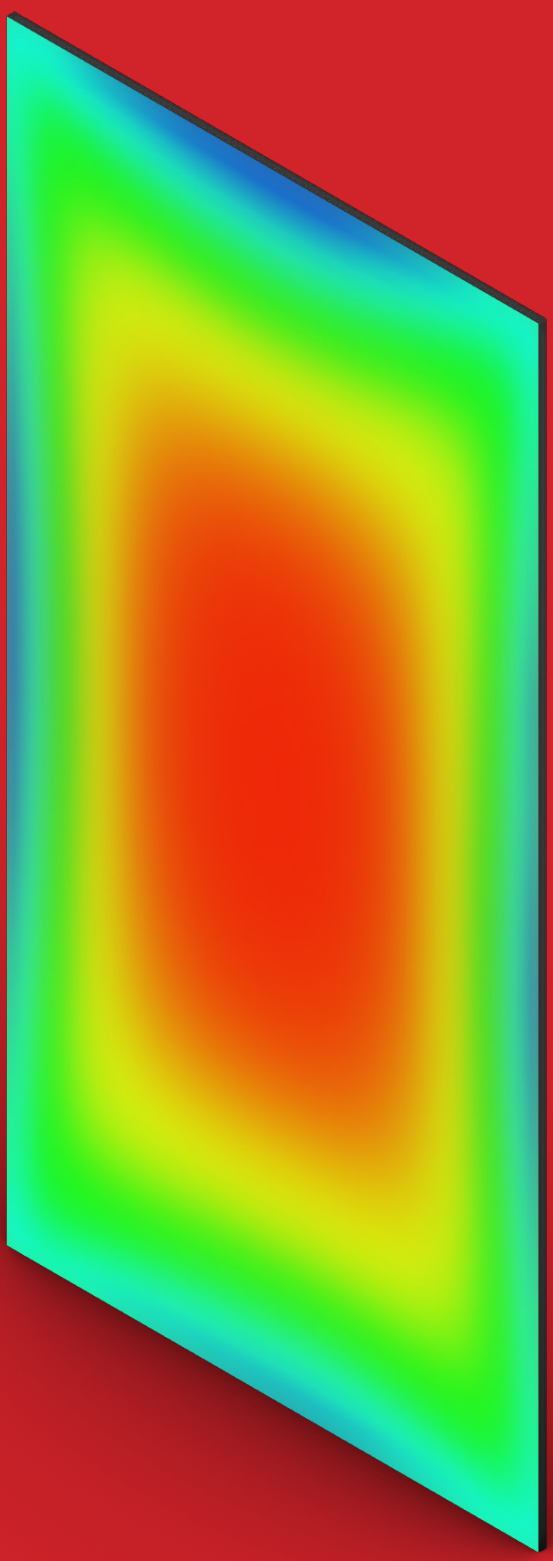

6. Thermal performance

6.1 U-value According to EN-673

As highlited in chapter 3.2 the calculation of opaque construction components is different to glazing. This European Standard outlines a calculation method for determining the thermal transmittance of flat and parallel glazing surfaces, applicable to uncoated glass, coated glass, and materials not transparent in far infrared. It is suitable for multiple glazing but not for those with far infrared transparent sheets or foils. The procedure determines the central area U-value, excluding edge effects, solar radiation, and Georgian bars. Used for product comparison and predicting heat loss, heat gains, condensation, and solar factor effects, it serves as a reference for calculating overall U-values in windows, doors, and shutters (European Commitee for Standardization, 2011).

The following chapter addresses the calculation method of the U-value for glazing and the translation of this method into a computational workflow. Since the calculation method only considers flat glass panes, some adjustments are required. The norm only accounts for a single U-value, defined as the center pane value. The glass surface of the inflated glazing will be non-uniformly shaped. Ultimately, the surface must be evaluated, and a U-value assigned at virtually every point of the pane. The final output will include the average, minimum, and maximum U-values, as well as the change in U-value from fully inflated to completely deflated, signifying total conduction.

6.2 Calculation Method

U-value

The U-value represents the overall thermal transmittance of the glazing, calculated as the inverse of the sum of external, internal heat transfer coefficients and the total thermal conductance of the glazing (Formula 1 + 2). It also includes the thermal conductance of each gas space and material layer (Formula 3).

$$\frac{1}{U} = \frac{1}{h_e} + \frac{1}{h_t} + \frac{1}{h_i} \qquad \text{(Formula 1)}$$

$$\frac{1}{h_t} = \sum_{1}^{N} \frac{1}{h_s} + \sum_{1}^{M} d_j \cdot r_j \qquad \text{(Formula 2)}$$

$$h_{s,k} = h_{r,k} + h_{g,k}$$ (Formula 3)

Radiation conductance

Radiation conductance (hr) accounts for heat transfer due to radiation between surfaces bounding the gas space. It is calculated using the Stefan-Boltzmann's constant, mean absolute temperature of the gas space, and corrected emissivities of the surfaces including coatings (Formula 4).

$$h_r = 4\sigma \left(\frac{1}{\varepsilon_{1,k}} + \frac{1}{\varepsilon_{2,k}} - 1 \right)^{-1} T_{m,k}^3$$ (Formula 4)

Gas conductance

Gas conductance (hg) represents heat transfer through the gas space between the glass panes. It is calculated using the width of the gas space, the thermal conductivity of the gas, and the Nusselt number (Formula 5). The Nusselt number, Grashof number, and Prandtl number are determined using formulas 6, 7, and 8, respectively, considering constants, temperature differences, density, dynamic viscosity, and specific heat capacity.

$$h_{g,k} = Nu \frac{\lambda_k}{s_k}$$ (Formula 5)

$$Nu = A \cdot (Gr \cdot Pr)^n$$ (Formula 6)

$$Gr = \frac{9,81\ s^3 \Delta T \cdot \rho^2}{T_m \mu^2}$$ (Formula 7)

$$Pr = \frac{\mu c}{\lambda}$$ (Formula 8)

The Nusselt number is calculated from Equation (6) and it represents the ratio of convective to conductive heat transfer in the gas space between the glass panes. It helps quantify the effectiveness of heat transfer due to fluid movement and is used

to calculate the gas conductance (hg) in Equation (5).

If the calculated Nusselt number (Nu) is less than 1, the value of unity (1) is used for Nu in Equation (5) instead. This is done because a Nu value less than 1 would imply that conduction is more effective than convection for heat transfer in the gas space. However, in practice, convection is always present to some extent. Using the value of unity ensures that the gas conductance calculation takes into account the minimum contribution of convection in the heat transfer process (European Commitee for Standardization, 2011).

Monitoring the Nusselt number is essential to prevent exceeding the cavity width. This consideration has been incorporated into the computational script, which consistently finds the optimal cavity width, ensuring the cavity remains primarily conductive.

The gas properties of Air, Argon, Krypton, and Xenon used in this study can be found in the Appendix.

The external heat transfer coefficient (he) depends on factors such as wind speed, emissivity, and other climatic elements. For standard comparisons of glazing U-values, he is set to 25 W/(m2K) for vertical glass surfaces. The internal heat transfer coefficient (hi) is the sum of the internal radiative (hr) and convective (hc) heat transfer coefficients. The radiation conductance for uncoated soda lime glass is 4.1 W/(m2K).

6.3 Computational Workflow

To determine the U-value of an uneven surface, a custom thermal model has been developed using Rhino/Grasshopper with the Python developer component. Basic Grasshopper sliders were used to make the inputs parametric and quickly calculate for different iterations. Two Python component contain an altered script of the EN-673 to calculate the inputs for both the inflated and deflated condition of the Inflatable Glazing. The script has both a numerical output as well as a visual one with a scaled appearance to depict the curvature and the associated U-values in the 3D space.

Next to the sliders that adjust the glazing parameters, the surface of the inflated glass must be evaluated to make the most accurate thermal calculation possible. However, accurately determining the curvature of a surface using generic measuring devices proves to be ambitious. For this reason, the Center of Design for Advanced Manufacturing (CDAM) at the faculty of Industrial Design was contacted to perform a 3D scan on the unit. The inflation and 3D scan were carried out in five inflation

steps using two different glass units. Chapter 9 will delve deeper into the details of the experiment setup and the results. The computational workflow to determine the thermal performance involved cleaning up the mesh from the 3D scan and preparing it for input into the script. The following steps explain the method to prepare the mesh:

1. The 3D scanner (Artec Eva) can output meshes; in this case, the .stl file format (stereolithography) was used to import the mesh into Rhino Grasshopper. The mesh lacked context and consequently appeared around a random axis. To visualize deformation or curvature, an environment map was overlaid (see Figure 6.0).

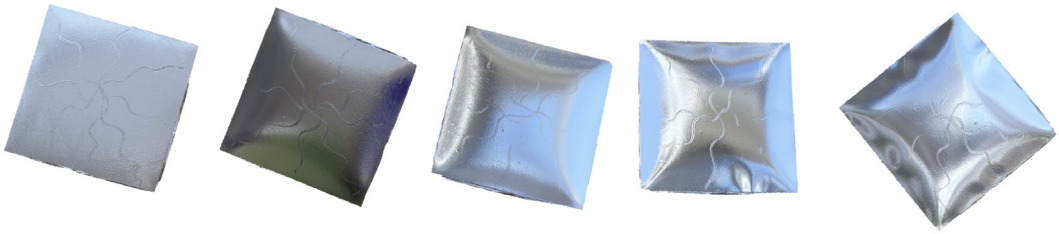

Figure 6.0 | Importing the 3D scans into Rhino - inflation steps (author)

2. The surface was leveled in Rhino and imported to Grasshopper. The 3D scan appeared to be highly detailed, with even the smallest imperfections visible. To make the file manageable and evaluable, the mesh was reduced from 300,000 vertices to 500 vertices. A Laplacian smoothing with a Catmull-Clark algorithm was applied, which enhances 3D mesh quality by repositioning vertices, minimizing surface roughness and irregularities. A Quad-Remeshing component was further applied to simplify and restructure the 3D mesh into a quad-dominant mesh. This step reduced complexity and created a more orderly, grid-like topology (see Figure 6.1).

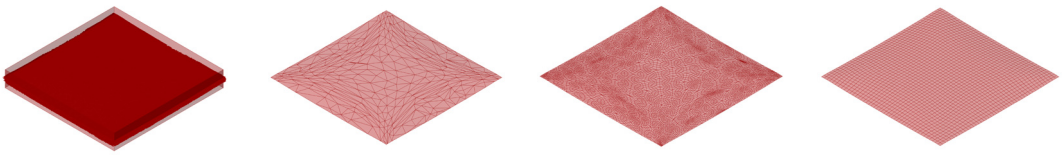

Figure 6.1 | Preparing the scanned mesh for the thermal simulation - improving mesh quality (author)

3. With an evenly divided mesh, it was possible to analyze it properly. Measuring deformation in the z direction accurately was achieved by deconstructing the mesh into its vertices. The mean curvature was estimated by calculating the angle of the normal at the center of each mesh face (see Figure 6.2). Environment maps and zebra stripes are visualization techniques that highlight curvature and surface features.

An environment map reflects the surrounding scene onto the surface, making curvature changes visible through distortions in the reflection. Zebra stripes, due to their high contrast, accentuate surface deviations and curvature changes. They create visually distinct patterns that change according to the surface shape, helping identify subtle surface details and imperfections (Figure 6.2).

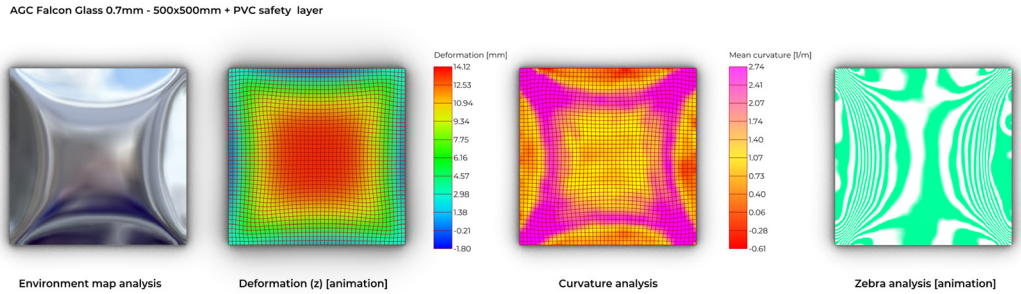

Figure 6.2 | Mesh analysis on deformation and curvature - Environment map and Zebra stripes for visual inspection (author)

4. To simulate the inflation in the thermal performance script, it was necessary to divide the inflation into steps. A flat mesh and the fully deformed scanned mesh were used to tween between a series of meshes. In this case, 60 steps were used to transition from relaxed to fully inflated. The computer-generated inflation steps have been checked to be similar to the scanned steps. The mesh was then scaled to a 1:2 ratio, which is common for office windows.

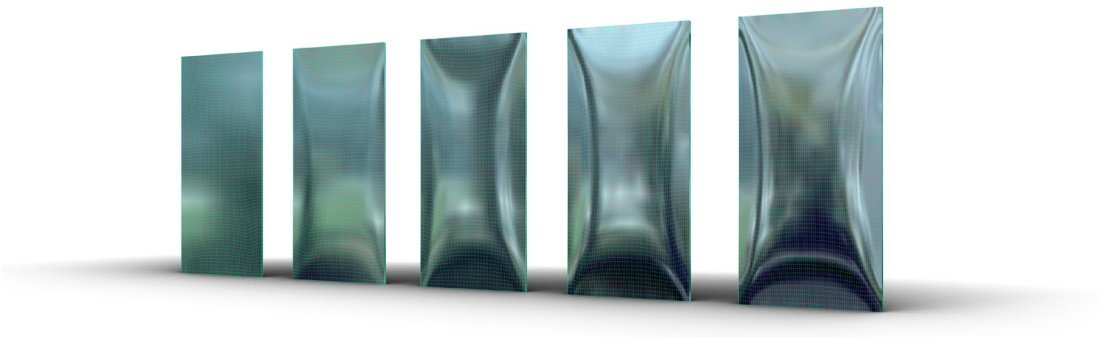

Figure 6.3 | Mesh can now be simulated with different inflation steps - e.g. above 0, 25, 50, 75 and 100% inflation (author)

The prepared mesh from the 3D scan is now imported into Grasshopper, where the inflation can be simulated. By using the cavity width slider, the inflation can be adjusted. The maximum cavity width is always associated with the maximum center pane cavity width. The mesh can be divided into virtually an infinite number of points that represent the surface. A realistic grid of points with a suitable resolution

is chosen and the number of points is matched on the flat surface, which represents the PMMA core pane. The distances of all opposing points can then be individually measured and output as a list. This list is fed into the Python component that contains the calculation script (Appendix).

Now the calculation is only missing the base parameters of the glazing. Which are given as follows (figure 6.4):

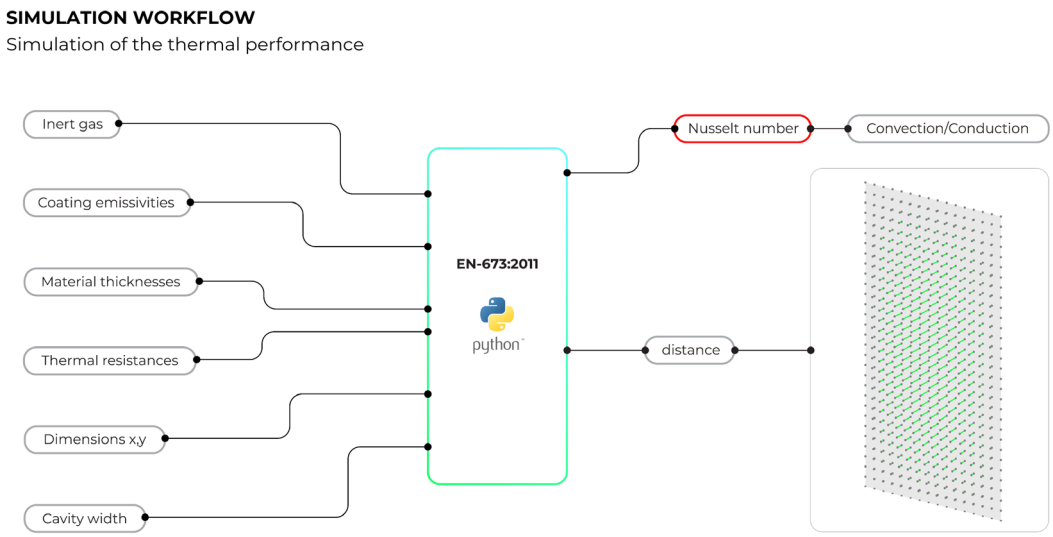

Figure 6.4 | Thermal simulation workflow - distance in each point (author)

1. Gas properties: The inert gas can be switched between Air, Argon, Krypton and Xenon. The input is given from the table in the Appendix and contains the density, dynamic viscosity, conductivity and specific heat capacity of each gas.

2. Emissivity: The emissivities range from 0.02 - 0.837 for uncoated soda lime glass and 0.92 for PMMA. They can technically be applied for all surfaces #1 to #6, however, it has been limited to the surfaces #2 to #5 since exterior and interior coatings were not intended in this product. The specific coating emissivity can be looked up on glass suppliers websites such as from AGC YourGlass.

3. Thickness: The thickness of all panes, in this case both thin glass panes and the core pane is entered here.

4. Thermal resistance: The thermal resistance is defined for the thin glass as alumino silica glass. Depending on the core pane material the thermal resistance value can be switched between alumino silica glass or PMMA.

5. Cavity width: The cavity width can range from 0.1 - 20.0mm. 0.1mm have been defined as the minimum to account for the fact that the panes might not be in direct contact across the whole surface. Depending on the outcome of the Nusselt

number, the cavity width needs to be adjusted to avoid convection inside the cavity.

6. Dimensions: Technically, all shapes (recutangular, round) can be inserted and defined as a mesh. In this version, it can be adjusted via x, y values.

The final output can be made visual with a legend stating the range of U-values asocciated with an RGB colored mesh.

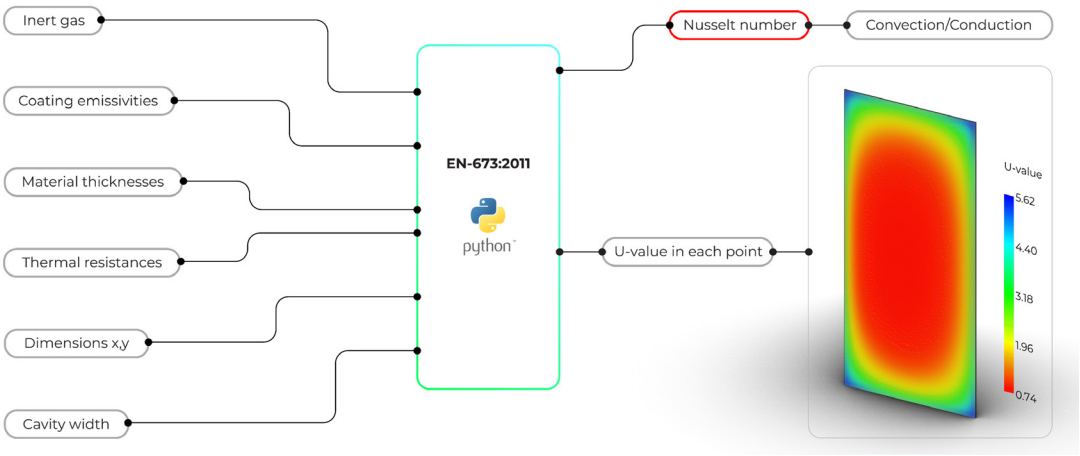

Figure 6.5 | Thermal simulation workflow - U-value in each point (author)

In order to determine the optimal set of values as well as the ideal cavity width per unit, the machine learning algorithm plugin Galapagos was integrated into the script and connected to the glazing parameters and Nusselt number (see Figure 6.6). Upon running the algorithm, it was discovered that the low-e coating has the most significant impact on the U-value, particularly when applied to two surfaces. The cavity width and the inert gas were the second most influential factors. Subsequently, material thicknesses and resistivity factors were also important contributors.

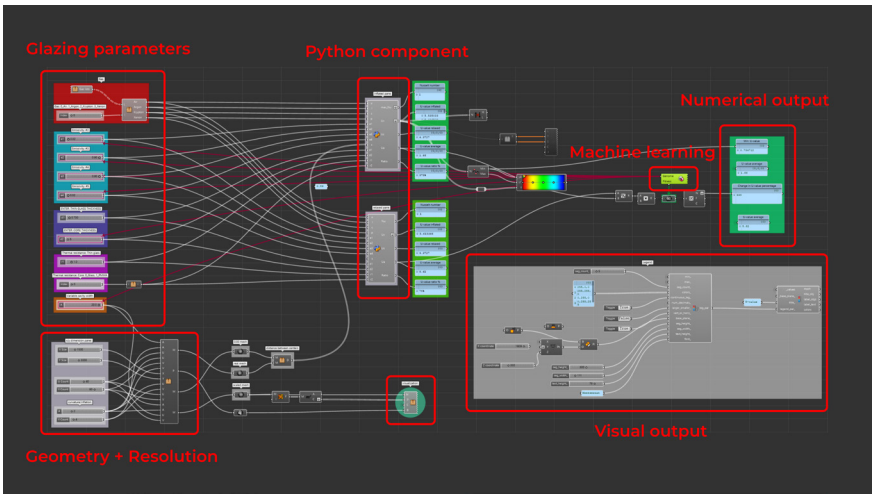

Figure 6.6 | Thermal simulation GH script - annotated (author)

6.4 Results

The thermal testing has been performed to explore the maximum potential of Inflatable Glazing. Therefore, the parameters have been consecutively altered, one at a time, to keep track of significant changes. In total, six different setups have been simulated.

The simulation output is given as the average U-value (U_{av}), which is calculated as the sum of all U-values divided by the number of measured U-values. The minimum U-value (U_{min}) is determined as an extreme value that appears anywhere on the pane. The maximum U-value (U_{max}) is determined when the unit is fully conductive and the material is in direct contact. Finally, the change in U-value is defined as a percentage increase between U_{av} and U_{max}. This percentage value is used as the main indicator of performance.

The coating used for the calculation is a thermally insulating coating, selective for the wavelengths λ = 3000-50,000nm, with an emissivity of 0.02. The coating is always calculated on either none or two surfaces at positions #2 and #5. Ideally, this coating should be bendable and scratch-resistant due to the constant flexure of the glass pane.

Firstly, a glass unit without coatings and inert gas has been calculated to gauge the minimum effect of Inflatable Glazing (see Figure 6.7). The result of over 200% shows the potential of Inflatable Glazing. However, the average U-value of 1.82 W/m2K is not satisfactory yet. One can also notice that the maximum U-value of 3.90 W/m2K is relatively low due to the PMMA core, which has a higher thermal resistivity than glass.

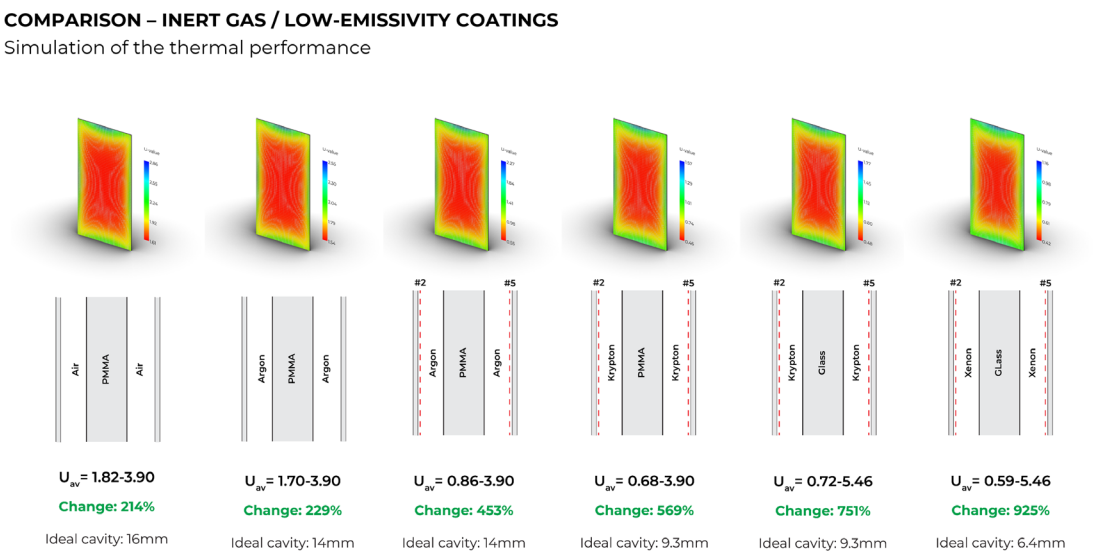

Figure 6.7 | Comparison of different U-value calculation setups 1-6 (author)

Consequently, Argon has been introduced as an inert gas. The change in U-value is relatively insignificant. However, when adding the coatings on #2 and #5, a substantial increase can be observed. By incorporating Krypton as an inert gas, the change in U-value significantly rises to over 500%. The average U-value is now also within the range of high-performance triple glazing. However, the maximum U-value is still far from the single glazing properties that have been defined in the design criteria. As a result, the PMMA pane has been replaced with a glass pane.

The fully glass unit with Krypton and coatings achieves the U-values of both triple and single glazing with 5.46 W/m2K. The change in U-value is now over 700%. Finally, the super-insulating inert gas Xenon has been added to the calculation to determine the maximum potential. The final numbers of U_{av} 0.59 W/m2K up to U_{max} 5.46 W/m2K result in a change of 925% and a U_{min} of 0.42 W/m2K (see Figure 6.8).

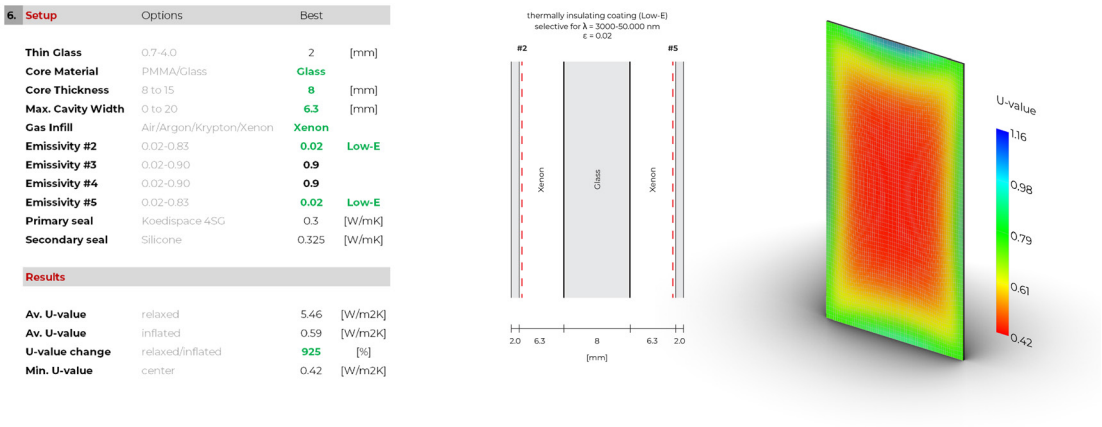

6. Setup	Options	Best	
Thin Glass	0.7-4.0	2	[mm]
Core Material	PMMA/Glass	Glass	
Core Thickness	8 to 15	8	[mm]
Max. Cavity Width	0 to 20	6.3	[mm]
Gas Infill	Air/Argon/Krypton/Xenon	Xenon	
Emissivity #2	0.02-0.83	0.02	Low-E
Emissivity #3	0.02-0.90	0.9	
Emissivity #4	0.02-0.90	0.9	
Emissivity #5	0.02-0.83	0.02	Low-E
Primary seal	Koedispace 45G	0.3	[W/mK]
Secondary seal	Silicone	0.325	[W/mK]
Results			
Av. U-value	relaxed	5.46	[W/m2K]
Av. U-value	inflated	0.59	[W/m2K]
U-value change	relaxed/inflated	925	[%]
Min. U-value	center	0.42	[W/m2K]

Figure 6.8 | Setup of glazing parameters with resulting U-value for the xenon infill (author)

Revisiting Figure 6.7, the decrease in cavity width is evident. The Inflatable Glazing with air infill requires a cavity width of 16mm to reach its full potential, whereas the xenon infill only needs 6.4mm. The thermal performance of an IGU filled with inert gas peaks at a specific cavity width due to two heat transfer mechanisms: conduction and convection. At smaller widths, conduction dominates; the inert gas slows heat transfer, improving insulation. As cavity width increases, the insulating effect initially improves, reducing conduction. However, beyond a certain width, convection currents begin to form within the gas layer, enhancing heat transfer and reducing the unit's insulating effectiveness. This creates an optimal cavity width where the combined effects of conduction and convection are minimized, maximizing thermal performance. This width varies depending on the specific gas used, its thermal properties, and the ambient conditions.

In the simulation, this phenomenon could be measured from the Nusselt number explained earlier. The machine learning component has been connected to the output of the Nusselt number to keep it as close to the value 1 as possible. This

always resulted in achieving the lowest possible U-value. Keeping the cavity width and the resulting ratio of conduction and convection constant is even difficult in modern IGUs. Respondek's (2020) study examined how the shrinkage of an IGU cavity impacts heat loss during winter. The study, which analyzed both double- and triple-glazed IGUs, revealed that deformation due to climatic loads increases the heat loss in these units. For instance, under mild winter conditions, the heat loss in triple-glazed IGUs could rise by up to 5%, while in double-glazed IGUs with 10–14 mm gaps, the increase could be around 4.6%. Thus, he suggests that these considerations should be incorporated into IGU design.

The graph depicted below illustrates the disparity in U-value relative to the Nusselt number. In this scenario, the Inflatable Glazing was simulated using a krypton infill and a PMMA core. The data was collected in increments of 1.3mm. It can be observed that the U_{av} reaches its minimum around the Nu_{max} value of 1, where the lines intersect.

Figure 6.9 | Cavity width versus U-value - krypton/PMMA core (author)

Discussion

It can be concluded that the application of a low emissivity coating, coupled with a low conductive inert gas at the appropriate cavity width, can significantly enhance the performance of the unit. The material's thickness is also crucial. The already low conductive material, PMMA, requires a higher thickness, resulting in a lesser alteration in U-value. The glass units indisputably outperform the PMMA units, as they permit a substantially higher shift in U-value.

The insulation of the warm edge spacer and the secondary sealant have not been considered in the calculations. As previously noted, these elements are not part

of the EN673 standards. However, the warm edge spacer can notably influence the U_w-value when the glass unit has a low U-value. Scherer et al. (2016) observed significant improvement with thermoplastic spacers such as the 4SG Ködispace by Kömmerling. With a psi-value of 0.04 W/mK for triple glazing, they surpass ordinary aluminium spacers, which have a psi-value of around 0.111 W/mK. Consequently, improvements of up to 10% in thermal performance in U_w-values can be observed (Scherer et al., 2016).

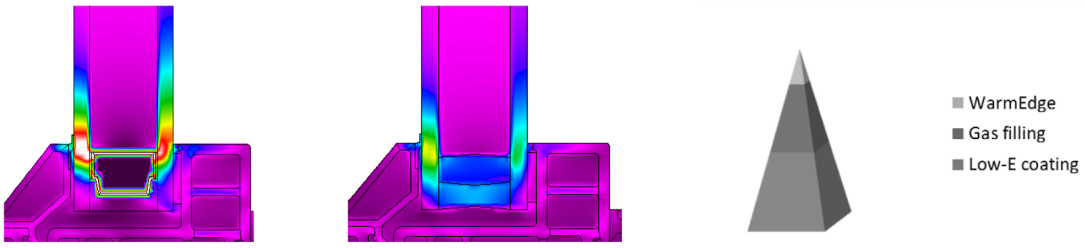

Figure 6.10 | Left: Aluminium spacer vs 4SG Ködispace thermal simulation (Kömmerling, 2019) - Right: Contribution to U-value (Scherer et al., 2016)

However, these values should be treated with caution since they are theoretical and still require validation in a testing facility. In practice, the U-value of an IGU is determined through two primary laboratory methods: the hot box method and the guarded heat flow meter method. The hot box method involves placing the IGU between two climatic chambers with differing temperatures, then measuring the heat transfer. The guarded heat flow meter method (also known as the hot plate method) involves positioning a heat flux sensor on the IGU surface to measure the heat flow rate. Both methods provide an accurate measurement of the U-value, which quantifies the IGU's thermal transmittance.

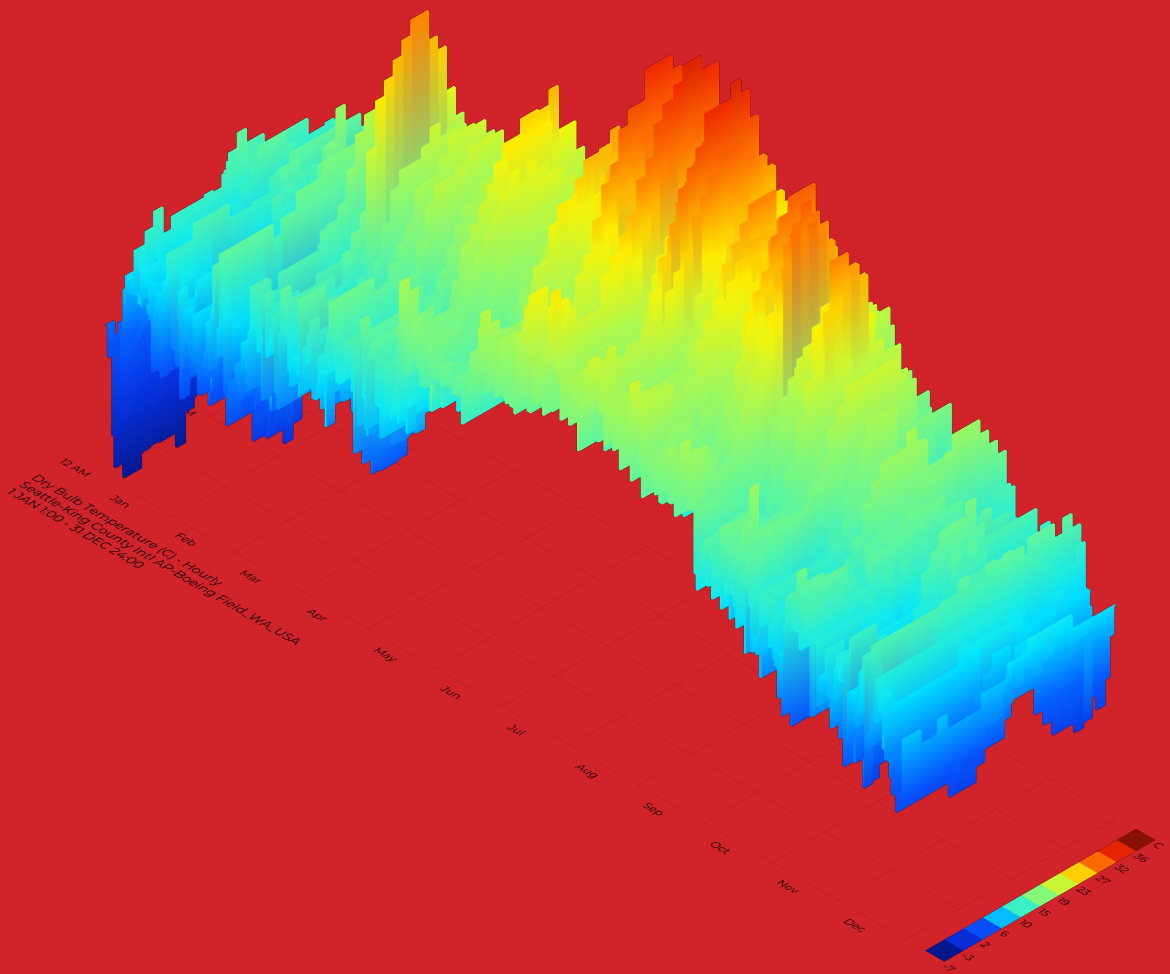
Dbt Bulb Temperature [C] - Hourly
Seattle-King County Intl AP-Boeing Field, WA, USA
1 JAN 1:00 - 31 DEC 24:00
12 AM
Jan
Feb
Mar
Apr
May
Jun
Jul
Aug
Sep
Oct
Nov
Dec
C
36
32
27
24
19
15
10
6
2
-3
-7

7. Energy Efficiency

The ultimate goal of Inflatable Glazing is to reduce the energy demand of buildings and enhance thermal comfort for occupants. Thermal simulations have indicated that a significant change in the U-value is achievable. However, it has not yet been determined how the transition between insulating and conducting states impacts a building's energy demand. To ascertain when and how it is beneficial, an energy model needs to be developed. Consequently, the ideal location for Inflatable Glazing will be determined and the boundary conditions will be set. Finally, the glass unit will be tested in both a passive state, with no HVAC involvement, and an active state, where HVAC is operational throughout the entire year.

7.1 Boundary Conditions

Setting the boundary conditions in an energy model is a critical step in the modelling process. Boundary conditions serve as constraints or limits that govern the behavior of the system under study. They represent a set of assumptions and parameters that define the environmental conditions and specific characteristics of the building. When well-established, these boundary conditions allow for a more accurate and reliable prediction of the energy performance of the building.

In the realm of modern architecture, the trend towards fully glazed office buildings with a low window to wall ratio has gained significant traction. Therefore, the designed building with the dimensions of 12x6m (see Figure 7.0) has a fully glazed facade in all orientations. The designed building is a single-storey office structure with large overhangs providing shade to the fully glazed facade. The presence of these overhangs plays a significant role in the energy model as they protect the facade from direct solar radiation The office building is also surrounded by other structures, which further shield the building from low angle solar rays.

Given this setting, the energy model mainly considers the energy flow caused by the difference in interior and exterior temperatures. The impact of solar radiation on the building is significantly reduced due to the architectural design and the context of the surrounding buildings. Therefore, the model primarily focuses on the heat transfers that occur as a result of the temperature gradient between the building's interior and the outside environment.

However, it is important to note that while direct solar radiation does not directly strike the glazed facade, indirect solar radiation in the form of ground-reflected radiation does contribute to the building's thermal load. Furthermore, the building's roof is exposed to direct solar radiation and will be a main factor of heat gain during warm periods.

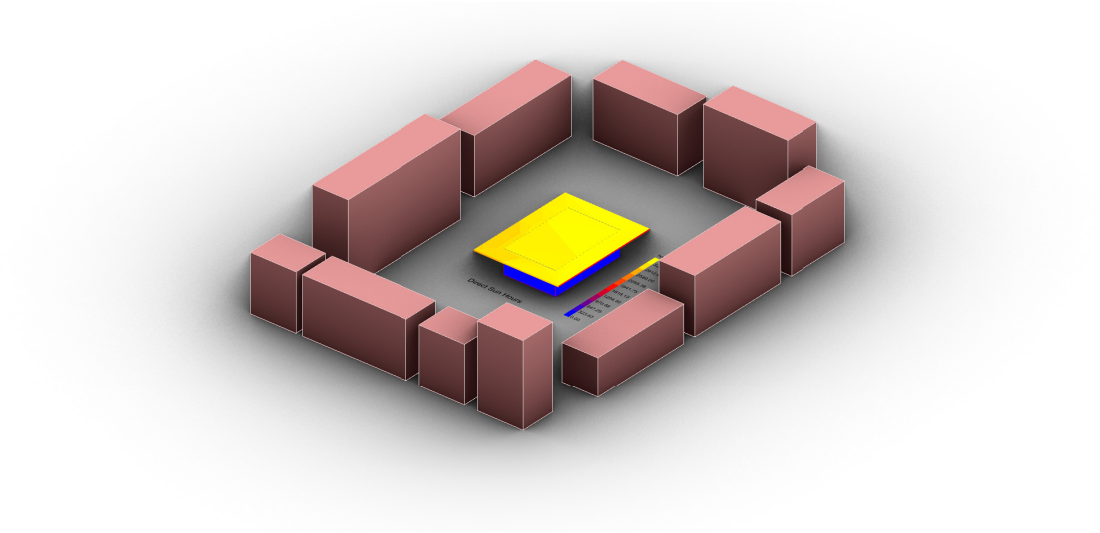

Figure 7.0 | Energy model - Fully glazed office building (blue) with overhang (yellow) and context (red) (author)

7.2 Computational Workflow

First, the building's geometry had to be defined in Rhino. This included the building volume, shading, glazing, and the surrounding context, which also acts as shade. Once the geometry was established, the Ladybug Sun Hour Analysis component in Grasshopper was used to ensure that all glazed facades did not receive any direct solar radiation. This step was necessary because only heat flows due to temperature differences needed to be analyzed. Following that, the energy model was established using the Honeybee plugin, which operates with EnergyPlus in OpenStudio. EnergyPlus is a powerful energy simulation software developed by the U.S. Department of Energy. It is used to model energy consumption and thermal comfort in buildings. The software considers a variety of factors including heating, cooling, lighting, and ventilation, as well as water heating and renewable energy systems. By simulating these energy flows, EnergyPlus helps in understanding the energy performance of a building and aids in making design decisions for energy efficiency.

Preparing the location

The location preparation began by importing the EnergyPlus Weather (epw) files of four vastly different climate zones, as per ASHRAE classifications, ranging from zone 1 (hot) to zone 6 (cold). Following this, the weather file was deconstructed into the hourly dry bulb temperature, which was used to calculate the heating and cooling degree days from the outdoor dry bulb temperature. This data was then further deconstructed into a list of heating and cooling probabilities, and conditional formatting was applied to define of a certain day would either require heating or cooling. Each day was then transformed into a binary code consisting of 0s and 1s, indicating whether a specific hour of the year required an insulating or a conducting window.

Defining the building properties

The process started by determining if the building was conditioned, allowing for an on or off toggle for the HVAC system to test both active and passive states. Next, the building program was established for a medium-sized office, including standard settings for elements like lighting, equipment, occupants, heating, and ventilation.

The climate zone, as per ASHRAE, was defined based on location, which adjusts the building program parameters to suit the local climate. This is a refinement to the construction set, reflecting local building practices. The building vintage, following ASHRAE 90.1 2019/IECC 2021 standards, refers to the energy efficiency standards in place at the time of construction. The construction type was set as mass (concrete). Lastly, shading was applied, and all these parameters were included in the energy model's construction set.

Glazing properties

The properties of glazing are defined by a static window component for comparison purposes, as well as a dynamic window component, namely the Inflatable Glazing. The static component is characterized by a single U-value and a g-value, while the dynamic window component is defined by two extreme U-values and a single g-value. This component can shift between either of the extreme values, effectively toggling between the fully insulating and fully conducting states of the glass unit.

The decision to adopt either state is determined by a schedule. To reduce complexity in this context, the binary code of heating and cooling dates, based on the outside dry bulb temperature, was used to determine whether the insulating or conducting state is activated.

The types of glazing used for comparison include single glazing, coated double glazing, coated triple glazing and coated quadruple glazing. The choice among these depends on the climate zone of the location being used in the simulation.

Output

A Python component has been used to read from the Input Output Reference document by EnergyPlus. The first analysis was conducted on a non-conditioned space throughout the year to evaluate if the glazing is capable of passively cooling the building or storing heat when needed. This analysis focused on the Zone Air Temperature.

In the second analysis, a conditioned space was considered to assess the heating and cooling demand. The HVAC's cooling and heating load is calculated based on

the interior air temperature. The heating will commence at 18 degrees, while cooling will be initiated at 23 degrees.

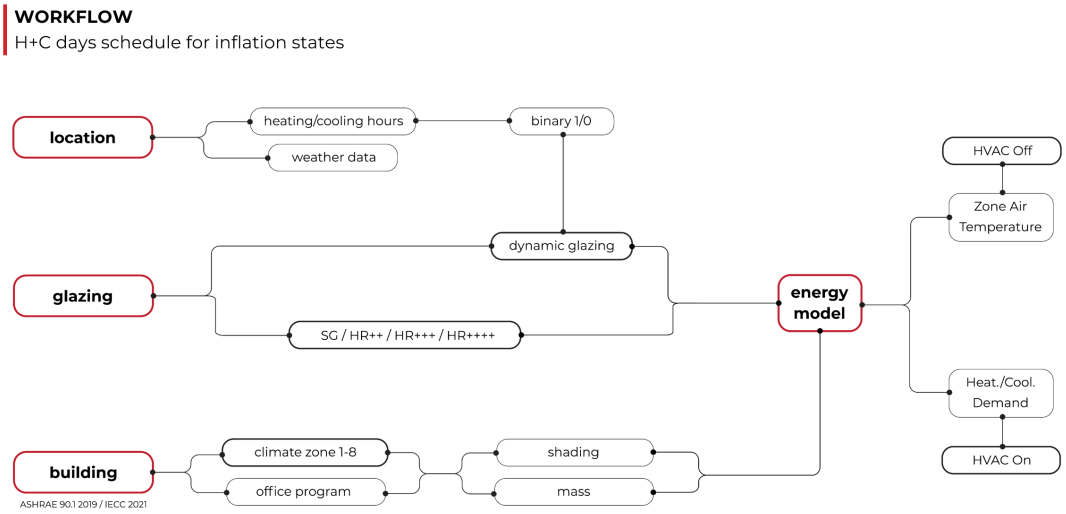

Figure 7.1 | Energy model computational workflow based on H + C hours (author)

Discussion

The energy model provides a general idea of the Inflatable Glazing's performance, but there are several other parameters that need to be considered to create a more accurate energy model. At present, standard building parameters are employed, which should be adequate to provide a realistic outlook. However, the energy required to inflate the glazing is not considered in the model.

The schedule is perhaps the most critical factor, as it determines when it is best to inflate or deflate the glazing. A deeper study of this aspect could significantly enhance the energy model's accuracy. Additionally, the energy model could gradually adjust the U-value or adjust it in smaller increments rather than merely turning it on or off.

Finally, it would be beneficial to investigate the building's geometry itself further. It is possible that there is an ideal orientation for Inflatable Glazing that could result in optimal energy efficiency.

7.3 Classification of Climate Zones

As described by Ladybug Tools (2022) climate zones are categorized based on long-term weather data, specifically temperature and precipitation, to outline the expected meteorological conditions in a given region. These climate classifications serve as a valuable resource for architects and engineers, enabling them to benchmark structures and make preliminary decisions concerning building HVAC

systems, types of facades, fenestrations, and insulation levels. The Koppen-Geiger Climate Classification and the International Code Council (ICC) / American Society of Heating, Refrigeration, and Air Conditioning Engineers (ASHRAE) climate zones are the two primary climate classification systems utilized in the construction industry. Furthermore, a simplified method known as Design Degree Days amalgamates temperature and time data.

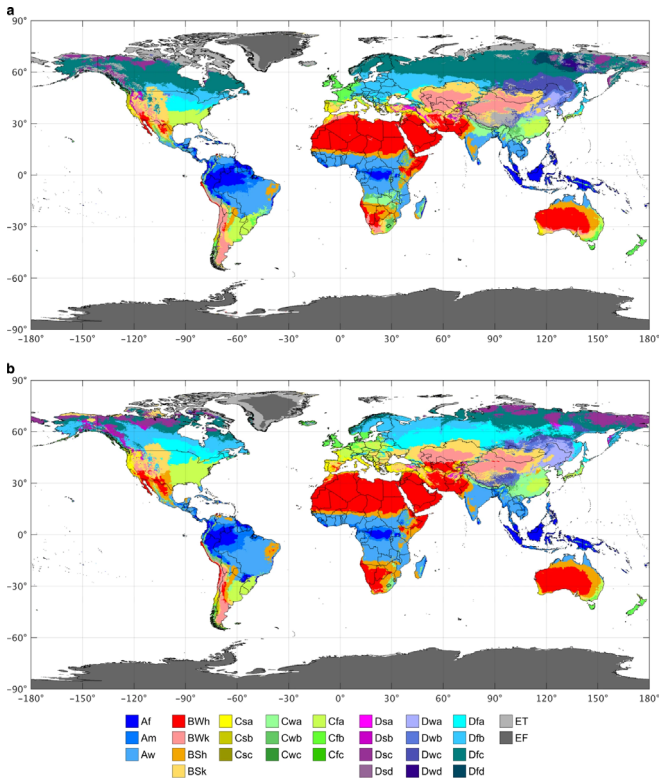

Figure 7.2 | Panel (a) illustrates the current-day map (spanning from 1980 to 2016), while panel (b) depicts the projected future map (from 2071 to 2100). (Beck et al., 2018).

The Koppen-Geiger Climate Classification is a globally recognized system, primarily employed for ecological modeling and assessments of climate change impacts. This system segments the world into five principal climate groups: equatorial (A), arid (B), warm-temperate (C), snow (D), and polar (E). These primary climate groups are further divided based on specific temperature and precipitation conditions. For precipitation, the classifications include desert (W), steppe (S), fully humid (f), dry summer (s), dry winter (w), and monsoon (m). For temperature, the categories are hot arid (h), cold arid (k), hot summer (a), warm summer (b), cool summer (c), extremely continental (d), polar frost (F), and polar tundra (T) (Ladybug Tools, 2022).

7.4 Optimal Location for Inflatable Glazing

The U-value of glazing does not have the same effect in different climate zones. There are specific climate zones that consistently rely on insulation, like the very cold zones including Alaska, Northern Canada, Northern Europe, and Siberia. These

regions endure frigid temperatures for the majority of the year, making insulation critical to retain heat within buildings. This reduces the amount of energy needed for heating and ensures a comfortable indoor environment. Historically, vernacular architecture in these zones featured few and small openings. Today, this tradition of small openings persists, and the use of high-performance glazing is highly recommended.

Conversely, there are climate zones, particularly those near the equator, that maintain warm temperatures year-round. In some instances, glazing isn't even necessary. These climate zones predominantly fall under the tropical category, such as the Amazon, Central Africa, the Caribbean, and Southeast Asia. In these areas, temperatures stay relatively consistent throughout the year, and humidity remains consistently high. Consequently, there's little need for insulation to maintain comfortable indoor temperatures. Instead, considerations for ventilation and moisture control take precedence in these climates. Here, shutters or nets are commonly employed to maintain high ventilation rates.

Figure 7.3 | Left: Vernacular architecture in the Dominican Republic without glazing and shutters (Martínez, n.d.). Right: A typical house in Northern Canada with a few small openings (Barrow Alaska Photograph by Jeffrey Sward, 2010).

In conculsion, the above stated climate zones are not ideal for the Inflatable Glazing. A static window solution as they exist now, work well enough. A switchable insulation therefore, only makes sense if the temperature over the year signigicantly fluctuates. Two scenarios have been identified where switchable insulation makes a significant impact on energy efficiency as well as occupancy comfort.

Scenario 1:

Mixed climate zones, are regions characterized by moderate temperatures and varied weather patterns, including both warm and cold periods. These zones typically experience (very) hot summers and (very) cold winters. In developed countries, insulated glazing is often installed in buildings to mitigate heat loss during winter. However, in the summer, insulated glazing can enhance the greenhouse effect. During temperature peaks, this may result in the overheating of spaces. Seattle has

been identified as a location with a mixed climate and is being used as a case study in this context.

Scenario 2:

Climate zones characterized by warm, dry summers and mild, wet winters exhibit less severe temperature extremes compared to areas with very cold or very hot climates. This reduces the need for high-performance windows. In general, temperatures are comfortable throughout the year, allowing buildings to maintain a comfortable interior temperature without requiring much heating. However, cooling becomes a significant concern. Single glazing can exacerbate heat ejection or build-up inside the building. Due to the widespread use of equipment such as PCs and servers in office buildings, as well as the heat generated by occupants, the internal heat load is significant. However, during the transitional seasons and winter, buildings are much more reliant on heating than they would be with insulated glazing. San Jose fits the described climate zone and has therefore been selected for this case study.

The following graph depicts the annual dry bulb temperature (hourly) for both Seattle and San Jose. It can be observed that Seattle's temperature fluctuates quite significantly, whereas San Jose maintains warmer temperatures over a longer period, with a temperature dip only in the winter season.

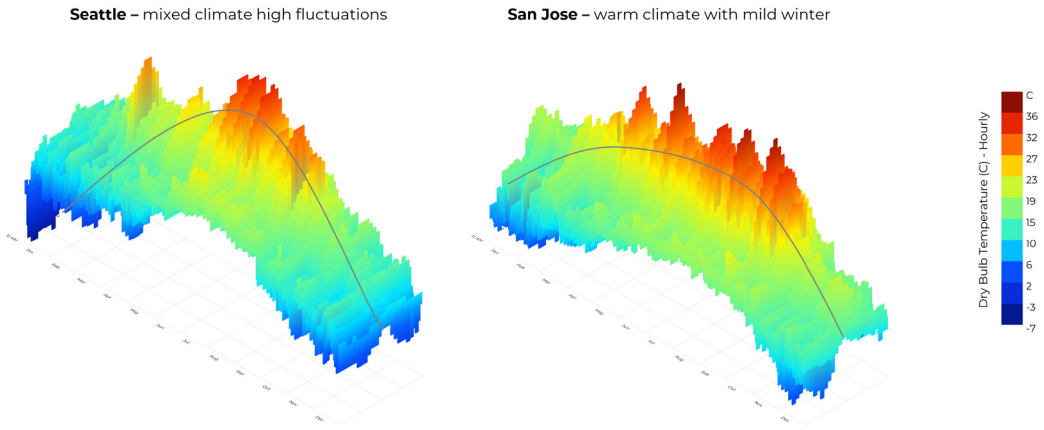

Figure 7.4 | Seattle vs. San Jose - annual dry bulb temperature (hourly) comparison (author)

To confirm that these two climate zones/scenarios indeed outperform static glazing, it's necessary to compare them with other climate zones. The ASHRAE climate zones, which can be easily accessed through the Honeybee plugin, range from 1 (hottest) to 8 (coldest) and include three moisture levels: Moist (A), Dry (B), and Marine (C) (Ladybug Tools, 2022). The annual dry bulb temperatures of cities in climate zones ranging from 1 to 7 have been plotted to understand the temperature patterns (refer to Figure 7.5). It can be observed that, despite Carlton being in climate zone 6-7 (very cold), it still exhibits a mixed climate with summer temperatures exceeding

30 degrees Celsius. San Juan, in climate zone 1 (very hot), displays a very consistent pattern due to its proximity to the equator.

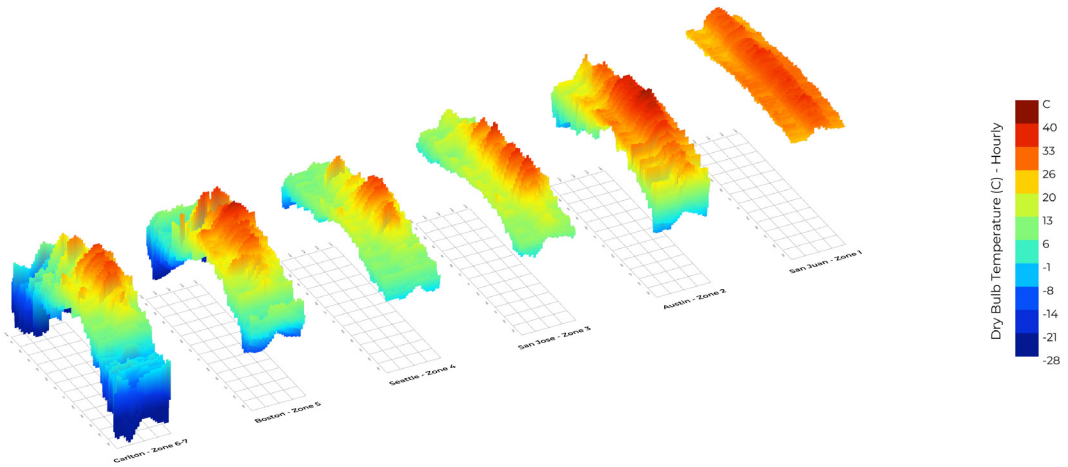

Figure 7.5 | Cities ranging from ASHRAE climate zones 1-7 annaul dry bulb temperature (hourly) comparison (author)

The following cities are being tested according to the previously described energy model against single glazing, triple glazing, and Inflatable Glazing. The locations that perform best with Inflatable Glazing will then be further investigated in terms of zone air temperature and annual energy balance:

- Carlton, Minnesota
- Boston, Massachusetts
- Seattle, Washington
- San Jose, California
- Austin, Texas
- San Juan, (Puerto Rico)

For the analysis the following U-values and g-values are assumed:

Glazing	Ug-value	g-value	Coating
Single Glazing	5.8	0.87	No
Double Glazing	1.1	0.5	Yes
Triple Glazing	0.6	0.3	Yes
Inflatable Glazing (Xenon)	0.6 - 5.46	0.3	Yes

Table 7.0 | Different glazing performances for comparison (author)

The following energy analysis is conducted for each glazing type, and the combined heating and cooling demand is calculated throughout the year. The schedule for the Inflatable Glazing is only seasonal in this analysis, meaning that it does not fully

demonstrate the technology's potential. The purpose is merely to identify the best location while maintaining the same settings throughout the year. Table 7.1 shows uncoated single glazing in the second row. It can be observed that the energy demand is high for both extreme temperature zones. Seattle and San Jose have approximately the same energy demand with single glazing, even though they exhibit quite different temperature patterns.

Improvements are noticeable when coated double glazing is employed, more so for heating-dominated climates than for cooling-dominated climates. The decreased energy demand for cooling-dominated climates can be attributed to the slower heat transmission through the window. The room will not heat up as quickly, and the air conditioning will not need to operate at maximum capacity.

The same applies to triple glazing, where improvements can be seen in both heating and cooling-dominated climates. This time, Seattle achieves the best result compared to single glazing. Inflatable Glazing outperforms triple glazing by 15% in San Jose and is 72% more effective than single glazing in Seattle.

Combined energy demand [kWh/m²]

	Carlton	Boston	Seattle	San Jose	Austin	San Juan
ASHRAE ZONE	6 - 7	5	4	3	2	1
Single Glazing (SG) Ug=5.8	410	289	176	173	327	495
Double Glazing (DG) Ug=1.1	186	145	81	113	237	392
Improvement DG to SG	55%	50%	54%	35%	28%	21%
Triple Glazing (TG) Ug=0.6	143	110	58	82	179	304
Improvement TG to SG	65%	62%	67%	53%	45%	39%
Inflatable Glazing (IG) Ug=0.6 - 5.46	127.12	98.16	49.32	69.58	179	304
Improvement IG to SG	**69%**	**66%**	**72%**	**60%**	**45%**	**39%**
Improvement IG to TG	**11.10%**	**10.76%**	**14.97%**	**15.15%**	**0.00%**	**0.00%**

Table 7.1 | Energy performance of different glazing types compared to Inflatable Glazing (author)

Neither San Juan nor Austin show any improvement when transitioning from triple glazing to inflatable glazing, as these climates are predominantly cooling-dominated. The glazing would remain inflated for almost the entire year, as it's best to mitigate heat transfer in both winter and summer. Therefore, climate zones 1-2 are not considered ideal for Inflatable Glazing. On the other hand, the technology demonstrates a significant effect on energy reduction in climate zones 3-7. Mixed climate zones with approximately equal heating and cooling periods seem to yield the best results for this technology.

Two climate zones will be further investigated. To mitigate analysis bias, climate zones 5-7 will not be examined further. In newly constructed buildings, triple glazing would be the recommended choice, as overall consumption drops from 410kWh/m²

to 143kWh/m². Inflatable glazing would then add an 11% improvement compared to triple glazing.

Seattle and San Jose exhibit a very mixed and moderately warm climate, respectively. In both locations, single glazing or uncoated double glazing is still an option to this day, as it is cost-effective, aesthetically pleasing, and helps keep out heat in the summer. This is especially the case in residential homes where air conditioning is not always installed. In such scenarios, Inflatable Glazing can actually be compared to single or double glazing, and in these instances, the improvement numbers increase significantly. As shown in Table 7.2, the improvement when transitioning from single glazing to Inflatable Glazing in Seattle is over 70%. Therefore, these two locations will be further analyzed.

Combined energy demand [kWh/m²]

	Seattle	San Jose
ASHRAE ZONE	4	3
Single Glazing (SG) Ug=5.8	176	173
Double Glazing (DG) Ug=1.1	81	113
Inflatable Glazing (IG) Ug=0.6 - 5.46	49.32	69.58
Improvement IG to SG	**72%**	**60%**
Improvement DG to SG	**39%**	**38%**

Table 7.2 | Energy performance of SG and DG to Inflatable Glazing in Seattle and San Jose (author)

7.5 Zone Air Temperature Simulation

In an EnergyPlus analysis without an active HVAC system and inoperable windows, the Zone Air Temperature represents the passive thermal behavior of a building zone or room. The analysis focuses on evaluating how the building's design, materials, and construction interact with external factors like solar radiation, outdoor temperatures, and wind to influence the indoor thermal conditions.

The results of this specific analysis would demonstrate the building's natural thermal performance and highlight its passive design features, such as insulation, thermal mass, and orientation.

To demonstrate the passive benefits of Inflatable Glazing on the interior climate, a variety of glazing types are compared. This comparison includes glazing types ranging from single to quadruple glazing, with minimum and maximum temperatures monitored. The Inflatable Glazing types vary from Air infill to Xenon infill, all featuring glass units with thermally insulating coatings applied. A schedule based on heating days has been implemented for the inflation, meaning that this analysis may not fully capture the complete potential. The following table presents the zone air temperature analysis:

Seattle

	Single Glazing	Double Glazing	Triple Glazing	Quadruple Glazing	IG (Xenon)	IG (Krypton)	IG (Air)
Ug-value [W/m²K]	5.8	1.1	0.6	0.35	0.6-5.46	0.72-5.46	1.18-5.46
g-value	0.87	0.3	0.3	0.3	0.3	0.3	0.3
Minimum temperature	8.17	11.9	13.89	15.43	13.87	13.28	11.58
Maximum temperature	46.96	47.47	52.63	56.46	38.48	37.66	37.4
Av. Temperature annually [°C]	**21.45**	**25.06**	**28.43**	**31.03**	**25.27**	**24.60**	**22.63**

San Jose

	Single Glazing	Double Glazing	Triple Glazing	Quadruple Glazing	IG (Xenon)	IG (Krypton)	IG (Air)
Ug-value [W/m²K]	5.8	1.1	0.6	0.35	0.6-5.46	0.72-5.46	1.18-5.46
g-value	0.87	0.3	0.3	0.3	0.3	0.3	0.3
Minimum temperature	9.85	13.12	14.28	15.03	14.3	13.98	12.96
Maximum temperature	48.01	45.28	48.09	49.87	38.43	38.43	38.41
Av. Temperature annually [°C]	**24.02**	**25.45**	**27.18**	**28.35**	**24.72**	**24.43**	**23.50**

Table 7.3 | Zone air temperature analysis - minimum, maximum and average annual temperatures of different glazing types (author)

From Table 7.3, it is observed that the results for the Inflatable Glazing are relatively similar across different instances. Interestingly, Seattle appears to experience hotter periods than San Jose, in addition to colder temperatures. This suggests that the climate with higher and lower peaks in Seattle levels out to similar temperatures as San Jose when using Inflatable Glazing.

It is also noteworthy that the internal temperature rises significantly with the use of increasingly static insulated glazing. With quadruple glazing, temperatures in Seattle can escalate up to 56 °C. However, all types of Inflatable Glazing manage to limit the maximum temperature to around 38 °C. The minimum temperature also stabilizes at approximately 13 °C, and the average maintains a comfortable level of 24 °C.

For a visual comparison, the Inflatable Glazing with Krypton infill has been analyzed alongside triple glazing. The subsequent graph illustrates the average monthly temperatures over a year in Seattle. It becomes evident from the graph that Inflatable Glazing significantly moderates peak temperatures, thereby reducing the overall temperature balance.

Zone Air Temperature with Triple Glazing:

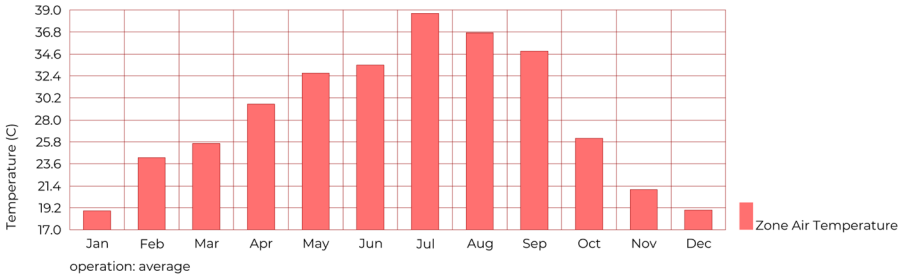

Zone Air Temperature with Inflatable Glazing:

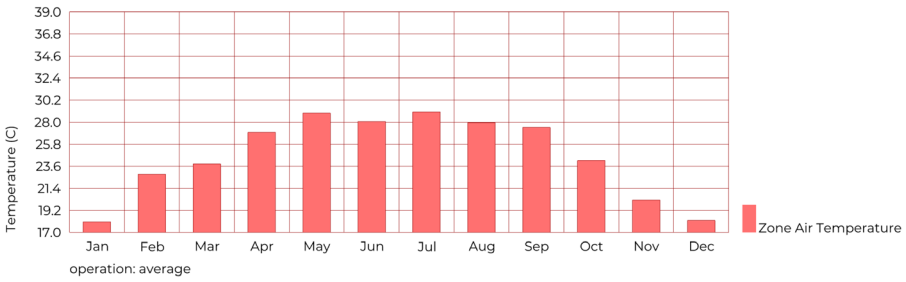

Figure 7.6 | Zone Air Temperature analysis showing the passive method of lowering air temperature (author)

7.6 Energy Balance Simulation

An energy balance analysis in EnergyPlus is a method of evaluating the energy flow within a building by accounting for all energy gains, losses, and exchanges that occur. It provides a comprehensive understanding of the building's energy performance, which can be used to optimize its design, HVAC systems, and operational strategies.

Energy balance analysis considers various factors, such as heat gains from occupants, lighting, and equipment, solar radiation, heat transfer through building elements, ventilation, and air infiltration. The analysis calculates the energy required for heating, cooling.

This analysis is treated similar as the Zone air temperature with the difference that HVAC is now turned on and the heating and cooling sets in at 18 and 23°C respectively. The same glazing types will be evaluated and the performance indicator is the total energy demand per year. The following table shows the energy balance for both locations Seattle and San Jose:

Seattle

	Single Glazing	Double Glazing	Triple Glazing	Quadruple Glazing	IG (Xenon)	IG (Krypton)	IG (Air)
Ug-value [W/m²K]	5.8	1.1	0.6	0.35	0.6-5.46	0.72-5.46	1.18-5.46
g-value	0.87	0.3	0.3	0.3	0.3	0.3	0.3
Cooling demand [kWh/m²]	50.1	29.73	32.82	43.75	22.23	22.23	22.23
Heating demand [kWh/m²]	125.92	41.93	25.57	17.61	25.68	29	45.67
Total energy demand [kWh/m²]	**176.02**	**71.66**	**58.39**	**61.36**	**47.91**	**51.23**	**67.90**

San Jose

	Single Glazing	Double Glazing	Triple Glazing	Quadruple Glazing	IG (Xenon)	IG (Krypton)	IG (Air)
Ug-value [W/m²K]	5.8	1.1	0.6	0.35	0.6-5.46	0.72-5.46	1.18-5.46
g-value	0.87	0.3	0.3	0.3	0.3	0.3	0.3
Cooling demand [kWh/m²]	96.07	56.91	61.67	64.56	45.52	45.52	45.52
Heating demand [kWh/m²]	75.8	29.24	20.28	15.77	20.18	22.03	30.96
Total energy demand [kWh/m²]	**171.87**	**86.15**	**81.95**	**80.33**	**65.70**	**67.55**	**76.48**

Table 7.4 | Energy balance analysis - cooling, heating and total energy demand for different glazing types (author)

It can be observed that with static glazing and increasing insulation, the heating demand decreases while the cooling demand rises. In the case of Seattle, it is evident that excessive insulation can be counterproductive. Triple glazing, in fact, has a lower total energy demand than quadruple glazing.

For Seattle, Krypton and Xenon infill Inflatable Glazing outperform all static glazing types. The air infill unit also performs well, exhibiting better performance than double glazing. In the context of Seattle, it would be more appropriate to compare Inflatable Glazing with double glazing instead of single glazing. **In this case, the total energy demand of an office building located in Seattle with double glazing (Ug=1.1) can be reduced by 33% when Inflatable Glazing is installed.**

In the case of San Jose, all Inflatable Glazing types, including the one with air infill, outperform the static glazing types. It would be suitable to compare the performance of Inflatable Glazing to single and double glazing in San Jose. **Consequently, the total energy demand of an office building located in San Jose with single glazing (Ug=5.8) or double glazing (Ug=1.1) can be reduced by 62% and 24%, respectively, when Inflatable Glazing is installed.**

Seattle	IG (Xenon)	IG (Krypton)	IG (Air)
HR++++	22%	17%	-11%
HR+++	18%	12%	-16%
HR++	33%	29%	5%
SG	73%	71%	61%

San Jose	IG (Xenon)	IG (Krypton)	IG (Air)
HR++++	18%	16%	5%
HR+++	20%	18%	7%
HR++	24%	22%	11%
SG	62%	61%	56%

Table 7.5 | Energy balance matrix - improvements with Inflatable Glazing in percentages (total energy demand) (author)

The energy balance is visually displayed below for comparison. To demonstrate the effectiveness of the air infill Inflatable Glazing in San Jose, it is compared to single glazing. A significant total energy reduction of 57% can be observed.

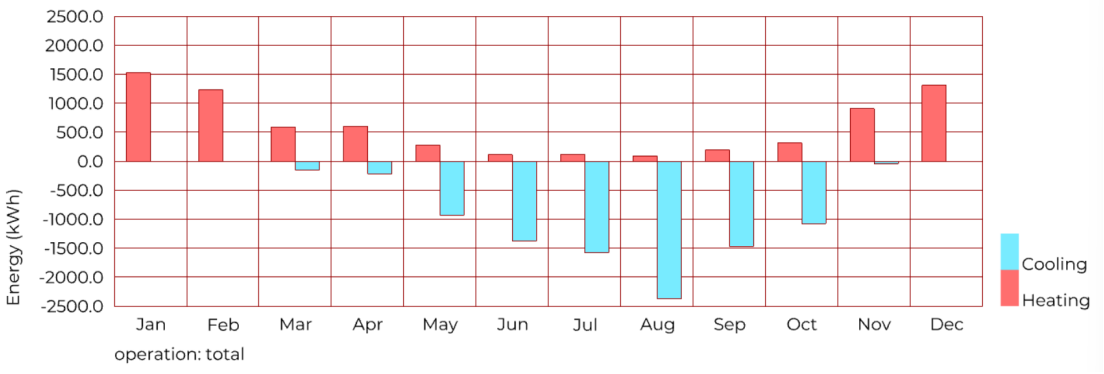

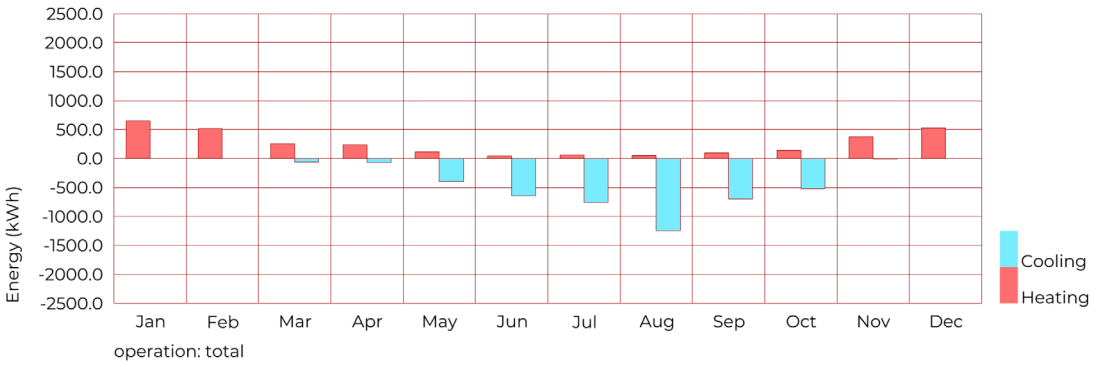

Figure 7.7 | Top: office building with single glazing equipped, bottom: office building equipped with Inflatable Glazing air infill (author)

7.7 Discussion

In conclusion, the energy model demonstrated the potential of Inflatable Glazing, but there is room for improvement in simulation. The boundary conditions were set for a fully glazed building with large overhangs to avoid direct solar radiation. However, the glazing has not been tested on a single orientation, such as only the northern facade. Additionally, there is potential to make better use of direct solar radiation by deflating the unit. This free solar gain is particularly useful in colder periods, as heat transmission would be faster with a deflated unit.

The energy model itself is based on the approximate heating hours of a specific location, so the schedule might not have been ideal for showcasing its full potential. The model only works in one direction and does not provide feedback to the schedule when, for example, there is a heating or cooling demand. For more accurate calculations, the results of each hour in the model should be sent back to the model and reevaluated. Similar to an interior and exterior sensor in real life, the model currently only considers the exterior sensor. If this were implemented, the model could better capitalize on solar gain, nocturnal cooling, or other optimizations.

Lastly, the model's results and numbers are quite impactful. However, it is important to consider that some of the high numbers result from comparing Inflatable Glazing to, for example, single glazing, which has highly conductive properties. Moreover, the best Inflatable Glazing unit is specified with xenon gas, which is an uncommon filling even for high-performance IGUs. Krypton infill already delivers a cutting-edge IGU standard. The energy analysis and air temperature analysis simply demonstrate that by changing the insulation value throughout the year, cooling capacity can be significantly reduced, and it is possible to outperform static glazing. Even with new technologies like static quadruple glazing, there are flaws, especially during hot seasons. The overall slowing down of heat transmission can be counterproductive.

8. Structural Performance

8.1 Developable Surfaces

Developable surfaces are a unique class of geometric shapes that can be formed by smoothly bending a flat, two-dimensional sheet, such as paper or thin metal, without stretching or compressing the material. These surfaces can be flattened back into a plane without distortion, and thus, they have zero Gaussian curvature. Common examples include cylinders, cones, and tangent developables.

The bending of thin glass follows the rules of developable surfaces because its material properties favor bending over stretching or compression. When bent, the glass experiences only curvature along one principal direction, leaving the other direction unchanged. This behavior minimizes the potential for fractures or deformations in the material. Consequently, the shaping of thin glass, like other developable materials, adheres to these geometric constraints to preserve its structural integrity and prevent breakage or warping.

As described by Neugebauer and Wallner-Novak (2019) to determine if a surface is “developable,” Gaussian curvature is used, which applies mathematical geometric principles to analyze 3D surfaces. Normal planes, defined by normal vectors perpendicular to the surface, intersect with surface geometries to create space curves. The minimum and maximum curvature values, or principal curvatures (k1 and k2), are obtained by analyzing other points on the surface. Gaussian curvature (K) is found by multiplying both principal curvatures and can be positive, negative, or neutral (zero). For a surface to be developable and suitable for manufacturing or processing from cold-bent thin glass, it must have zero Gaussian curvature.

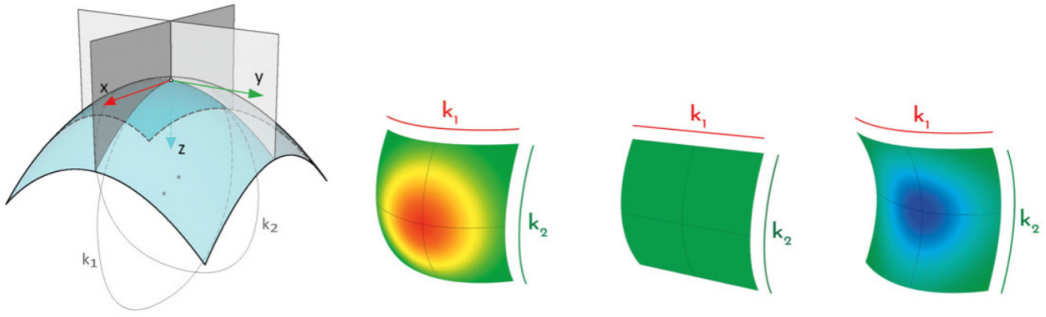

Figure 8.0 | Left: Gaussian curvature, Right: kind of gaussian curvatues ((Neugebauer & Wallner-Novak, 2019))

In the case of Inflatable Glazing the thin glass is going to be in a state of double curvature and thus might not follow the previously described zero-Gaussian curvature. A ring-on-ring test by Neugebauer (2016) involves placing a glass sample on a circular steel reaction ring and applying load through a steel loading ring until the glass breaks. This test aims to create a uniform tensile stress field inside the loading ring, independent of edge effects. This test other tests were performed to determine the the ultimate bending tensile strength of thin glass.

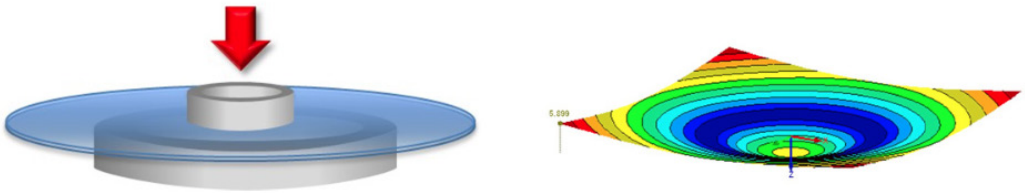

Figure 8.1 | Ring-on-ring test setup with steel loading rings and thin glass (Neugebauer, 2016)

As described by Neugebauer (2016) in the ring-on-ring test, various effects occurred due to the glass sample's deformation. Non-linear stability effects emerged at the edges, and large asymmetric deformations were observed at certain loading levels. Additionally, snap-through effects were noticed at the corners, caused by the glass's dead weight. The described imperfections can arise from factors like flawed test setups, irregular glass samples, and inaccurately centered load rings. The following graphic shows the deformation of thin glass in both FEA and a real setup.

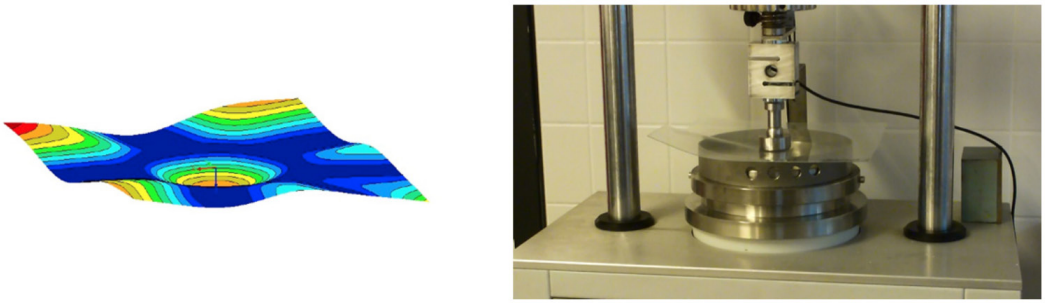

Figure 8.2 | Large deformations can be seen in both FEA and experiment setup (Neugebauer, 2016)

The experiment conducted by Neugebauer (2016) to determine the bending tensile strength demonstrates that glass can be distorted without breaking. This indicates that the material can accommodate slight double curvatures, making it suitable for Inflatable Glazing applications. The test setup by Neugebauer also revealed that reducing imperfections and ensuring precision enhances the resulting curvature. With Inflatable Glazing, the primary force comes from gas pressure, which ensures a uniform load application. However, the main challenge lies in the edge sealants' quality and purity.

8.2 Finite Element Analysis

Finite element analysis (FEA) is a powerful computational method used to simulate, analyze, and predict the behavior of complex physical systems under various conditions. The technique works by breaking down the system into smaller, more manageable components called finite elements. These elements are interconnected at specific points, known as nodes, creating a mesh that represents the geometry and properties of the entire structure (Fish & Belytschko, 2007).

FEA is widely used across many engineering disciplines, including mechanical, civil, aerospace, and biomedical engineering, to tackle problems such as stress analysis, heat transfer, fluid dynamics, and electromagnetic phenomena. By using FEA, engineers can optimize designs, identify potential failure points, and evaluate the performance of materials and structures under diverse loading and environmental conditions, ultimately leading to safer and more efficient products.

The process of finite element analysis typically involves creating a detailed geometric model, assigning material properties and boundary conditions, and discretizing the model into a mesh of finite elements. Once the model is prepared, mathematical equations representing the physical behavior of the system are solved numerically, yielding results that can be visualized and interpreted to inform design decisions or validate theoretical predictions (Fish & Belytschko, 2007).

FEA software and settings

SJ MEPLA is a specialized software tool designed for analyzing and designing glass structures. The software is particularly useful for calculating the load-bearing capacity, stability, and performance of glass components under various loading conditions, including wind, snow, and dead loads. One of the key advantages of SJ MEPLA is its ability to model and analyze different types of glass, including monolithic, laminated, and insulating glass units.

The software also accommodates various support conditions, such as point, linear, and continuous supports. Additionally, SJ MEPLA incorporates advanced calculation methods, such as linear and non-linear analysis, as well as the ability to account for geometric and material non-linearities. The software also adheres to international standards and guidelines, ensuring that the analysis and design are compliant with industry norms.

The following paragraph outlines the calculation setup. In general, all elements (thin glass and PMMA) have been calculated individually to determine the thickness, deformation and principal stresses for the final design:

1. Defining geometry: The first step involved defining the geometry size, which was in this case the pane size in x and y dimensions, as well as establishing the mesh element size for the pane. Generally, the panes were calculated using element sizes ranging from 25 to 50 mm.

2. Layers: The layers are created by the materials, in this case, the properties of AGC Falcon glass and generic PMMA. For interlayers, a PVB long-time loading layer has been applied. The subsequent table presents the values used:

	Modulus of elasticity	Possios ratio	Thickness	Density	Thermal expansion coefficient
	[N/mm²]	/	[mm]	[to/mm³]	[1/K]
AGC Falcon Glass	70000	0.21	x	2.48E-09	9.61E-06
PMMA	3300	0.45	x	1.18E-09	7.30E-05
PVB long-time loading	0.03	0.5	0.38	1.07E-09	8.00E-05

Table 8.0 | Material properties for FEA calculation (author)

3. Supports: Springs provide a flexible, punctual bearing method for supports, accounting for displacement and rotation in finite element mesh nodes. Springs can have movement stiffness in x, y, and z directions, as well as rotational stiffness around the x and y axes. Figure 8.3 shows the placement of the springs, always 150mm from the corner.

Elastic edge supports were chosen as the main support since they are used for system borders with elastic profiles or bonded materials. Unlike rigid edge supports, these allow for transversal and shear deformation consideration. Using the shear modulus, this boundary condition can also be applied to structural glazing. Additionally, contact conditions can be considered, allowing for lifting corners. Elastic edges act like simple supports (hinges) perpendicular to the edge.

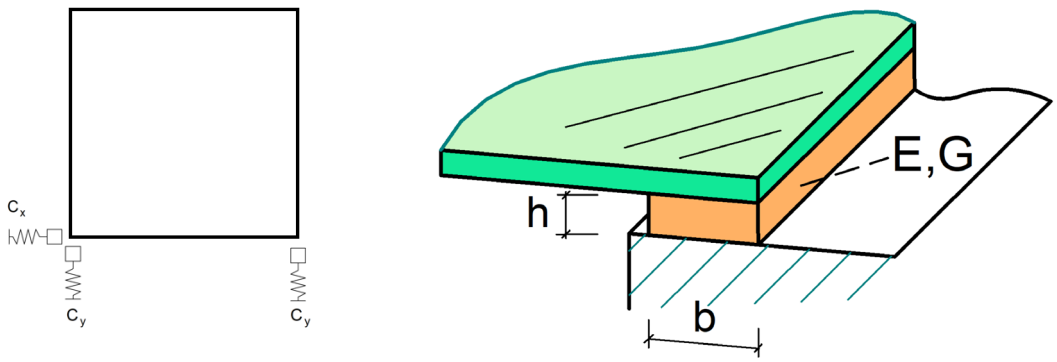

Figure 8.3 | Left: location of spring supports (Cy 150mm offset) - Right: Elastic edge supports (author & SJ Mepla)

4. Loads: To simulate pressure, a constant, uniformly distributed face load has been applied. Depending on the material thickness, this load has been adjusted between 2000 and 3000 Pa. The load has been applied in five steps to accurately simulate the inflation of the cavity (see Figure 8.4). The dead weight has also been taken into

account.

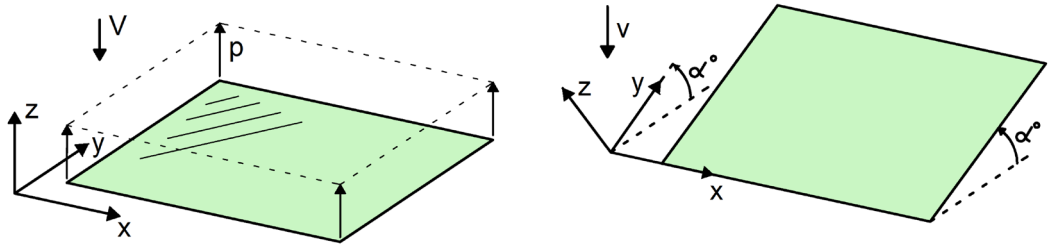

Figure 8.4 | Left: Constant uniformily distributed load - Right: Dead load (SJ Mepla)

5. Calculation: Some settings need to be adjusted before the simulation: geometrically non-linear analysis is necessary for glass calculations due to significant deformations, resulting in non-linear stress-strain behavior. Principal stresses should be enabled to identify maximum stress locations under loading. The calculation should also output deformation (w), elastic spring supports, and spring reaction forces.

The FEA model has now successfully been set up and the inputs for different setups can be made. The analyed panes are listed below.

- **Prototype (thin glass 500x500 t=0.7 and 1.1)**
- **Typical Office window dimension (thin glass PVB package, PMMA - 1500x3000)**
- **Residential window (thin glass PVB package, PMMA - 1200x1200)**

8.3 FEA Results

Prototype (500x500)

The thin glass dimensions delivered by AGC are 500x500mm Falcon Glass panes with the thicknesses 0.7 and 1.1mm. All panes have been chemically strengthened and came with a lasercut edge. The simulation has been performed with a 25mm mesh element size. The following graphics shows the results for both 0.7mm and 1.1mm.

AGC Falcon Glass: 2000Pa + self load in 5 steps

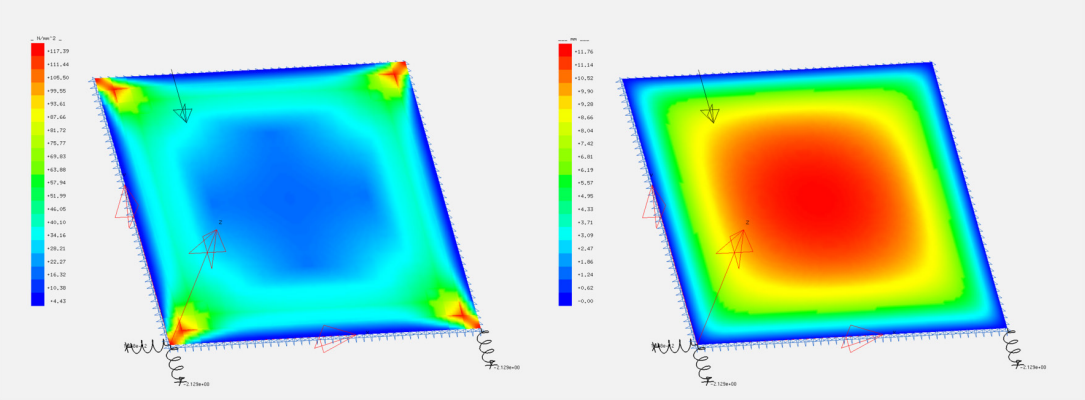

Thickness: 0.7mm

Deformation: up to 12mm

Principal stress: up to 117N/mm² in the corners

Figure 8.5 | FEA simulation 500x500mm, t= 0.7mm (author, obtained through SJMEPLA)

AGC Falcon Glass: 3000Pa + self load in 5 steps

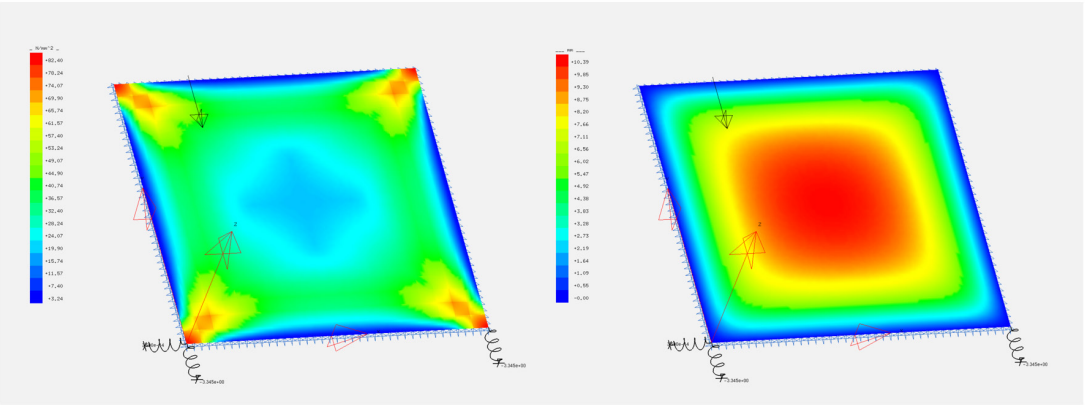

Thickness: 1.1mm

Deformation: up to 11mm

Principal stress: up to 83N/mm² in the corners

Figure 8.6 | FEA simulation 500x500mm, t= 1.1mm (author, obtained through SJMEPLA)

In Figures 8.5 and 8.6, it can be observed that the highest stresses occur at the corners of the pane. The edges and the center of the pane experience relatively low stresses. It can be assumed that these stresses also indicate the extent of curvature. As the thickness of the pane increases, the stresses are reduced. Pressure of 2000-3000 [Pa] should be adequate to achieve the desired deformation of around 12mm. This would equal to 0.02-0.03 [bar] using a bicycle pump or air compressor.
The PMMA for the prototype has not been calculated because the design thickness of 15-20mm is similar to the real-life dimensions of the larger panels. In this case, there would be minimal deformation due to air pressure.

Typical office window dimensions (1500x3000)

For the office window calculation, the deformation of the PMMA pane is taken into account, as the deformations due to wind loads can be quite significant. The allowed deformation should be anywhere between L/100 and L/250. The following outcomes for PMMA and thin glass are shown in Figure 8.7.

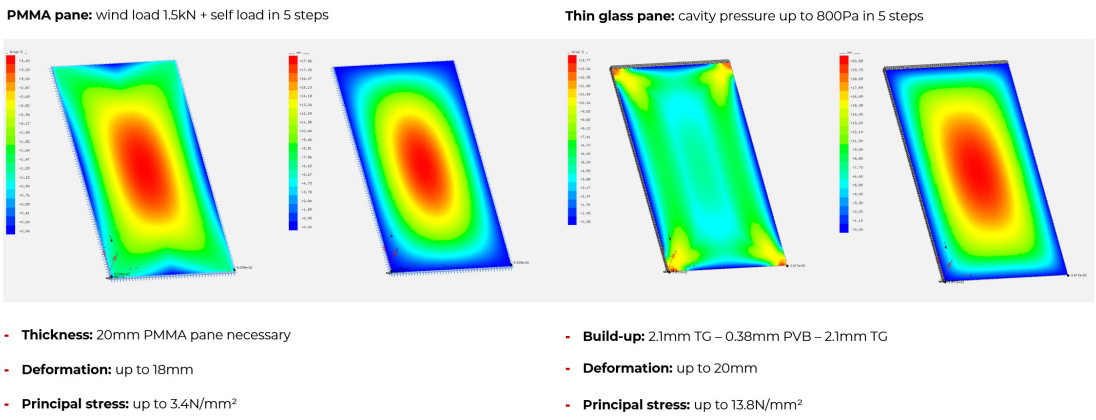

Figure 8.7 | FEA simulation 3000x1500mm (author, obtained through SJMEPLA)

The results for the office window indicate that a 20mm PMMA would be necessary to withstand the wind load. Thin-glass has been found to be optimal at around 800 Pa with a 4mm thickness. For safety reasons, the thin glass should be laminated if it is in close proximity to occupants or pedestrians. Therefore, two 2.1mm thin glass panes should be laminated with a PVB interlayer. It can be observed that with larger panes, the principal stresses are significantly reduced since the curvature radii are lower to achieve the same deformation as with smaller dimensions. Now, cavity widths between 0 and 20mm are possible, depending on the inert gas used. The resulting glass edge design is the following:

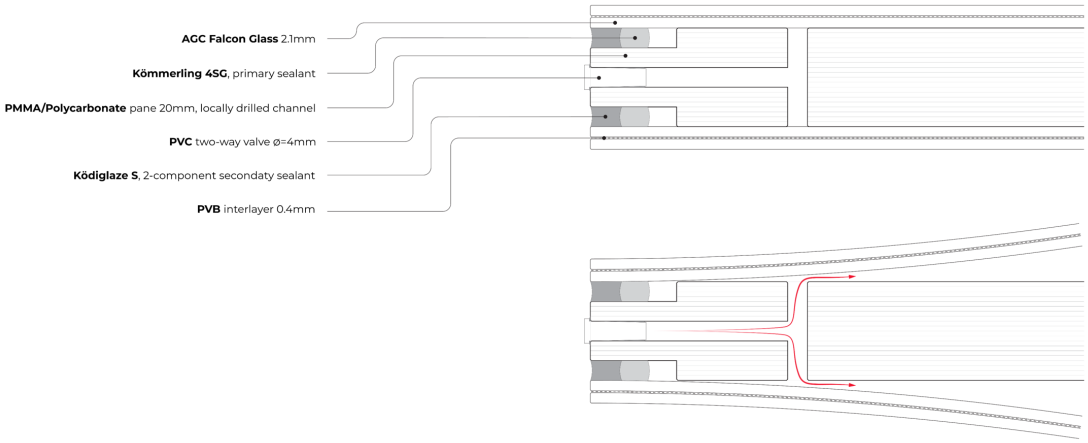

Figure 8.8 | Edge detail of the office window dimensions (1500x3000mm) Inflatable Glazing (author)

Residential window (1200x1200)

For the residential window the same settings apply than to the office window dimensions. This time however, the shape of the window is square. The following figure shows the FEA analysis of the residential window:

PMMA pane: wind load 1.5kN + self load in 5 steps

Thin glass pane: cavity pressure up to 800Pa in 5 steps

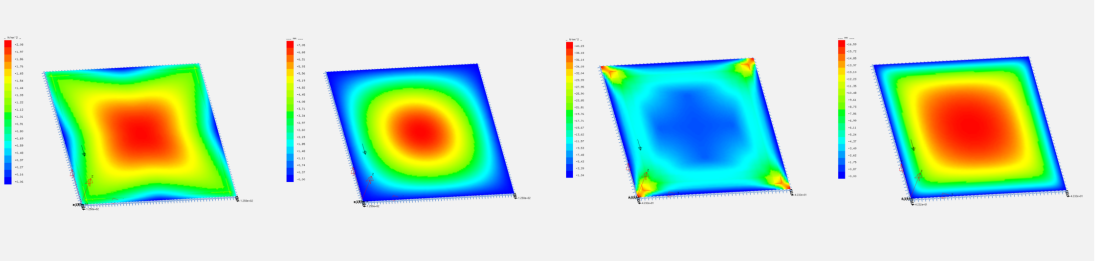

- **Thickness:** 15mm PMMA pane necessary
- **Deformation:** up to 7mm
- **Principal stress:** up to 2.1N/mm²

- **Build-up:** 1.1mm TG – 0.38mm PVB – 1.1mm TG
- **Deformation:** up to 16mm
- **Principal stress:** up to 40.2N/mm²

Figure 8.9 | FEA simulation 1200x1200mm (author, obtained through SJMEPLA)

The results for the residential window show increased principal stresses due to its smaller dimensions compared to the office window. However, it can be observed that the square glass unit has significantly lower stresses at the center of the pane. One could assume that the square shape is more beneficial for inflation than a rectangular ratio. The principal stresses are also relatively high due to the reduced thin glass thickness. The laminated panes are each 1.1mm thick with a 0.38mm PVB interlayer. The resulting edge design can be seen in Figure 8.10.

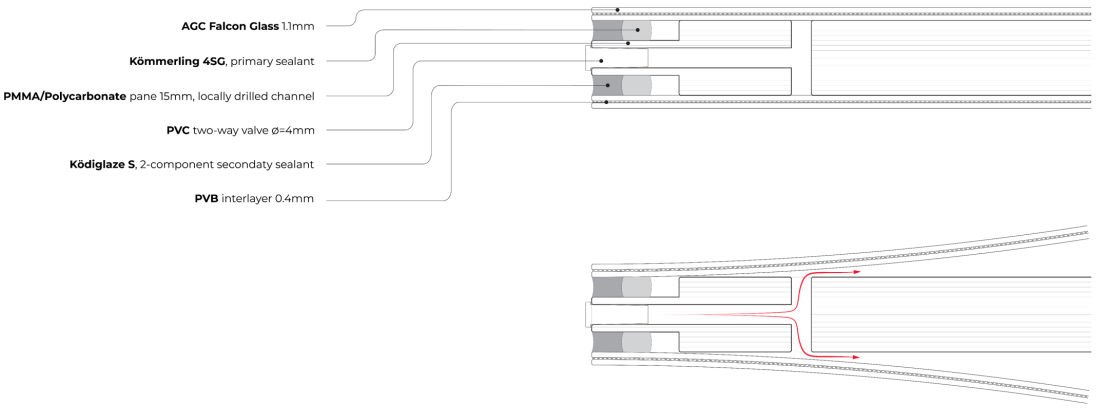

Figure 8.10 | Edge detail of the residential window dimensions (1200x1200mm) Inflatable Glazing (author)

8.4 Weight Comparison

The weight of Insulated Glass Units (IGUs) is a crucial aspect to consider in the design process due to several factors. Firstly, labor requirements are impacted by the weight of the glass units, as heavier panes demand more manpower to install, increasing labor costs and time. Additionally, there are health and safety regulations in place regarding the maximum weight that workers can handle, which must be taken into account.

Transporting heavier IGUs also presents logistical challenges, such as requiring specialized vehicles or equipment for handling and potentially increasing fuel costs. In terms of manufacturing, heavier units may necessitate more robust and sophisticated machinery to process, assemble, and maneuver the glass, leading to increased capital costs.

Furthermore, the overall building structure must be designed to accommodate the weight of the IGUs, which can influence material choices, structural reinforcement, and overall costs. Therefore, carefully considering the weight of IGUs in the design stage can lead to more efficient, cost-effective, and safe solutions in both construction and operation.

The following table outlines a weight comparison for the two discussed window sizes, comparing the weights of triple glazing versus Inflatable Glazing with a PMMA and a glass core.

Glazing type	Build-up	Weight per m2	1200x1200	3000x1500
	Composition	[kg/m2]	[kg]	[kg]
Double glazing	**6** - 15 - **6**	30.0	43.2	135.0
Triple glazing	**6** - 12 - **4** - 12 - **8**	45.0	64.8	202.5
Triple glazing (laminated)	**8** - 16 - **6** - 16 - **44.2**	55.0	79.2	247.5
Triple glazing (double-laminated)	**44.2** - 12 - **6** - 12 - **66.2**	65.0	93.6	292.5
Inflatable Glazing PMMA(Office)	**22.2** - x - **20.PMMA** - x - **22.2**	43.6	62.8	196.2
Inflatable Glazing PMMA (Residential)	**11.2** - x - **15.PMMA** - x - **11.2**	27.7	39.9	124.7
Inflatable Glazing Glass (Office)	**22.2** - x - **8** - x - **22.2**	40.0	57.6	180.0
Inflatable Glazing Glass (Residential)	**11.2** - x - **8** - x - **11.2**	30.0	43.2	135.0

Table 8.1 | Weight comparison of various IGU compositions versus Inflatable Glazing (author)

From Table 8.1, it can be observed that Inflatable Glazing, whether it has a PMMA core or a glass core, is lighter in weight compared to standard triple glazing. Moreover, the residential PMMA unit is even lighter than standard double glazing. Considering that Inflatable Glazing features laminated glass on both the interior and exterior sides, it has also been compared to acoustic triple glazing. A weight reduction of over 50% can be achieved when comparing the residential PMMA glass unit to a double laminated TGU acoustic glass.

An overall weight reduction from Inflatable Glazing to standard IGUs is difficult to determine, as the composition of glass panes is always project-specific. Factors such as thermal requirements, acoustic insulation, structural requirements, safety/security, and aesthetics primarily influence the build-up of an IGU.

Upon examining the thicknesses of the various glazing types presented, it becomes clear that the double glazing, at 28mm thick, matches the thickness of the thickest Inflatable Glazing (office). This makes it particularly attractive for renovation projects that aim to maintain the existing frame. Notably, the thinnest Inflatable Glazing presented has a thickness of just 12mm.

8.5 Discussion

The FEA analysis provided a rough understanding of the required thicknesses, deformations, stresses, and pressures. The results of the FEA were useful in specifying the edge details of the units. Additionally, the sizing of panels and upscaling of the prototype were investigated. The principal stress pattern offers insight into potential curvature locations; however, the inflation geometry cannot be determined from the analysis.

Several aspects have been identified that require further research. Predicting the edge support of the entire unit is challenging, and edge deformation might affect the clamping/dry-glazing of the pane. Moreover, the edge support of individual panes has only been roughly calculated. The primary and secondary sealants would need to be modeled in a separate calculation (e.g., Ansys or Abaqus) to determine the shear forces experienced by the spacer due to frequent inflation and deflation.

Another undetermined parameter is the stiffness of the inflated glass. Stresses have only been calculated in a windless state. In reality, the panel should withstand forces up to 1.5kN from the exterior side without significant deflections of the thin glass. Additionally, the durability of the PVB layer needs to be investigated. While it has been calculated with a long-time loading layer, high movements will occur, resulting in substantial shear forces.

9. Prototyping

The prototyping phase was crucial for the proof of concept and determining the inflation geometry, curvature, and deformation of the unit. Several different prototypes were built with various edge designs, materials, and dimensions to identify the best configuration. The final outcome was a fully functional prototype and 3D scans that helped evaluating the inflation geometry. The material suppliers Kömmerling | H.B. Fuller and AGC supported the design phase with technical input and manufacturing advice. Additionally, they provided state-of-the-art materials to construct the prototypes. The companies Röhm and Innotech-Rot offered discounts on their products to support the prototyping phase of Inflatable Glazing.

The manufacturing of the unit was primarily accomplished with the help of Marcel Bilow in his workshop, where the precision of cutting and drilling was a high priority. The first assembly of a glass unit, as well as the initial test, was conducted in his workshop. Later on, the TUDelft ThinkLab was used to assemble the pre-cut/drilled units.

9.1 Thin Glass Double Curvature Test

The initial test to determine the extent of double curvature achievable with thin glass involved clamping and bending a 600x600 mm, 0.7 mm-thick Corning glass sheet on a table. All corners have been moved a few millimeters towards the center of the pane. Thus, a consistent double curvature has been achieved. The chemically strengthened glass featured ground edges. While the test did not yield a comprehensive understanding of thin glass bendability, it provided insight into the possibility of attaining a cavity width of approximately 16 mm. The constraints have been setup in an FEA and the deformation and principal stresses showed promising results.

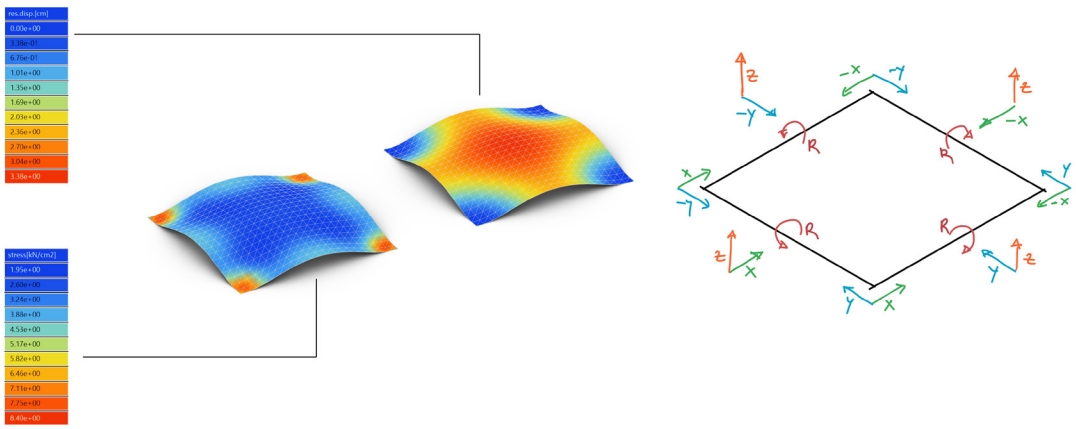

Figure 9.0 | FEA of the first clamping test with thin glass (author)

The following picture shows the clamped corners of the thin glass pane. A 22mm cavity was achievable with minimal force. The curvature of the glass seemed symmetrical.

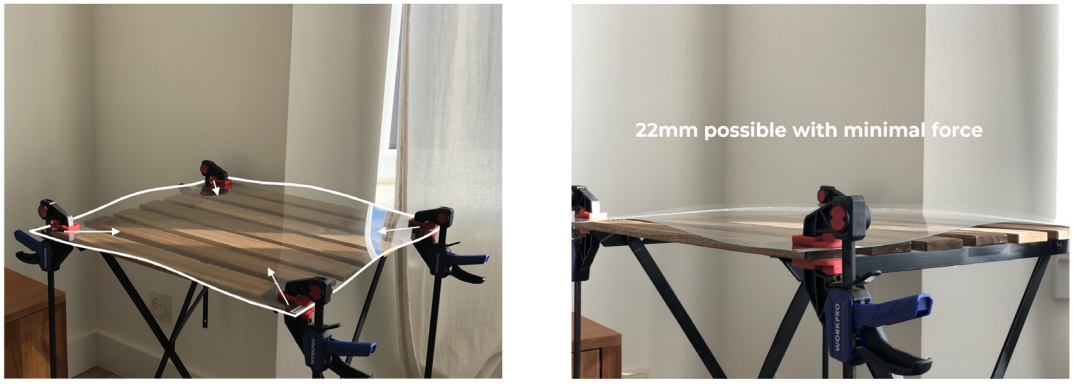

Figure 9.1 | Thin glass clamping test (author)

9.2 PETG Prototype

The first prototype was constructed to examine the behavior of thin glass when fixed at all corners and edges. Additionally, the edge design underwent testing for the first time. Since the project was still in its early prototyping stage, transparent PETG was utilized instead of thin glass. The behavior of the thin glass during inflation and the risk of glass bursting were uncertain at the time. The core pane was assembled using MDF plates, a drilled T-channel, and a Scladerland valve. Finally, ordinary sanitary silicone from a local DIY store served as the edge sealant. The overall thickness of the unit measured 24.5mm (refer to Figure 9.2).

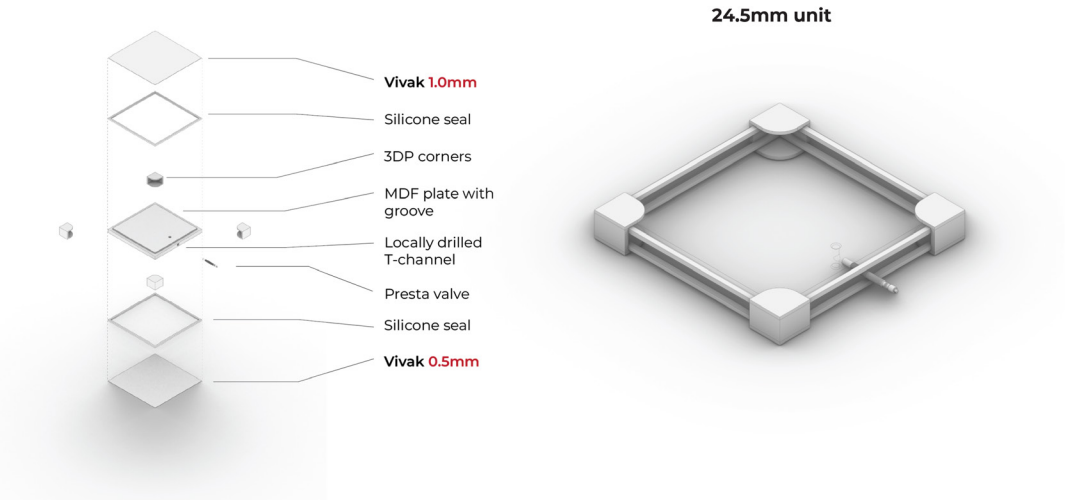

Figure 9.2 | Left: Exploded view of the individual components - Right: isometric drawing of the final setup (author)

The prototype was constructed using a 0.5mm PETG pane and a 1mm pane on opposite sides. Upon inflation, a pillowing effect was observed. This effect was amplified when stripes of tape were applied, and the shadow was projected onto the MDF plate. When the valve was reopened, the PETG quickly returned to its original position, and the panes came into direct contact again. A slight deformation of the sealant was also noticeable during the inflated state. Unfortunately, the unit was not entirely airtight, as the MDF may have been permeable enough to cause deflation after a few minutes. The following photos illustrate the relaxed and inflated states on both sides of the unit, with approximate deformations measured in millimeters.

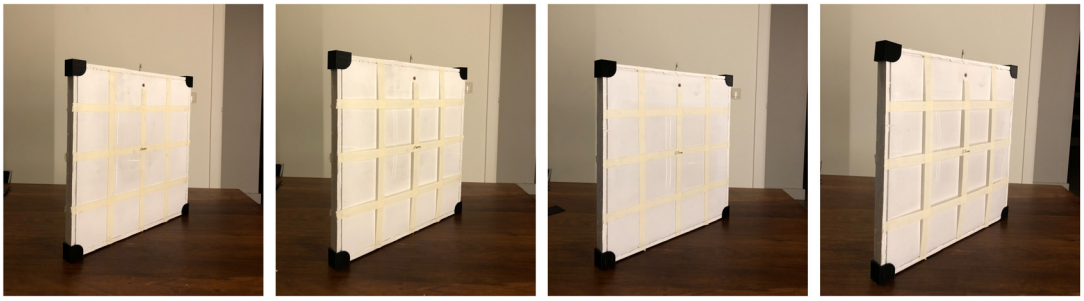

1.0mm Vivak
8mm deformation

0.5mm Vivak
12mm deformation

Figure 9.3 | Left: 1mm PETG with an 8mm deformation - Right: 0.5mm PETG with a 12mm deformation (author)

9.3 Annealed Thin Glass Prototype

The second prototype was designed to investigate the previously discovered pillowing effect, but now using thin glass. The edge has been redesigned as a one-sided unit (see Figure 9.4). The air supply has been moved to the bottom of the pane to ensure a properly sealed and airtight edge bond. Additionally, a foam bead has been glued to the corner of the groove. This resulted in a so-called “Zweiflankenhaftung,” which ensures that instead of three contact surfaces, only two contacts are structurally bonding. Consequently, this bond acts like a hinge and enhances the bendability of the glass.

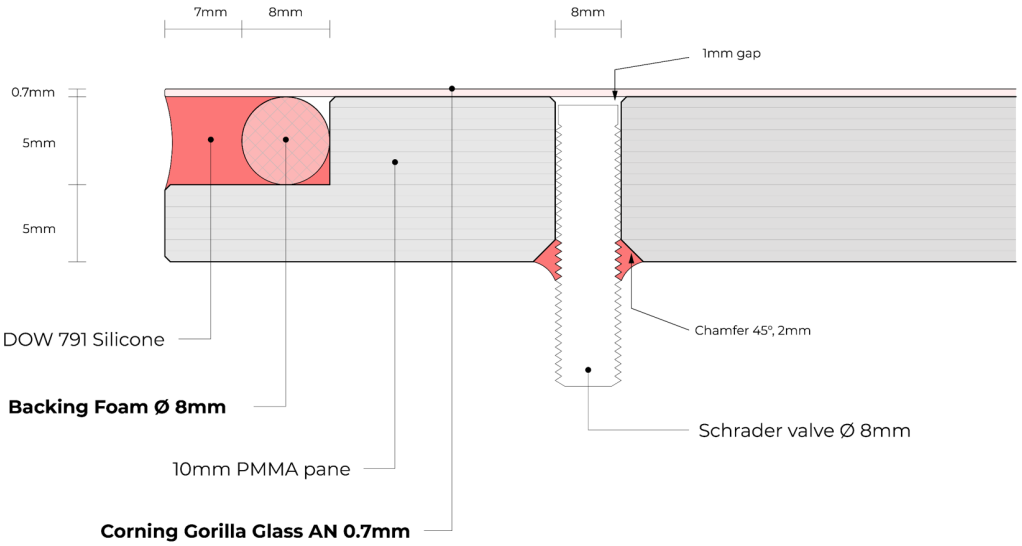

Figure 9.4 | Edge design of the one-sided prototype (author)

The following series of pictures shows the manufacturing process of the first glass unit:

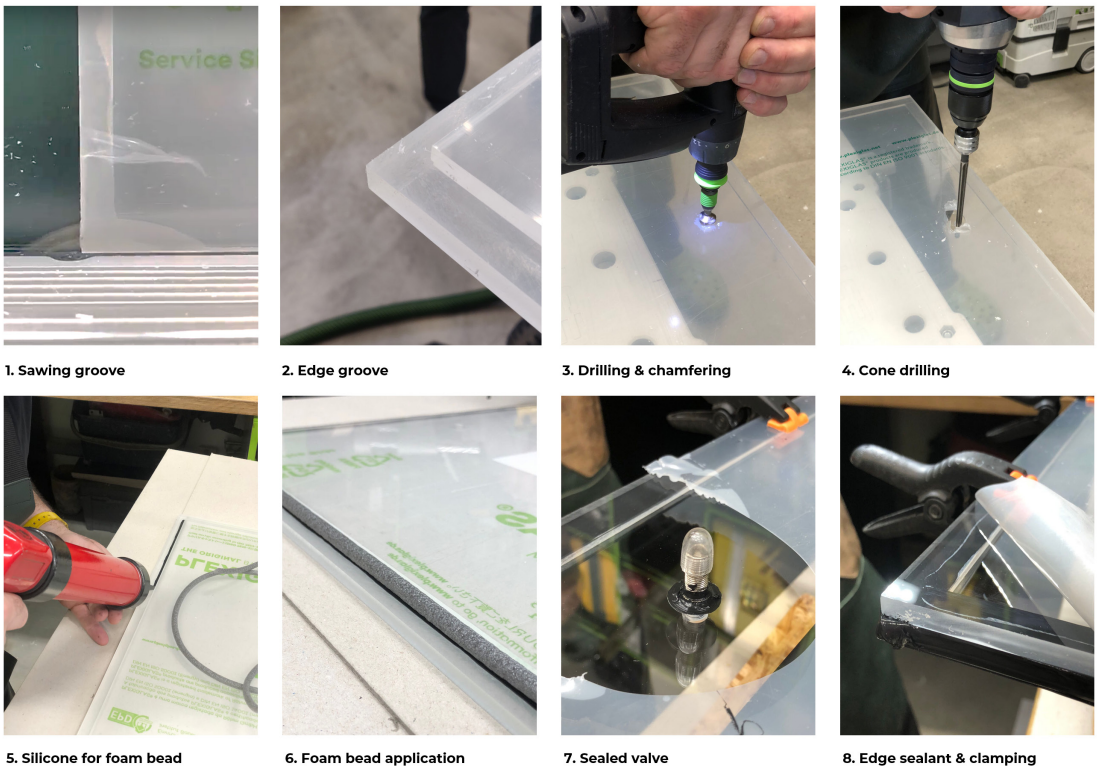

Figure 9.5 | Photo series showing manufacturing process of the first unit (author)

The glass for the prototype was a Corning 500x500, 0.7mm annealed pane with laser-cut edges. The silicone for the edge bond was the DOW 791 glass weather proofing silicone. After a curing period of 72 hours, the prototype was ready for testing. The prototype was positioned on four wooden blocks, and a bicycle pump was attached to the unit from below (refer to Figure 9.6). Subsequently, pressure was gradually applied to the cavity. After a few pumps, the curvature of the glass became clearly visible. Prior to shattering, the cavity expanded to approximately 10-15mm in width.

Figure 9.6 | Photo series showing inflation process of the first unit (author)

A slow-motion video captured the inflation process of the thin glass unit. Frame-by-frame analysis revealed the precise moment when the glass shattered. The crack originated from one of the corners and propagated towards the other corners. The previously conducted FEA also indicated that the stresses would be highest in the corners. Additionally, the curvature of the pane can be observed due to the reflections on the pane (see the grey lines in the first image of Figure 9.7).

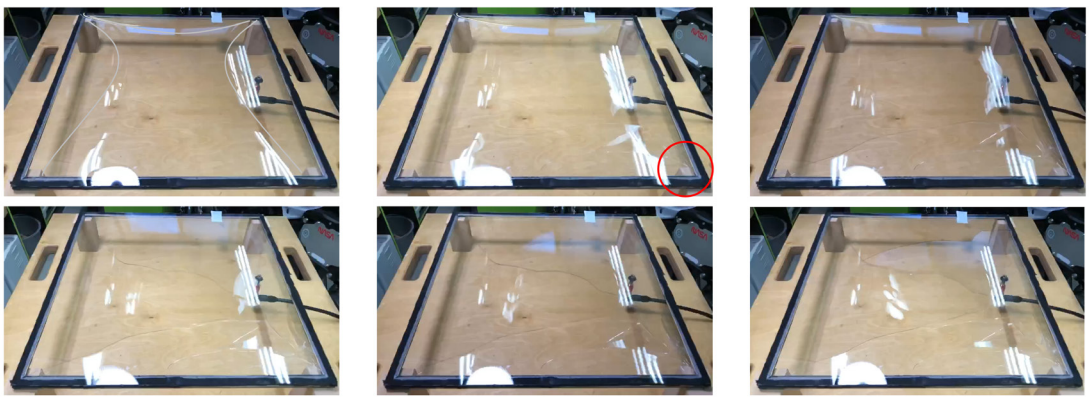

Breakage Frames: cracks emerged from corner bottom right

Figure 9.7 | Frames when crack emerged on the thin glass pane (author)

The break pattern is visible in Figure 9.8. However, more surprisingly, the silicone on the inner side of the edge bond did not cure at all. Only the outer portion of the unit exhibited a cured seal. Half of the sealant did not receive sufficient air to solidify completely. Consequently, it became evident that the next prototype would require a solution for the edge bond.

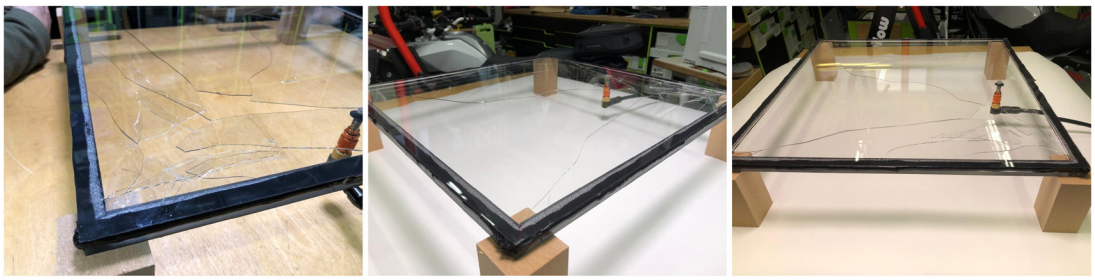

Figure 9.8 | Break pattern of the annealed glass pane (author)

9.4 One-Sided 3D Scannable Prototype

Since the setup from the previously described prototype proved to be working, the PMMA pane could be reused. Therefore, the residual glass pieces and silicone were removed using a cutter knife, and the surfaces were sanded down and cleaned with isopropyl alcohol. Another pre-cut PMMA pane, measuring 600x600mm, was prepared. Two different edge designs were planned for the one-sided prototype to compare the differences in inflation.

The 600x600 unit was constructed similarly to the edge design shown in Figure 9.4, but with chemically strengthened glass from Corning used instead.

Marco Zaccaria, from the thin glass research department of AGC, joined the project during the design phase, providing valuable input and offering to ship the desired thin glass to complete the project. A stack of both 0.7 and 1.1mm AGC Falcon Glass with chemical strengthening and laser-cut edges was produced and shipped to TU Delft. With the new glass, the second prototype could be completed.

For the second unit, a freshly produced 0.7mm AGC Falcon glass was used. This unit also incorporated a polyisobutylene (PIB) strip, typically employed as a primary seal in IGUs. The material is highly impermeable to gas, ensuring long-lasting airtightness. It has a soft consistency and can easily be applied by hand to the panes (see Figure 9.11). The sealant has been provided for free by Premseal based in the UK. It has a dynamic tensile adhesion of 0.2N/mm2 and a dynamic shear adhesion of 0.22N/mm2.

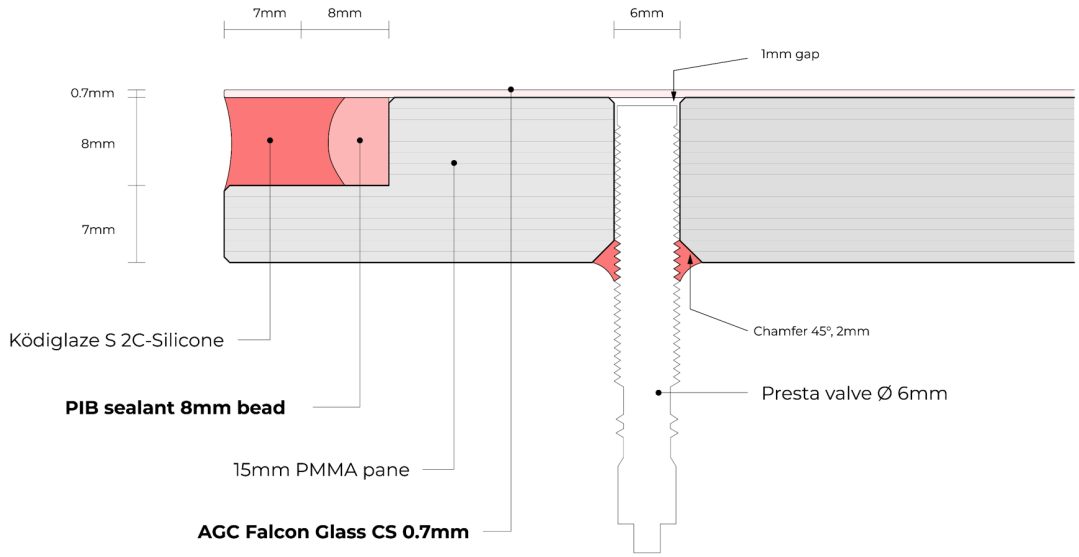

Figure 9.9 | AGC Falcon Glass prototype (author)

Finally, the edge seal remained a primary concern. After consultation from Christian Scherer from Kömmerling | H.B. Fuller, it became evident that a two-component silicone needed to be used to ensure a properly cured edge seal. Kindly, he sent over two boxes of Ködiglaze S, a two-component silicone featuring a double cartridge system with the required self-mixing extruders. The necessary silicone dispensing gun was ordered from Innotech-Rot, the main supplier for Kömmerling | H.B Fuller. The pneumatic dispensing gun VBA (MR) 400 A Alu Frame, manufactured by COX, is capable of extruding the Ködiglaze Silicone with a mixing ratio of 1:10 and offers adjustable extrusion speed (see Figure 9.10).

Figure 9.10 | Left: Ködiglaze S two component silicone with self-mixing extruder (author), Right: VBA (MR) 400 A Alu (Innotech-Rot)

Prototyping started with cleaning the PMMA panes and thin glass panes to achieve an almost sterile condition. This step is essential for removing any dust or particles that could end up in the cavity, as even the smallest grains can cause the glass to shatter if local pressure is applied to the unit. Consequently, both the working area and the panes were cleaned with compressed air. Subsequently, the panes were cleaned with 99% isopropyl alcohol, followed by glass cleaner, and wiped with

a microfiber cloth (see Figure 9.11). Afterward, the PIB seal was directly applied to the groove, and the thin glass pane was placed onto the PMMA pane.

Figure 9.11 | ThinkLab setup: cleaning process with compressed air, alcohol and glass cleaner. Right: PIB seal application (author)

After positioning the AGC Falcon Glass on the PMMA pane, the pneumatic silicone gun was used to fill the groove with Ködiglaze silicone. The groove has then been taped to ensure constant contact between the silicone and both panes. The valve was coated with the two-component silicone and inserted into the pre-drilled channel. The silicone on both panes was then left to cure for 72 hours.
Subsequently, a self-adhering PVC film was carefully placed on the glass to prevent glass fragments from flying off in the event of shattering. To make the prototype 3D-scannable, Bertus Naagen from the CDAM at Industrial Design advised spray painting the surface, as transparent materials are difficult to scan (see Figure 9.12).

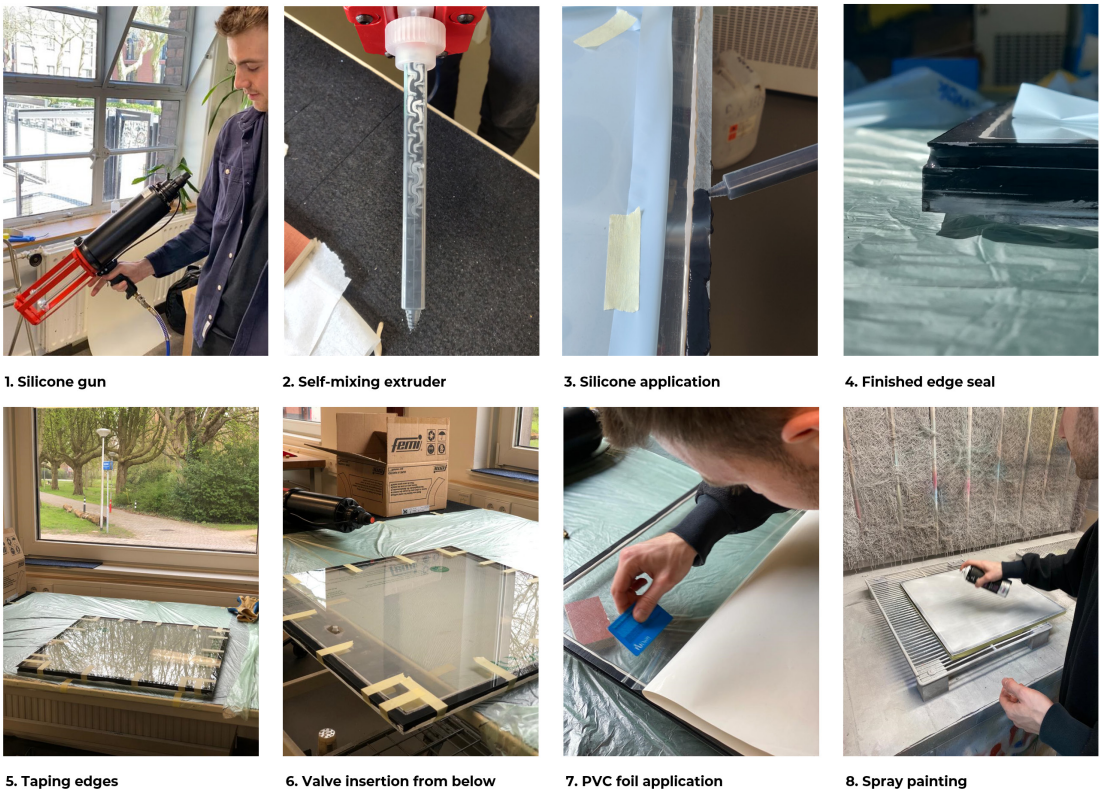

Figure 9.12 | Assembly of units + preparation for 3D scanning (author)

9.5 3D Scanning

After the paint on both units had dried, they were carefully transported to the Industrial Design Faculty. Bertus Naagen, an expert in 3D scanning, managed the entire 3D scanning process. He began by drawing random lines on both prototypes, providing the 3D scanner with more context for orientation. The scanner used was the Artec Eva, a handheld device with a point accuracy of up to 0.05mm and a resolution of up to 0.2mm. A powerful computer was connected to the 3D scanner, and the unit was placed on an automatically rotating table (Figure 9.13).

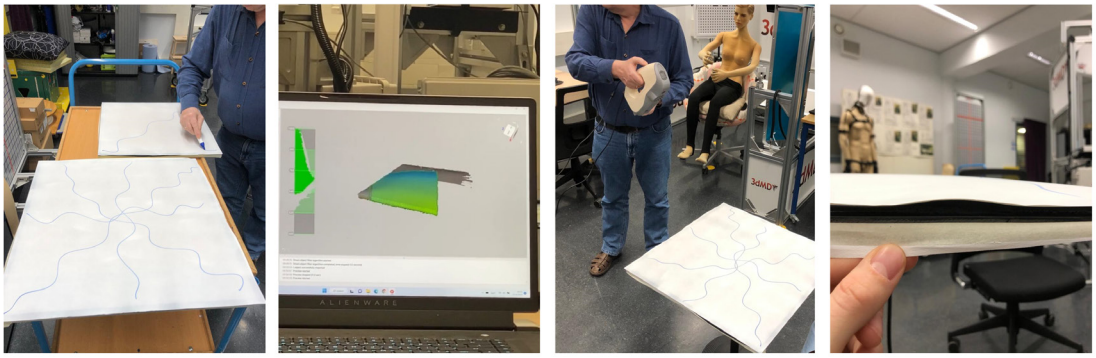

Figure 9.13 | 3D scanning by Bertus Naagen in the CDAM - right: flaw of the silicone in the first prototype (author)

The 3D scan of the first unit (600x600mm unit with Corning glass) was conducted in five steps of inflation. First, the relaxed state was scanned, and then progressively more air was pumped into the cavity in each subsequent step. The results from the first prototype revealed a flaw in the silicone. Since it was assembled first, it is likely that the mixture of silicone and additive was extruded in an undesirable ratio. This user error caused the silicone to be too flexible in that section of the edge. The bulging of the glass can be seen in Figure 9.14. However, the glass did not break in either prototype.

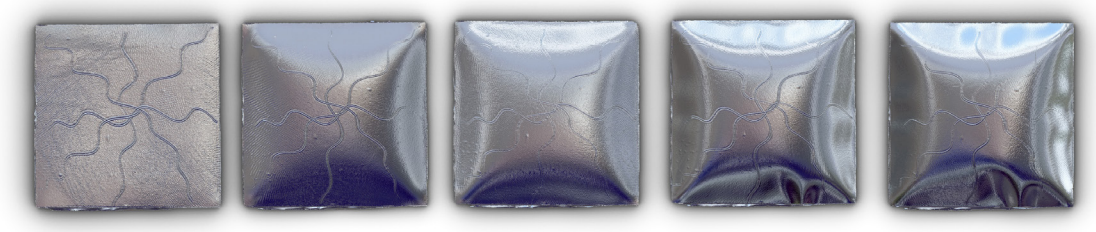

Figure 9.14 | Analysis of Corning prototype in Rhino with environment map - flaw in silicone evolved in the 4th inflation step (author)

AGC Falcon Glass Prototype

The second prototype has been scanned and appeared to be flawless. The prototype has been inflated to about the same pressure as in step 4 of the previous scan. After that, the sealant lost adhesion to the PMMA and caused the unit to deflate. The graphic below shows the high resolution scan of the inflated AGC Falcon Glass unit.

Figure 9.15 | Inflatable Glazing with AGC Falcon Glass scan - cleaned mesh with environment map (author)

Deformation

Both units has been imported into Grasshopper as described in Chapter 6. The meshes have been deconstructed and the center points of each mesh face was determined in its x,y,z coordinates. The z-coordinates were used to measure the deformation of the unit. The following graphic shows the deformation analysis of the AGC pane and the Corning pane.

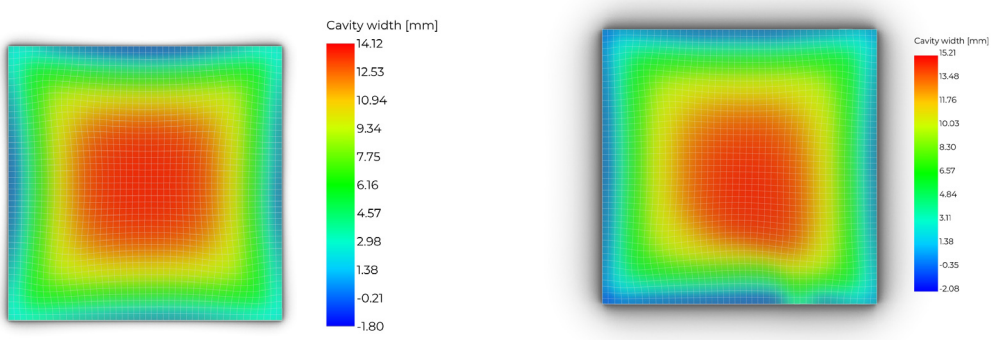

Figure 9.16 | Left: Deformation AGC pane - Right Deformation Corning pane (with edge flaw) (author)

Both thin glass panes reach a maximum deformation of around 15mm. Interestingly, the edge curvature of both panes seem to be different. The AGC pane has slightly higher corners than the edges, whereas the Corning pane seems to have fairly straight edges and corners. When looking at both panes in a close-up it is perceivable that the corners tend to bend downwards a little bit. It can be observed that the AGC thin glass also has a more conistent curvature over the length of the edge, even though it was expected that the larger pane would easier accomodate that. However, the flaws in the Corning pane are most probably traced back to the user error in assembly. Following grapgic shows the edge deformations of both panes in an elevation. The curvature has been scaled by x3 to make the edge condition more visible. The arrows indicate the movement of the edges and corners during inflation. Thus, the silicone around the edges experienced compression while the silicone at the corner has been streched.

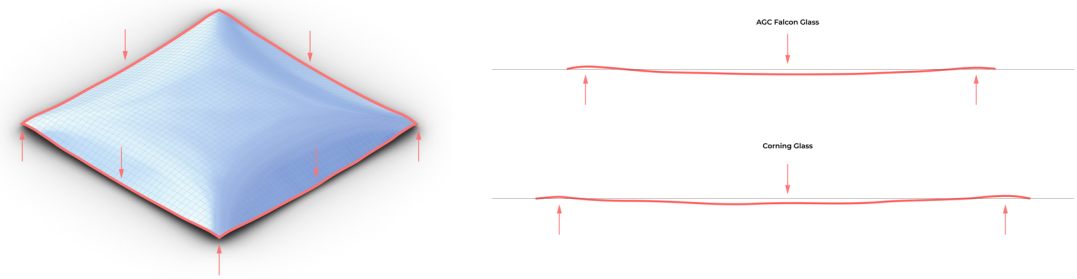

Figure 9.17 | Left: Isometric Falcon Glass edge deformation - Right: Elevation edge deformation. Both drawings scaled x3 (author)

Curvature

The curvature analysis shows the mean curvature across the thin glass surface. For this analysis the AGC Falcon Glass prototype has been used since the overall curvature is more consistent.

Mean curvature analysis on meshes is a method used to examine the local shape and smoothness of 3D surfaces represented by a collection of vertices, edges, and faces. This analysis computes each vertex's mean curvature (H) by approximating the local surface properties. The mean curvature is defined as the average of the principal curvatures (k1 and k2), which are the maximum and minimum curvatures at a point:

$$H = (k1 + k2) / 2$$

The unit 1/m (inverse meters) is used to express curvature because it represents the inverse of the radius of a circle that best approximates the local surface at a given point.

The following graphic shows the outcome of the curvature analysis. Interestingly, the curvature pattern and the prinicpal stress pattern is quite similar. High curvature regions can lead to stress concentrations, as the local shape affects how forces are distributed and absorbed, resulting in a similarity between the two patterns .

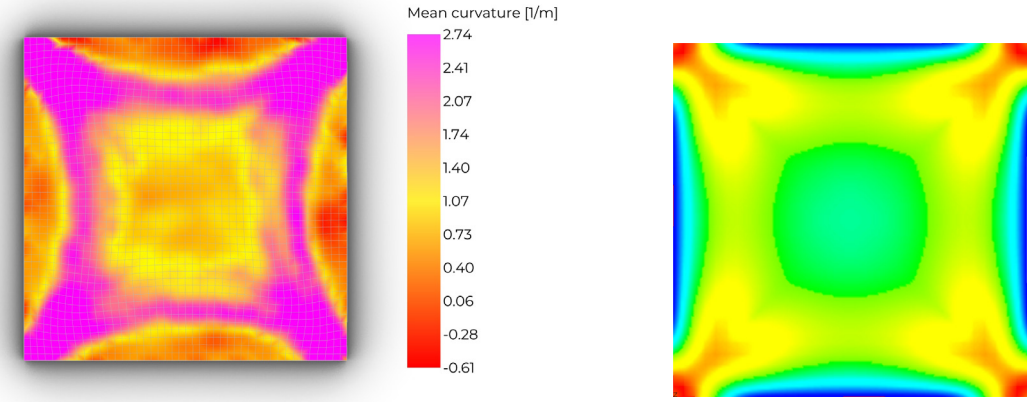

Figure 9.18 | Left: Mean curvature analysis from 3D scan - Right: Principal stress pattern obtained from FEA (author)

Finally, for visual examination a zebra analysis has been performed. It is a visualization technique that helps perceive curvature by applying a pattern of alternating light and dark stripes on a 3D surface. The stripes bend and distort according to the surface's curvature, emphasizing the changes in shape. This technique enhances the ability to visually identify high and low curvature areas and better understand the surface's overall geometry.

Figure 9.19 | Zebra stripes analysis - vertical and horizontal pattern. (author)

9.6 Final Prototype

The prototype showcases a two-sided build-up with a similar edge detail to the prototypes outlined in Chapter 8. The one-sided AGC glass prototype with the PIB seal from previous testing was found to be the most effective. Consequently, the edge is designed with the PIB seal, imitating the 4SG thermoplastic spacer from Kömmerling. For the secondary seal, the Ködiglaze Silicone is used, as it would be in an actual product. For the possibility of an exhibition and to ensure safety, the prototype is fully made from PMMA. It was found that the deformation behavior and the resulting reflections of PMMA are similar to the ones of thin glass. The final PMMA edge detail can be seen below (see Figure 9.20).

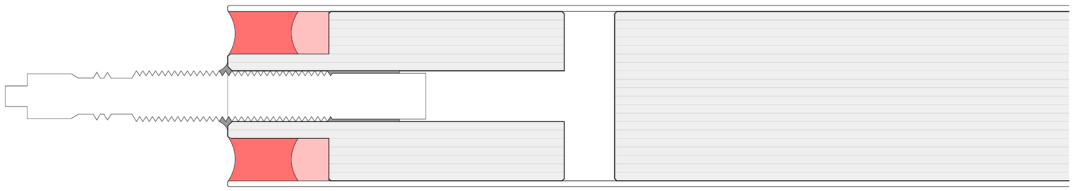

Figure 9.20 | Final prototype - glass edge detail (author)

For showcasing, the prototype is placed in a wooden frame. The dimensions of this frame are based on the FWS 50 Schüco system. For replicating the gaskets, an EPDM door sealant is used. This demonstrates how the prototype behaves in a dry-glazed system. Also, the prototype helps to see accurate reflections and determine how they change from different angles. It can be checked if a lensing effect occurs due to the curved panes. Finally, the prototype can be evaluated on aesthetic appeal and potential uses in architectural applications (See Figures on the next pages).

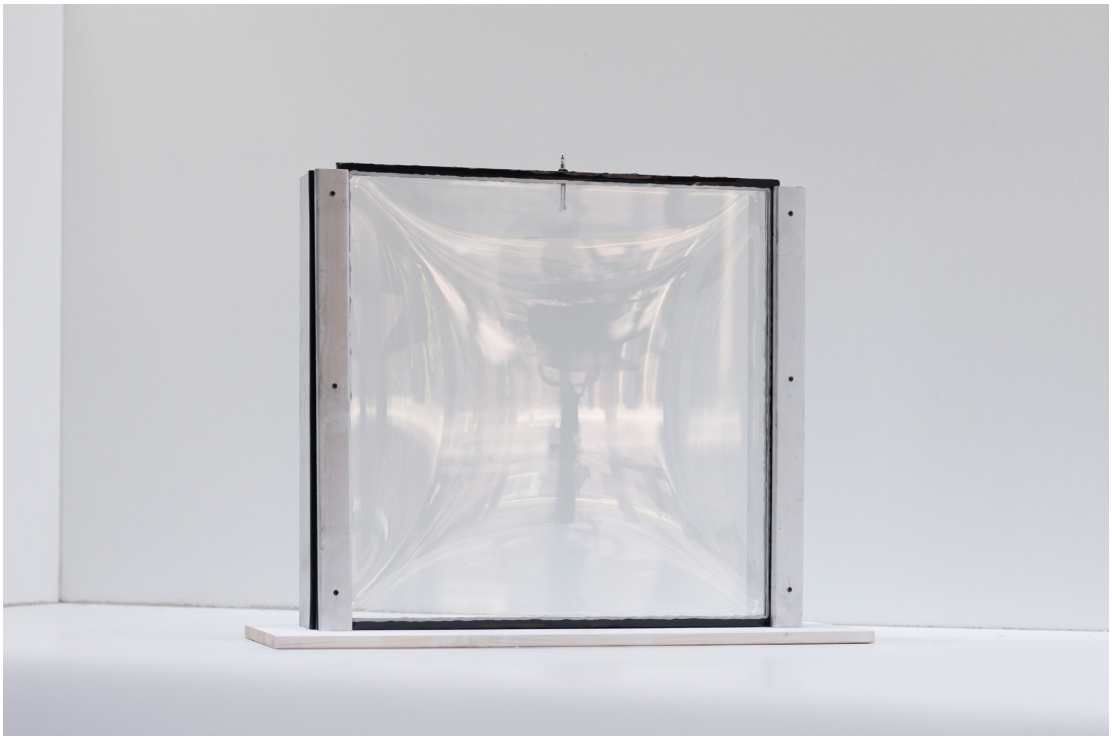

Figure 9.21 | PMMA double sided prototype (author)

Figure 9.22 | PMMA double sided prototype (author)

Figure 9.23 | PMMA double sided prototype (author)

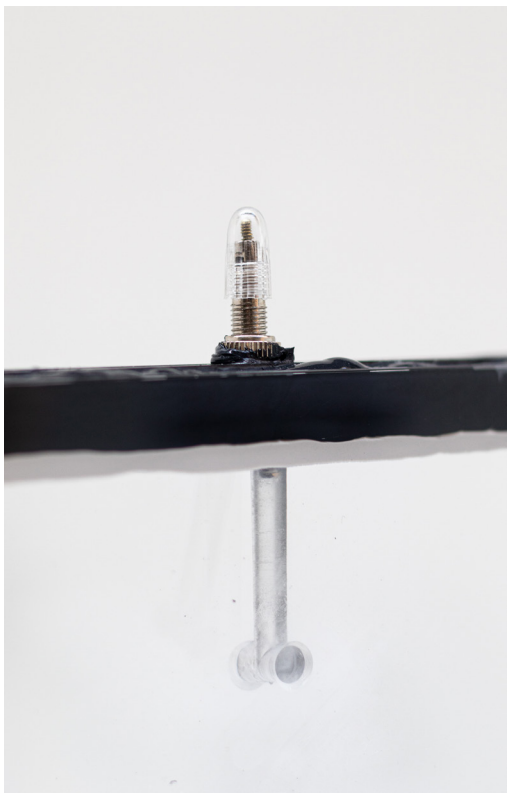

Figure 9.24 | PMMA double sided prototype (author)

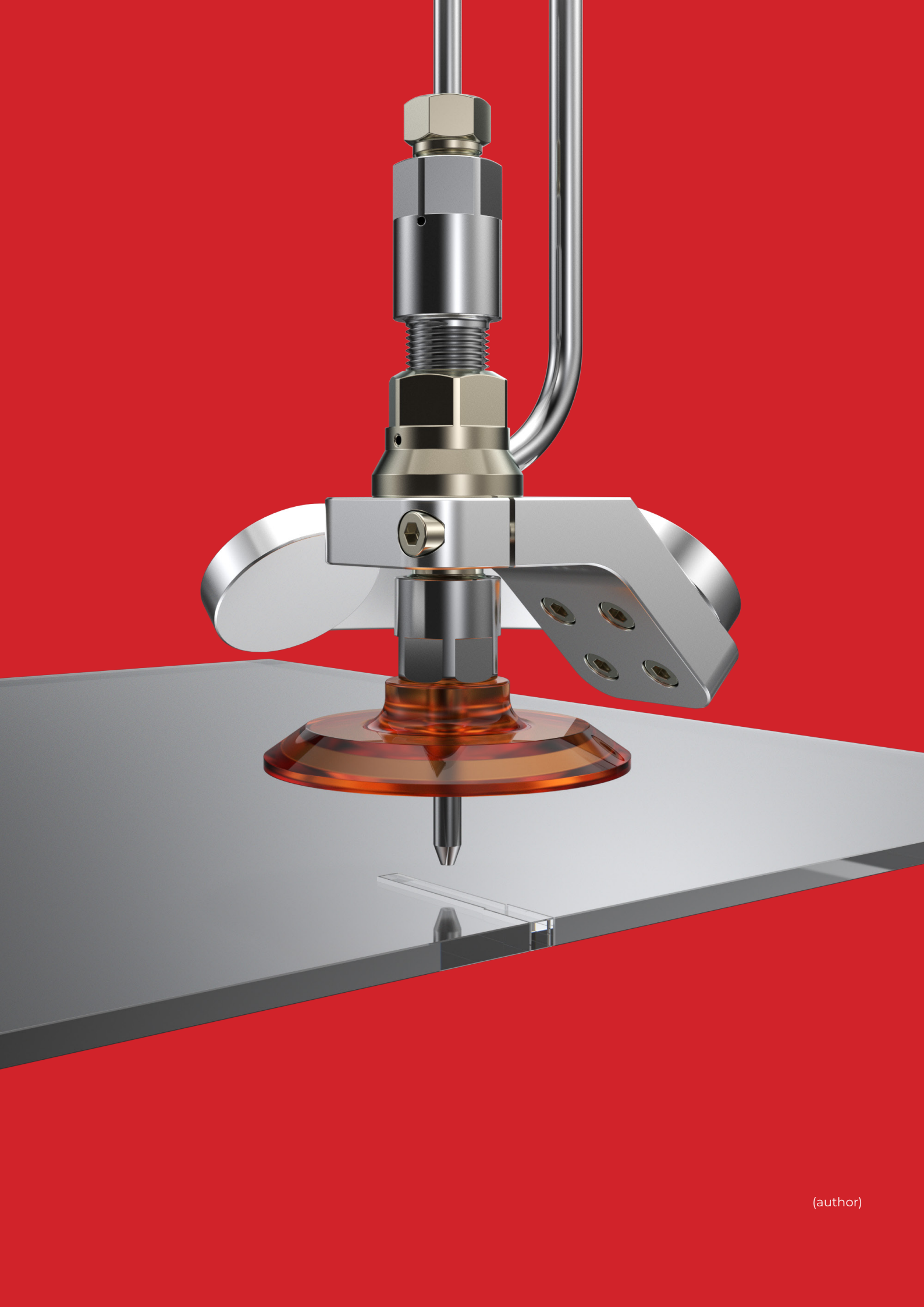

(author)

10. Inflatable Glazing as a Building Product

10.1 Core Pane: PMMA vs. Glass

Throughout the thesis, it has become clear that PMMA is an ideal material for prototyping, especially considering the distinct shape of the core pane. It's lightweight, highly transparent, and easy to cut, mill, or drill. However, thermal analysis, manufacturability, and durability tests have shown that there are benefits to using an all-glass unit.

Glass as a core pane offers better adhesion for both the primary and secondary sealant. Compared to PMMA, there's no gas permeability through the glass pane. This isn't necessarily a problem due to the constant adjustability of gas pressure. A major concern, however, is the significantly higher thermal expansion coefficient of PMMA compared to glass, which is 7-8 times greater. This could cause increased stress on the components, leading to a less durable product. PMMA can also develop microcracks when exposed to sunlight, resulting in reduced transparency over time. When designing larger panes, a thicker PMMA pane is needed to withstand the same wind forces as with a glass core pane. Lastly, thermal analysis showed that a greater change in U-value can be achieved with an all-glass design since the thermal resistivity of glass is lower than that of PMMA.

Therefore, the following paragraph presents two concepts on how the prior research on edge design is be applied to achieve an all-glass design.

10.2 All Glass Unit

The two subsequent building product concepts have similar performance in terms of U-value change, albeit with differing methods of manufacturing, complexity, and potential visual light transmittance.

Glass Composition 1

The first concept was developed to function as closely as possible to the previous final PMMA design. Since shaping the glass core pane isn't as straightforward as the PMMA pane, an alternative manufacturing method had to be selected. The possibilities of glass grinding, milling, waterjet cutting, laser cutting, and molding were explored. Rapid production of multiple glass panes with reliable edge conditions could only be achieved by waterjet cutting. The core pane would need to be cut and laminated with PVB interlayers. The 2D cuts of the waterjet cutter would only allow straight sides to fit the T-channel. Thus, a square aluminum T-channel with a round inner channel is inserted into the cutouts of the core pane.

The following edge detail demonstrates the number of panes needed for the glass composition. The unit thickness will ultimately be at least 20mm.

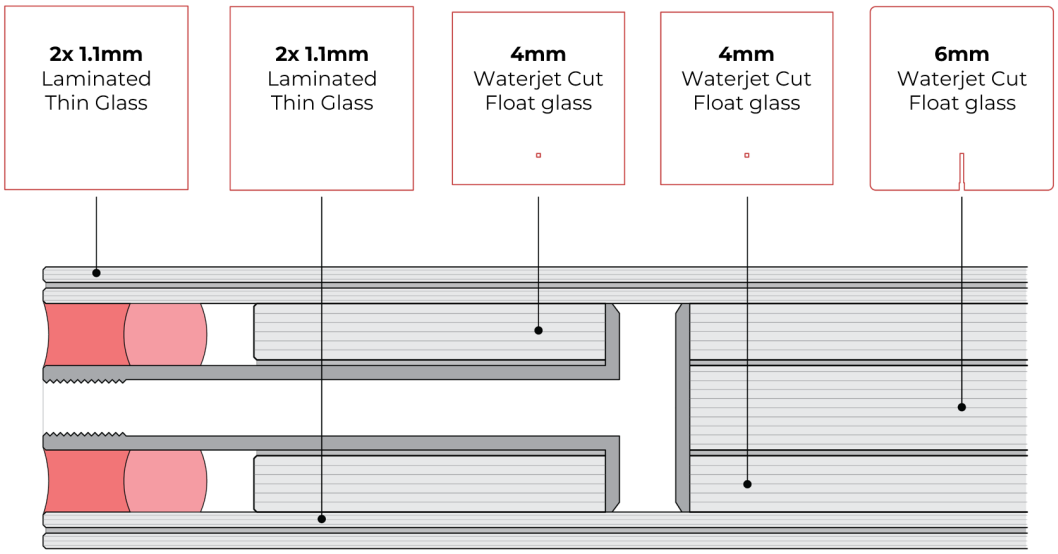

Figure 10.0 | All glass edge detail - composition 1 (author)

This unit can be manufactured and assembled using current production techniques, however, it comprises many panes (see Figure 10.1). The layering of glass would necessitate the lamination of the float glass panes, thereby permanently integrating the T-channel into the pane. Disassembling or maintaining this unit could be challenging if there's breakage or leakage. The numerous lamination layers might also result in lower visual light transmittance. Nonetheless, this unit would be durable and meet the requirements for consistent inflation and a significant change in U-value.

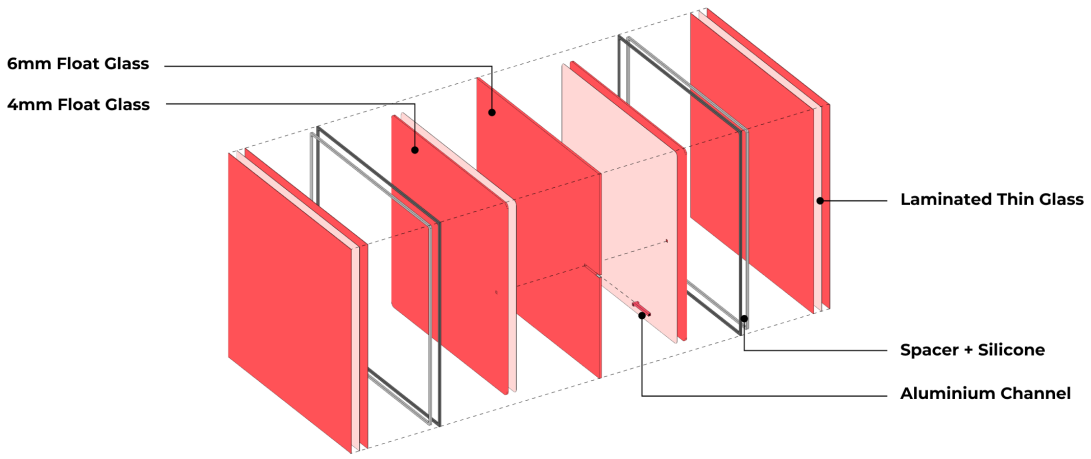

Figure 10.1 | Composition 1 exploded view (author)

The following graphic shows a step-by-step assembly of the glass composition as a fragment of the glass edge detail.

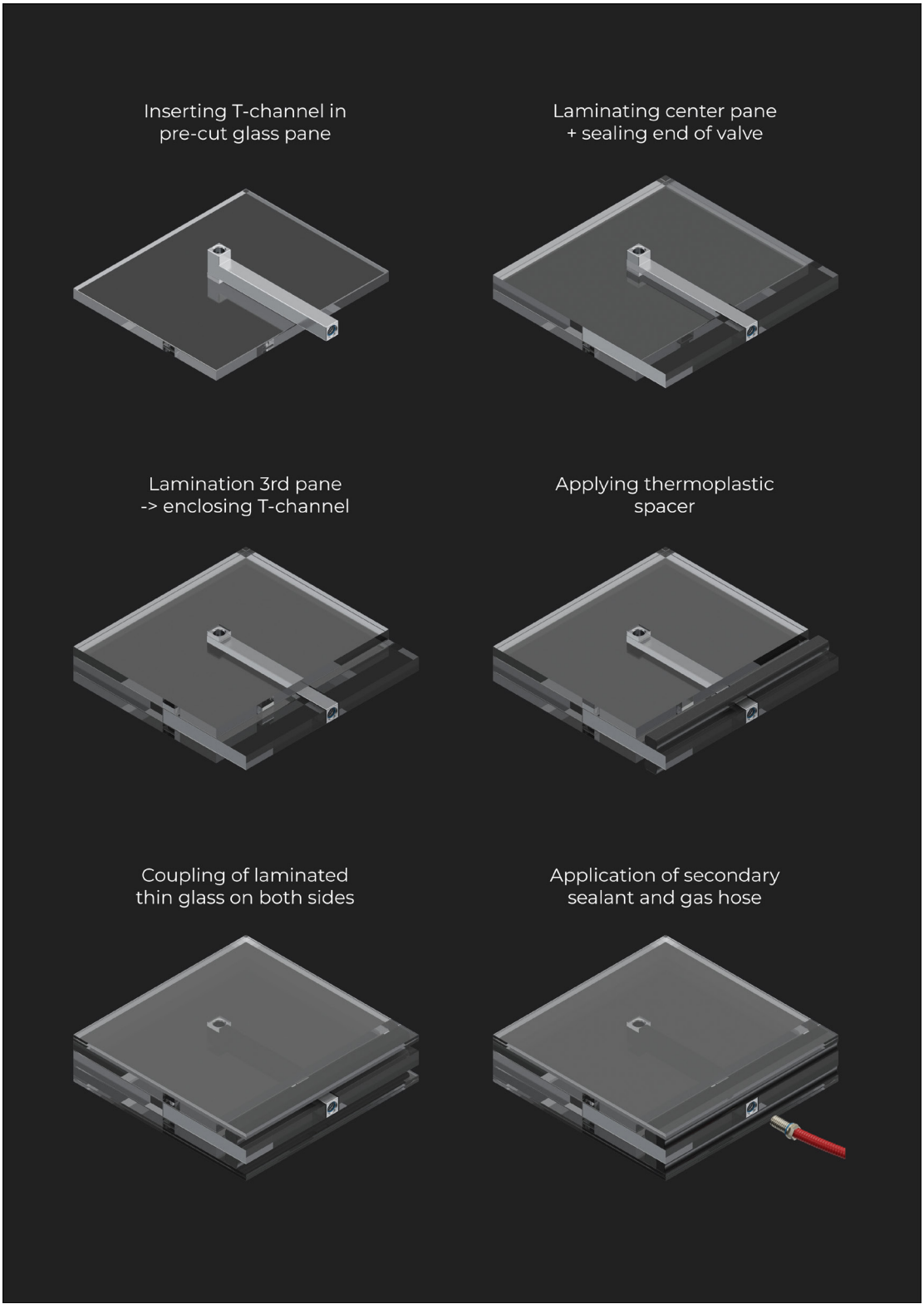

Figure 10.2 | Composition 1 assembly frames (author)

Glass Composition 2

The second all-glass unit design relies on a much simpler assembly method. Here, the core pane is a single float glass pane with two cutouts to accommodate the aluminum channels, which are filled with transparent silicone. The aluminum channels are designed for a flush fit with the glass pane and an offset at the edge to allow room for the secondary seal and movement of the thin glass panes. In this design, the primary seal is completely omitted, which lets the secondary seal form a structural bond on all three glass surfaces. This isn't necessarily a major drawback, since the secondary seal still offers low gas permeability and the gas pressure can be constantly adjusted by the gas supply.

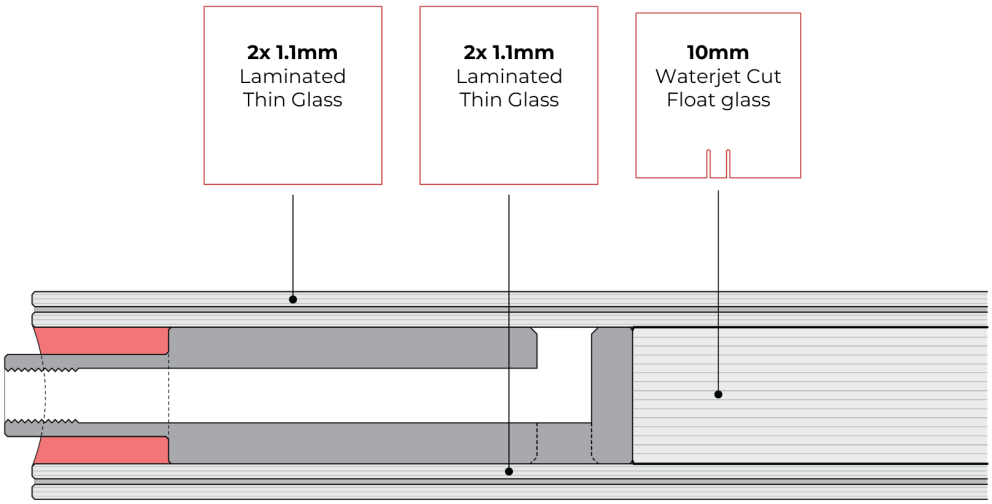

Figure 10.3 | All glass edge detail - composition 2 (author)

With this configuration, the thinnest possible glass unit of 15mm can be achieved. The core pane is now 10mm thick and requires only one seal. The decision to use two instead of one aluminum channel introduces another feature to Inflatable Glazing. Now, each side of the pane can be inflated separately, allowing for more control over the U-value and reducing the risk of convection in the area of the channel exhaust. The following exploded view illustrates the simplicity of this design (see Figure 10.4).

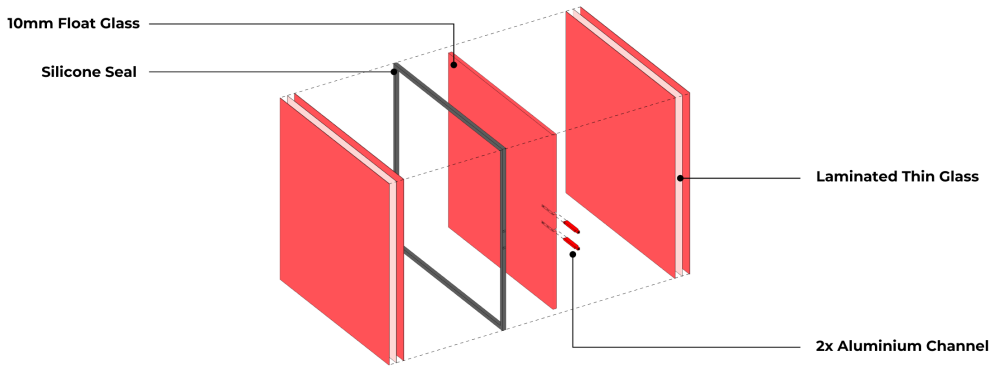

Figure 10.4 | Composition 2 exploded view (author)

The following graphic shows a the step-by-step assembly of the glass composition as a fragment of the glass edge detail.

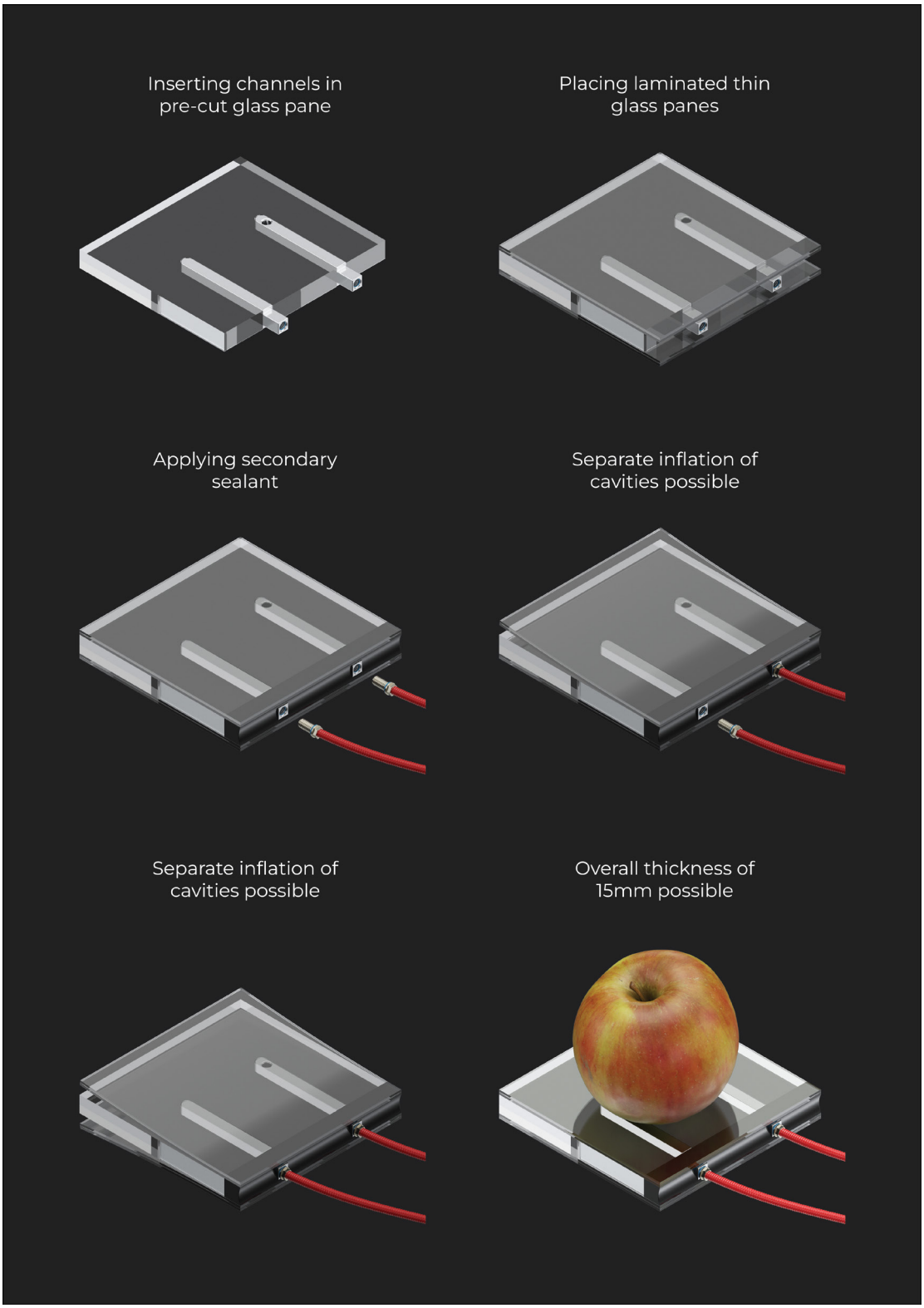

Figure 10.5 | Composition 2 assembly frames (author)

The second all-glass unit seems to have a promisable manufacurability and even has the possibility to be repaired if one of the panes break/fail. The sealant can in this case be scraped off and reapplied and the channels can be removed. This unit provides the highest change in U-value, has a realitvely low weight compared to generic triple glazing and uses less material.

Embodied Energy Comparison

Primary embodied energy refers specifically to the energy used in the initial phase of a product's life cycle, particularly in the extraction and processing of raw materials. This includes activities such as mining, refining, and the initial manufacturing steps, up to the point the raw material is transformed into a finished product. It does not include the energy used in transportation, storage, use, and disposal. The primary embodied energy is quantified in terms of energy intensity per unit of weight, typically measured in megajoules per kilogram (MJ/kg), allowing for an understanding of a material's energy footprint.

The following graph shows the comparison of different IGUs and Inflatable Glazing (INGL) types from this report (see Table 10.0)

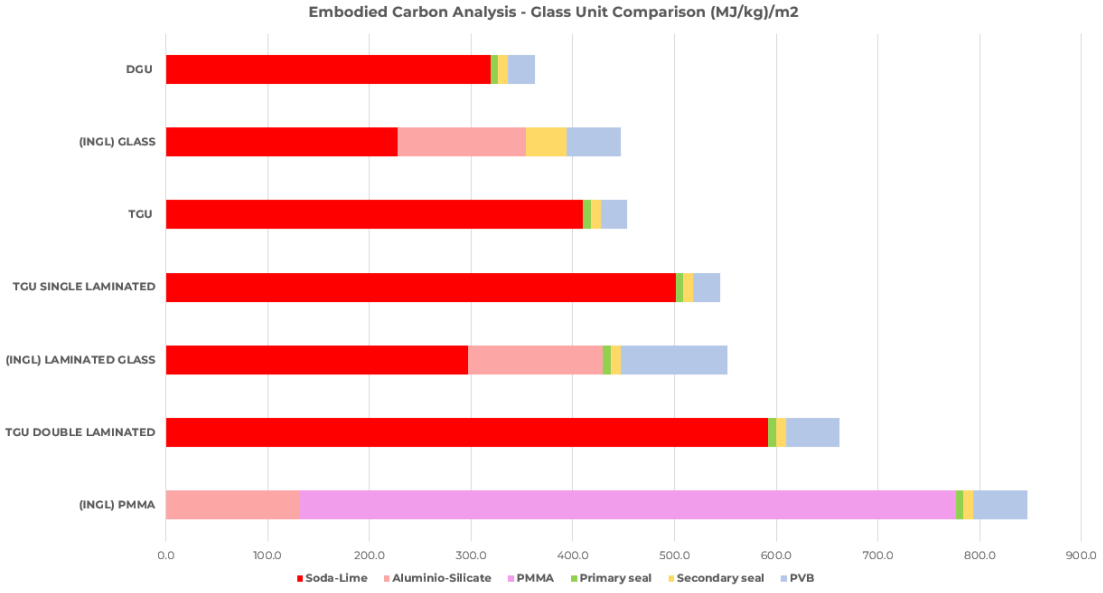

Table 10.0 | Embodied Energy (primary production) comparison (author)

The calculation is based on the materials and components used for 1m² of a unit. It's clear that glass/PMMA constitutes the largest part of embodied energy. PVB interlayers are the second largest contributor, while the primary and secondary sealants account for only a small portion of embodied energy. Surprisingly, PMMA has a very high embodied energy, making it the worst-performing unit.

Examining the previously presented slim all-glass (INGL GLASS) composition, it's noticeable that it has a similar embodied energy to standard triple glazing. Since Inflatable Glazing has laminated outer and inner layers, it can also be compared to single/double acoustic triple glazing, which also have laminated inner and outer panes. In comparison, an embodied energy reduction of 32% can be achieved. However, this comparison isn't valid until the acoustic properties of Inflatable Glazing are proven to be comparable to double laminated triple glazing.

10.3 Mullion Design

The mullion design for Inflatable Glazing needs to be adjusted to provide access for the gas hoses. To illustrate this, a 50mm mullion from a stick system has been redesigned to allow for access (see Figures 10.6 and 10.7). A square cutout in the mullion can be pre-manufactured by sawing or punching. A custom thermal break with channels can be plugged into these cutouts, and gas hoses can be run through them. They should be installed at the height of the aluminum channel in the glazing and can be secured by a screw valve or a pressure valve. The mullion has a rear cap which can be opened from the inside, allowing hoses to be routed towards the suspended ceiling or the raised floor. From there, they can be connected to the HVAC unit if the glazing is supplied with dry air, or to a separate supply system if noble gases are used.

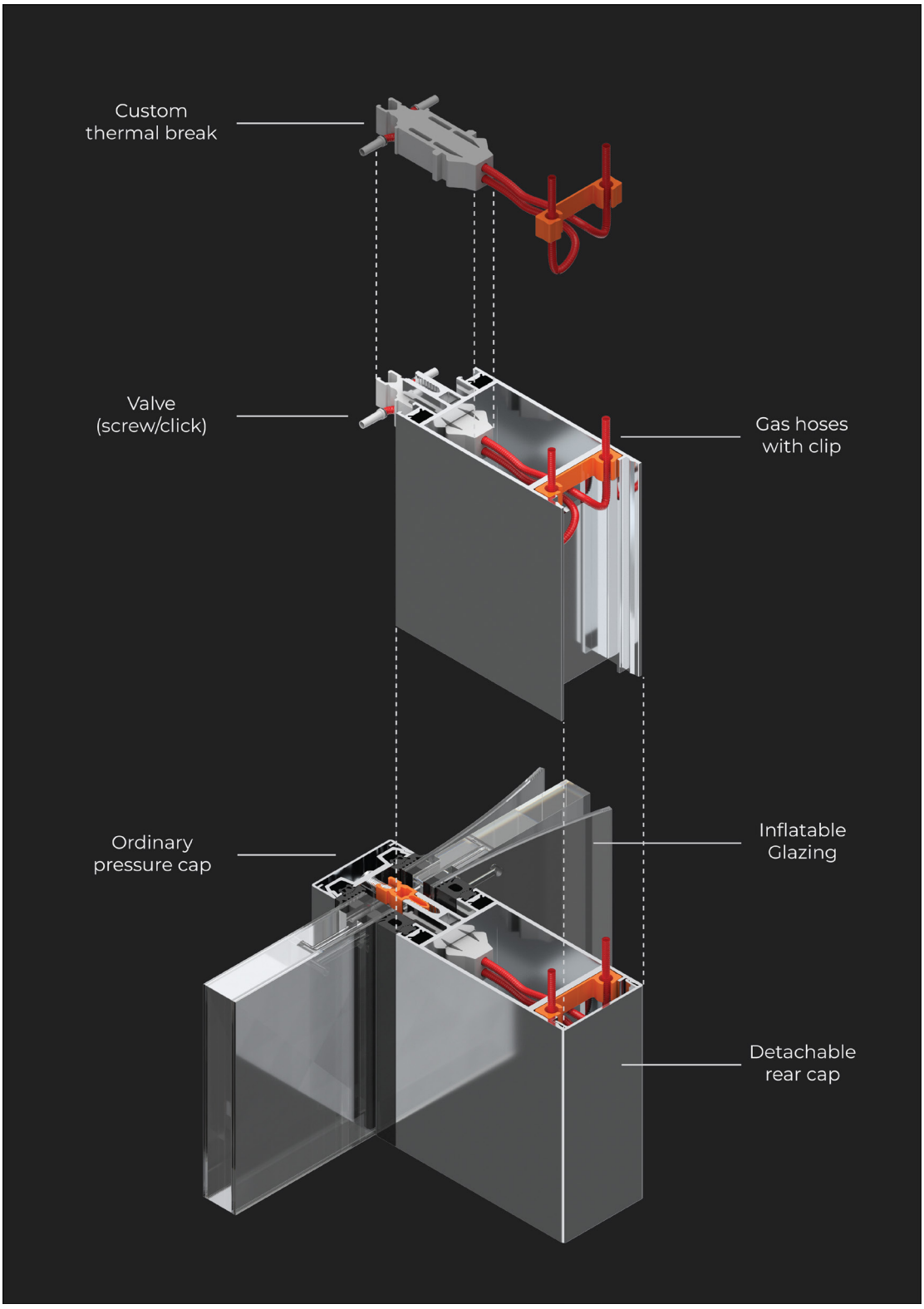

Figure 10.6 | Mullion design (author)

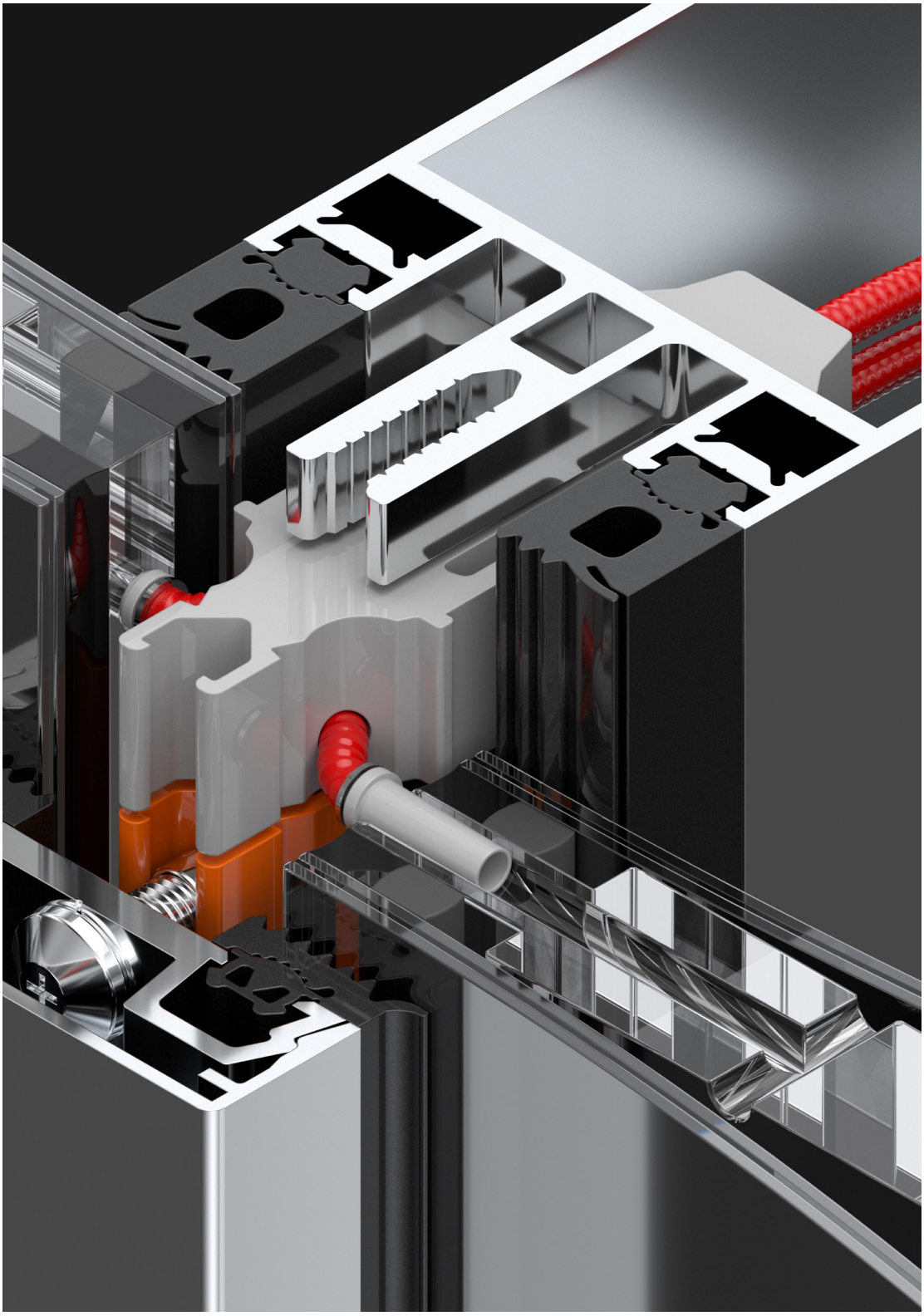

Figure 10.7 | Mullion design section - close up (author)

10.4 Architectural Use of Inflatable Glazing

This thesis focused on the prototyping of a potential building product and the proposal of a functional unit. The product has proven to effectively balance the thermal insulation requirements of a glass facade. However, the remaining question is whether this unit also offers aesthetic value. The observed deformation of the glass unit presents a consistent curvature, resembling an X-shape. The study that follows showcases the anticipated reflections/deformations of a glass facade on a building scale. Ultimately, it can be determined whether architects could employ Inflatable Glazing not only as a sustainability feature but also as a design element.

A building model was created in Rhino and rendered in V-ray using ray tracing. Broadly speaking, ray tracing works by simulating rays of light as they bounce around a scene. Instead of just calculating the light that hits an object directly (as with traditional rendering methods), ray tracing calculates light that bounces off other objects before it hits the target object. This can provide a more accurate and lifelike representation of lighting, reflections, refraction, and shadows in a scene.

Exterior

The following graphics depict a building with ordinary triple glazing installed, followed by Inflatable Glazing with cavity widths ranging from 6mm (Xenon infill), 10mm (Argon infill), to 16mm (Air infill). The inflation of the glazing has been simulated in Grasshopper, accurately reflecting the deformation measured from the 3D scan.

Figure 10.8 | Building with ordinary triple glazing installed (author)

Figure 10.9 | Building with Inflatable Glazing 6mm cavity width (Xenon infill) (author)

Compared to the triple glazing, Inflatable Glazing with xenon infill exhibits a slightly visible curvature. Especially the reflections in the right part of the building are showing the bulging effect. Overall, this effect is not directly noticeable.

Figure 10.10 | Building with Inflatable Glazing 10mm cavity width (Argon infill) (author)

Inflatable Glazing with an Argon infill (10mm cavity) already shows a defined deformation. The X-shape is now clearly visible in almost all openings of the building and reflections show a clear distortion of the opposing street/objects.

Figure 10.11 | Building with Inflatable Glazing 10mm cavity width (Argon infill) (author)

The deformation with a 16mm maximum cavity is now clearly defined and the glazing has a distinct shape. Reflections from objects of the opposing side are heavily distorted. Actual distortions of the objects behind the facade could not be determined from the visuals. A lensing effect might occur in regions of high curvature or close to the edge of the panes.

Interior

When light encounters a boundary between two different materials, such as a gas and glass, part of it is reflected, transmitted and refracted through the material. The proportion of light that is reflected versus refracted depends on several factors, including the angle of incidence and the difference in refractive index between the two materials .

During the day, most light comes from the brighter outside environment, whereas the interior is relatively dark. Thus, a large portion of that light is reflected outward, making the glass look reflective or mirrored from the outside. The relatively small amount of light from inside the building is mainly transmitted through the glass to the outside rather than reflected into the building, which is why one does not see strong reflections on the inside.

However, the situation can reverse at night if the lights are on inside the building and it is dark outside. In this case, more light hits the glass from the inside than the outside. This results in more light being reflected into the building, making the windows look more like mirrors when viewed from the inside. At the same time, people outside the building may be able to see in because the light being transmitted through the glass from the inside is more significant than any light reflecting off the glass from the outside.

The following graphics show the reflections during the day from an interior point of view with the same inflation steps:

Figure 10.12 | Building with ordinary triple glazing installed - interior (author)

Figure 10.13 | Building with Inflatable Glazing 6mm cavity width (Xenon infill) - interior (author)

From the interior view, it can bee seen that particularly bright surfaces, such as windows on the opposite side as well as bright furniture, are reflected in the glazing. The deformation of the glass can be observed in the form of a “squeezing” effect on the objects/windows in the building.

Figure 10.14 | Building with Inflatable Glazing 10mm cavity width (Argon infill) - interior (author)

Figure 10.15 | Building with Inflatable Glazing 16mm cavity width (Air infill) - interior (author)

The final two images show the inflation with argon and air infill. Strong deformations of the pane are now clearly visible. Especially, ceiling lights are distorted in the reflection, and opposing objects are strongly squeezed. The reflections from a frontal point of view also exhibit a larger area of reflection, much like in a wide-angle camera.

Discussion

The exterior and interior renders revealed the reflection behavior of Inflatable Glazing in a realistic context. It can be concluded that the deformation of the pane with a xenon infill is only slightly visible due to the narrower cavity width. In this case, it is almost equivalent to an IGU with deformations due to thermal pressure. These deformations are generally viewed as results due to a poor glazing choice. If the glazing is designed to be too thin, unwanted bulging in the pane can be observed. However, in the case of controlled inflation, this behavior of bulging is more consistent compared to thermal effects, and thus, has a more appealing appearance.

Deformations with 10+ mm are clearly visible from both the interior and exterior. In both cases, the X-shape is clearly defined. Unarguably, this effect can vary due to many factors. The time of day, weather, visibility, angle of the sun, etc., all play major roles. Also, moving in front of the building can create different visual effects. Passing by a building with Inflatable Glazing could display a variety of reflection patterns. There is certainly a risk of visual discomfort; however, this could be balanced with different coatings or anti-reflective treatments.

Lastly, there is the question of aesthetics. This is very individual, and designers should be cautious when using this technology. It would definitely need to be integrated into the architectural language of the building. For instance, overhangs, whether small or large, have a major impact on the appearance of the glazing since they result in more contrast. On the other hand, a building could alter its appearance with Inflatable Glazing by implementing parametric inflation patterns. The following figure shows examples of deformed glass panes as an architectural language.

Figure 10.16 | Examples - top: Finiglas Veredelungs GmbH (2023), bottom left: Herzog & de Meuron (2017) bottom right: REX (2010)

11. Conclusion

The Building Technology Graduation Project - Inflatable Glazing investigates the thermal performance, effects on energy efficiency, and manufacturability of a new type of switchable insulating glazing. This chapter concludes the thesis by answering the main research question and the sub-research questions. Finally, a discussion and recommendations for further research are provided in Section 11.2.

11.1 Answers to the Research Questions

Sub-research questions:

1. *What are the resulting U-values when the unit's cavity is either open or collapsed?*

The results described in Chapter 6 (Thermal Performance) demonstrate that it is possible to achieve values ranging from high-performance triple glazing to single glazing when the unit is specified with a super low-conducting inert gas (xenon) and low-e coatings. The resulting change of 925% represents the average U-value shift from the insulating state, which is around 0.6W/m²K, to the fully conducting state, which is 5.46W/m²K. While Inflatable Glazing did not outperform static triple glazing, which can reach values even lower than 0.4W/m²K, it shows that it can compete with highly insulating glazing when inflated.

A more realistic glass unit, however, would feature a cheaper gas infill, such as dry air, since it could be supplied just like in a closed cavity facade and does not need to be stored. The dry-air could be ejected every time the unit deflates and fresh dry-air could be supplied for the next inflation. The U-value change with air still achieves a change of around 460%, with U-values ranging from 1.18W/m²K to 5.46W/m²K. This change in U-value would more accurately represent a switch from double glazing to single glazing. Nevertheless, the results appear very promising and should therefore be validated in a laboratory environment. Based on the simulated values, the design criteria have been fulfilled.

2. *What is the effect on energy efficiency of a building with Inflatable Glazing equipped and where is it the most effective?*

The energy model simulations demonstrated that Inflatable Glazing has the potential to reduce a building's energy demand significantly. Accelerating heat flux through the glazing in summer substantially lowers the need for cooling. As a result, heat accumulation can be eliminated, addressing a primary flaw of static insulating glazing. In addition, the passive analysis revealed that air temperatures can be maintained more consistently throughout the year compared to static glazing.

Inflatable Glazing proves particularly effective in mixed and mild climate zones with cold winters and hot summers. This is because selecting appropriate static glazing in these locations can be challenging. When employing high or low-insulating glazing, a designer must consider the risk of overheating in summer or a substantial increase in heating demand during winter. Inflatable Glazing, on the other hand, allows for adjustment of the U-value based on exterior and interior temperatures, thereby controlling the indoor climate. With connected sensors and weather forecasts, the glass unit could automatically adjust its inflation state.

In conclusion, Inflatable Glazing is most effective in reducing a building's cooling load compared to equally well-insulating static glazing, assuming the unit will likely remain inflated throughout the winter. However, the energy model could be further developed to account for solar gain. By doing so, free heat would also contribute to a reduction in heating demand during winter.

3. *What are the main challenges in manufacturing a dynamic thin glass unit and how could the process be improved?*

The primary challenge throughout the manufacturing process was maintaining a high level of accuracy. This began with sawing the groove and drilling the T-channel in the PMMA pane. Although the achieved result was satisfactory and precise enough for a prototype, it is advisable to use CNC milling for a real product in order to achieve the most precise cuts. Alternatively, if glass is used for the center pane, one could consider waterjet cutting the glass pane or laminating multiple panes to achieve the desired shape.

The second challenge involved working with great precision during the assembly of the panes. Utilizing automatic dispensing of primary and secondary sealants and accurate assembly by robots would result in a more consistent curvature of the inflated pane. Additionally, working in a near-sterile environment during the process is crucial to avoid particles in the cavity that could cause the glass to crack.

Lastly, the valve used in Inflatable Glazing is a key driver of the overall unit thickness. Therefore, the thickness and resulting weight could be significantly reduced by minimizing the diameter of the valve.

4. *What are the desired cavity widths to achieve the best thermal results and which pressures and stresses can be expected?*

The thermal simulation showed that the ideal cavity width varies depending on the gas used. Generally, gases with higher conductivity, like air, require wider cavities than those with lower conductivity, such as xenon. As a result, lower-conducting gases are preferred since a narrower cavity will reduce the extent of curvature. Thus, principal stresses will decrease. Across the spectrum of gases, cavity widths ranged

from a maximum of 16mm (air) to a minimum of 6.4mm for xenon.

The pressure required to inflate a unit is calculated to be around 2000-4000 Pa before it fails. However, this result is theoretical and unconfirmed, as the sealant of the unit failed first during both test cases. This issue could be related to poor adhesion between silicone and PMMA or the surface quality of the PMMA. A full glass prototype would need to be constructed to determine the ultimate limit state of thin glass from air pressure, and silicone may need to be applied using a CNC for higher accuracy.

The calculated stresses were quite significant in the pane corners. For the smaller 500x500mm prototypes, the principal stresses were around 120 MPa, while the larger theoretical units of 1500x3000mm units were in the vicinity of 14 MPa. Consequently, larger units are expected to be much more durable, and sealants should experience less deformation. The maximum tensile strength of thin glass is around 700 MPa, so the extent of curvature that the panes undergo to achieve the desired cavity width is within the capabilities of thin glass. Therefore, the properties of thin glass are not expected to decline, and the edge bond of the glass should be able to accommodate multiple inflation cycles while remaining airtight and adherent.

5. *What is the resulting inflation geometry and curvature of the inflated thin glass unit?*

The inflated shape was determined using a 3D scanner, which provided a highly accurate digital representation of the surface. Throughout the process, the deformation of the shape remained uncertain, as finite element analysis (FEA) could not produce a realistic output of the pane's exact curvature. Consequently, the scan offered valuable insights into the actual deformation.

The inflation geometry seems like an X-shape, which becomes more defined as pressure increases. Also, the radii of the curvature decrease with more pressure, causing the X-shape to appear more pronounced. The pane's edge moves downward, compressing the silicone, while the area near the corners pulls the silicone upward. The ultimate corner exhibits a slight downward dip.

The surface scan also revealed the cavity width at every point of the unit. With this information, it became possible to predict the resulting U-values more accurately. Moreover, the scan highlighted flaws and unexpected deformations in the prototypes.

Main research question:

How can thin glass be utilized as a dynamic component to enable a switchable U-value in an insulated glass unit?

The primary objective of this master's thesis was to harness the bending properties of thin glass in order to create a mechanical movement that changes the insulating properties of a glass unit. Previous research has demonstrated the high potential for energy savings when switchable insulating systems are employed. However, there has not yet been a fully transparent prototype for all insulating states. The current smart glazing market primarily relies on changing the g-value, which controls solar radiation by adjusting the optical properties.

Combining thin glass with a gas pressure system allows for easy separation of materials when in direct contact, creating a consistent double-curved cavity. Moreover, since thin glass is not a stiff materia itself, the pressure stresses the pane, resulting in a stiff state. The build-up is designed to be similar to typical IGUs, allowing for the use of current glass assembly practices and ensuring low gas permeability.

Optically, Inflatable Glazing can offer aesthetic appeal and could be utilized by designers to create intriguing façade designs and enhancing the energy efficiency of the building at the same time.

11.2 Discussion and Further Research

The study demonstrates the concept and functionality of Inflatable Glazing, but many aspects still require further research for it to become an actual product. Additional research on structural, thermal, energy, visual, acoustical, and manufacturing topics can be conducted.

In general, the project shows that there are benefits in thermal performance and manufacturability when an all-glass prototype is employed. Discussions with Kömmerling | H.B. Fuller also suggested opting for an all-glass prototype since the adhesives and spacer are specifically designed for that purpose. PMMA has the issue of a much higher thermal expansion coefficient than glass, which could cause unwanted deformations within the unit. Additionally, PMMA's gas permeability is undesirable, but this is less of a problem since gas can be constantly adjusted.

Further research in structural performance would be highly interesting to understand the relationship between pressure and curvature. This knowledge could determine the maximum inflation and ultimate limit state. If these values could be validated through FEA and laboratory experiments, the effect of wind forces against the inflated pane could also be assessed. The structural capabilities, however, also depend on the durability of the sealants. A thorough FEA analysis using Ansys or

Abaqus would provide insight into the shear forces acting on the edge bond. A long-term experiment could be conducted by constantly inflating and deflating the unit to test the sealant's ability to withstand frequent movements over an extended period. The same applies to the coatings, where it remains undetermined which types of hard/soft coatings could be scratch-resistant enough to withstand frequent contact with the core pane.

The energy consumption of the frequent inflation and deflation over the year and its impact on the energy balance simulation is still unclear. The energy model has substantial room for improvement concerning the inflation schedule and understanding the ideal configurations.

The acoustic properties should be investigated, considering that the fully conducting pane has all materials in direct contact. Usually, the thicknesses of the pane, cavities, and laminated layers contribute to the overall sound insulation. Since the final design does have two panes with an interlayer, it might not be an issue, but this should be validated.

Lastly, the cost of the system should be determined. It is not confirmed how much the appropriate thin glass will cost per square meter for mass production, but it will likely be higher than a typical triple glass unit. Moreover, the glass panes would need to be connected to the HVAC system, requiring more labor for installation or glass replacement. The maintenance, cleaning, and gas costs are also crucial factors in conducting a cost analysis.

References

AGC. (2010). AGC Glass Unlimited: Your Glass Pocket.

Aguilar-Santana, J. L., Jarimi, H., Velasco-Carrasco, M., & Riffat, S. (2019). Review on window-glazing technologies and future prospects. International Journal of Low-Carbon Technologies, 15(1), 112–120. https://doi.org/10.1093/ijlct/ctz032

Apple. (2023, March 30). Apple awards Corning $45 million from its Advanced Manufacturing Fund. Apple Newsroom. https:// www.apple.com/newsroom/2021/05/apple-awards-corning-45-million-from-its-advanced-manufacturing-fund/

Awesome Infographic: The history of double glazing. (n.d.). Thetford Home Improvement Services. https://www.this-home.net/infographic-the-history-of-double-glazing

Barrow Alaska Photograph by Jeffrey Sward. (2010). https://www.jeffreysward.com/gallery/gallerybarrow/pages/r6c2.htm

Beck, H. E., Zimmermann, N. E., McVicar, T. R., Vergopolan, N., Berg, A., & Wood, E. F. (2018). Present and future Köppen-Geiger climate classification maps at 1-km resolution. Scientific Data, 5(1). https://doi.org/10.1038/sdata.2018.214

Berger, T., Amann, C., Formayer, H., Korjenic, A., Pospichal, B., Neururer, C., & Smutny, R. (2016). Impacts of external insulation and reduced internal heat loads upon energy demand of offices in the context of climate change in Vienna, Austria. Journal of Building Engineering, 5, 86–95. https://doi.org/10.1016/j.jobe.2015.11.005

Brandon. (2020, July 16). Chemical Tempering (Chemically Strengthened Glass). Materials Science & Engineering Student. https://msestudent.com/chemical-tempering-chemically-strengthened-glass/#e

Climate Change and Heat Islands | US EPA. (2023, February 15). US EPA. https://www.epa.gov/heatislands/climate-change-and-heat-islands

Corning. (n.d.). Corning's Fusion Process. Retrieved April 18, 2023, from https://www.corning.com/worldwide/en/innovation/the-glass-age/science-of-glass/how-it-works-cornings-fusion-process.html

Cwyl, M., Michalczyk, R., & Wierzbicki, S. (2021). Polyisobutylene and Silicone in Warm Edge Glazing Systems—Evaluation of Long-Term Performance. Materials, 14(13), 3594. https://doi.org/10.3390/ma14133594

Dabbagh, M., & Krarti, M. (2021). Optimal Control Strategies for Switchable Transparent Insulation Systems Applied to Smart Windows for US Residential Buildings. Energies, 14(10), 2917. https://doi.org/10.3390/en14102917

Delmastro, C. (2022, September). Buildings – Analysis. IEA. Retrieved January 13, 2023, from https://www.iea.org/reports/buildings

Dodoo, A., Gustavsson, L., & Bonakdar, F. (2014). Effects of Future Climate Change Scenarios on Overheating Risk and Primary Energy Use for Swedish Residential Buildings. Energy Procedia, 61, 1179–1182. https://doi.org/10.1016/j.egypro.2014.11.1048

EUROPEAN COMMITTEE FOR STANDARDIZATION. (2011). Glass in building - Determination of thermal transmittance (U value) - Calculation method. In NEN-Connect (NEN-EN 673).

Fish, J., & Belytschko, T. (2007). A First Course in Finite Elements. In John Wiley & Sons, Ltd eBooks. https://doi.org/10.1002/9780470510858

Forel. (2023). Insulating Glass Production Lines. https://www.forelspa.com/machinery-equipments/insulating-glass-production-lines/

How Structural Interlayers Work. (2023, February 13). Saflex. https://www.saflex.com/inspiration/how-structural-interlayers-work

IPCC. (2021). Sixth Assessment Report (AR6). IPCC. https://www.ipcc.ch/report/ar6/syr/

Kimber, M., Clark, W. W., & Schaefer, L. (2014). Conceptual analysis and design of a partitioned multifunctional smart insulation. Applied Energy, 114, 310–319. https://doi.org/10.1016/j.apenergy.2013.09.067

Knaack, U., Klein, T., Bilow, M., & Auer, T. (2014). Façades: Principles of Construction. Birkhäuser.

Kvasnin, S. (2014). Isolationsvorrichtung für Fenster oder Fassaden (Patent No. 20 2014 000 533.8). Deutsches Patent- und Markenamt.

Ladybug Tools. (2022). Climate Zone Classification. Ladybug Tools Academy. https://docs.ladybug.tools/ladybug-tools-academy/v/climate-analysis/climate-zone-classification

Luplow, M. (2021). Fahrradventile Arten: welche gibt es? Sclaverandventil, Dunlopventil und Schraderventil. Der Fahrradtour- Und Bikepacking-Blog. https://bikepacking-adventures.com/fahrradventile-arten-sclaverand-dunlop-schrader/

Martínez, E. (n.d.). FUNSAPDO - Fundación Salud para los Dominicanos. https://funsapdo.org/

Mavrogianni, A., Wilkinson, P., Davies, M. J., Biddulph, P., & Oikonomou, E. (2012). Building characteristics as determinants of propensity to high indoor summer temperatures in London dwellings. Building and Environment, 55, 117–130. https://doi.org/10.1016/j.buildenv.2011.12.003

McLeod, R. R., Hopfe, C. J., & Kwan, A. S. K. (2013). An investigation into future performance and overheating risks in Passivhaus dwellings. Building and Environment, 70, 189–209. https://doi.org/10.1016/j.buildenv.2013.08.024

Nature Picture Library. (2021, December 15). Emperor penguin imagesEmperor: A Survival Story | Nature Picture Library. https://www.naturepl.com/blog/2019/10/16/emperor-penguin/

Neugebauer, J. (2016). Determination of Bending Tensile Strength of Thin Glass. Challenging Glass - Conference on Architectural and Structural Applications of Glass, 5.

Neugebauer, J., & Wallner-Novak, M. (2019). 2.7 Movable and adaptive thin glass applications. In De Gruyter eBooks (pp. 84–87). https://doi.org/10.1515/9783035613629-024

Olbrich, H. (1989). Polystyrol-Schaumstoffkugeln für die bewegliche Wärmedämmung und Beschattung von transparenten Gebäudeteilen. (Patent No. 88114434.9). BASF Aktiengesellschaft.

Overbey, D. (2019, February 14). Gauging the Impact of Exterior Shading using the Projection Factor. 2019-02-15 | Building Enclosure. https://www.buildingenclosureonline.com/blogs/14-the-be-blog/post/88072-gauging-the-impact-of-exterior-shading-using-the-projection-factor

Overbey, D. (2022, February 24). Embodied Carbon and the Shearing Layers of Change. Building Enclosure. https://www.buildingenclosureonline.com/blogs/14-the-be-blog/post/90583-embodied-carbon-and-the-shearing-layers-of-change

Pflug, T., Bueno, B., Siroux, M., & Kuhn, T. E. (2017). Potential analysis of a new removable insulation system. Energy and Buildings, 154, 391–403. https://doi.org/10.1016/j.enbuild.2017.08.033

Pflug, T., Nestle, N., E. Kuhn, T., Siroux, M., & Maurer, C. (2018). Modeling of facade elements with switchable U-value. Energy and Buildings, 164, 1–13. https://doi.org/10.1016/j.enbuild.2017.12.044

Rammig, L. (2022). Advancing Transparency: Connecting glass with heat – An experimental approach to the implementation of heat bonding into glass connection design for structural applications. A+BE | Architecture and the Built Environment.

Respondek, Z. (2020). Heat Transfer Through Insulating Glass Units Subjected to Climatic Loads. Materials, 13(2), 286. https://doi.org/10.3390/ma13020286

Reunes-Vanhaevre, H. (n.d.). Pinguins info - penguin - information about Thermal insulation of penguins. © Hedwig Reunes-Vanhaevre. https://www.pinguins.info/Engels/Warmtebehoud_eng.html

Rezaei, S. D., Shannigrahi, S., & Ramakrishna, S. (2017). A review of conventional, advanced, and smart glazing technologies and materials for improving indoor environment. Solar Energy Materials and Solar Cells, 159, 26–51. https://doi.org/10.1016/j.solmat.2016.08.026

Schlösser, N. (2018). Thin Glass as Cold Bent Laminated Panels in Architectural Applications. TU Delft Repository, http://resolver.tudelft.nl/uuid:cf8fecc0-15f8-4f85-95da-6cb6b35fffa1.

SCHOTT AG. (n.d.). SCHOTT Glass Melting and Hot Forming. https://www.schott.com/en-lu/expertise/glass-melting-and-hot-forming?tab=e0366e25

Sodha, M., Nayak, J., Bansal, N., & Goyal, I. (1982). Thermal performance of a solarium with removable insulation. Building and Environment, 17(1), 23–32. https://doi.org/10.1016/0360-1323(82)90006-3

Stazi, F., Vegliò, A., Di Perna, C., & Munafò, P. (2012). Retrofitting using a dynamic envelope to ensure thermal comfort, energy savings and low environmental impact in Mediterranean climates. Energy and Buildings, 54, 350–362. https://doi.org/10.1016/j.enbuild.2012.07.020

Van Den Bergh, S., Hart, R., Jelle, B. P., & Gustavsen, A. (2013). Window spacers and edge seals in insulating glass units: A state-of-the-art review and future perspectives. Energy and Buildings, 58, 263–280. https://doi.org/10.1016/j.enbuild.2012.10.006

Van Der Linden, A. C. (2018). Building Physics (2nd ed.). ThiemeMeulenhoff bv.

Appendix

Gas	Temperature (°C)	Density (kg/m³)	Dynamic Viscosity (kg/(m*s))	Conductivity (W/(m·K))	Specific Heat Capacity (J/(kg*K))
Air	-10	1.326	1.661×10^{-5}	0.02336	1008
	0	1.277	1.711×10^{-5}	0.02416	
	10	1.232	1.761×10^{-5}	0.02496	
	20	1.189	1.811×10^{-5}	0.02576	
Argon	-10	1.829	2.038×10^{-5}	0.01584	519
	0	1.762	2.101×10^{-5}	0.01634	
	10	1.699	2.164×10^{-5}	0.01684	
	20	1.640	2.228×10^{-5}	0.01734	
Krypton	-10	3.832	2.260×10^{-5}	0.00842	245
	0	3.690	2.330×10^{-5}	0.0087	
	10	3.560	2.400×10^{-5}	0.009	
	20	3.430	2.470×10^{-5}	0.00926	
Xenon	-10	6.121	2.078×10^{-5}	0.00494	161
	0	5.897	2.152×10^{-5}	0.00512	
	10	5.689	2.226×10^{-5}	0.00529	
	20	5.495	2.299×10^{-5}	0.00546	

Appendix

4.1 Symbols

A	constant	-
c	specific heat capacity of gas	J/(kg·K)
d	thickness of material layer (glass	
	or alternative glazing material)	m
F	volume fraction	-
h	- heat transfer coefficient	W/(m^2·K)
	- also thermal conductance	W/(m^2·K)
M	number of material layers	-
n	exponent	-
N	number of spaces	-
r	thermal resistivity of glass (glazing material)	m·K/W
P	gas property	-
s	width of gas space	m
T	absolute temperature	K
U	thermal transmittance	W/(m^2·K)
ΔT	temperature difference	K
ε	corrected emissivity	-
ε_n	normal emissivity (perpendicular to the surface)	-
ρ	gas density	kg/m^3
σ	Stefan-Boltzmann's constant 5,67 x 10^{-8}	W/(m^2·K^4)
μ	dynamic viscosity of gas	kg/(m·s)
λ	- thermal conductivity of gas in space	W/(m·K)
ϑ	temperature on the Celsius scale	°C

4.2 Dimensionless Numbers

Gr	Grashof number	-
Nu	Nusselt number	-
Pr	Prandtl number	-

4.3 Subscripts

c	convection
e	external
i	internal
j	jth material layer
k	kth space
g	gas
m	mean
n	normal
r	radiation
s	space
t	total
1;2	first, second etc.

Appendix

```python
"""
Module Name: EN-673:2011 U-value calculation for uneven surfaces
Author: Patrick Ullmer
Last update: 2023-04-29.
"""

import rhinoscriptsyntax as rs

# Check if all input values are not None
if None in (u, l, c, p, s, e1, e2, d1, d2, r1, r2):
    Nu = None
    Uv = None
    Uc = None
    Ratio = None
    Max_Nu = None
else:
    # Define constants
    A, n, G, dT, Tm, he, hi, o = 0.035, 0.38, 9.81, 15, 283, 0.04, 0.13, 5.670374419 * 10 ** -8

    # Define input variables
    d1 = float(d1) / 1000
    d2 = float(d2) / 1000
    r1 = float(r1)
    r2 = float(r2)
    u = float(u)
    l = float(l)
    c = float(c)
    p = float(p)
    s = [float(x) / 1000 for x in s]
    e1 = float(e1)
    e2 = float(e2)
    e3 = float(e3)
    e4 = float(e4)

    # Initialize output lists
    Uv_list = []
    Nu_list = []

    # Calculate for each s value
    for i in range(len(s)):
        # Calculate Gr
        Gr = (G * s[i]**3 * dT * p**2) / (Tm * u**2)

        # Calculate Pr
        Pr = u * c / l

        # Calculate Nu
        Nu = A * (Gr * Pr) ** n
        Nu_list.append(Nu)

    # Determine the highest Nu
    Max_Nu = max(Nu_list)

    # Check if all Nu values are below 1, use 1 if true, else use the highest Nu value
    if all(val < 1 for val in Nu_list):
        Nu_to_use = 1
    else:
        Nu_to_use = Max_Nu

    for i in range(len(s)):
        # Calculate gas conductance
        hg = Nu_to_use * (l / s[i])

        # Calculate radiation conductance
        hr1 = 4 * o * (((1/e1) + (1/e2) - 1)**-1) * (Tm**3)
        hr2 = 4 * o * (((1/e3) + (1/e4) - 1)**-1) * (Tm**3)

        # Calculate heat transfer
        hs1 = hr1 + hg
        hs2 = hr2 + hg

        # Calculate total thermal conductance
        ht = 1 / ((1/hs1 + 1/hs2) + (d1*r1*2) + d2*r2)

        # Calculate U-value, inflated
        Uv = 1 / (he + 1/ht + hi)

        # Append results to output list
        Uv_list.append(Uv)

    # Calculate the average of Uv_list
    Ua = sum(Uv_list) / len(Uv_list)
```